DIPLOMARBEIT

HPLC Analysis of plasmid isoforms with chemoaffinity based media:

Method validation and

Application to in-process control (IPC) samples

angestrebter akademischer Grad

Magistra der Naturwissenschaften (Mag. rer.nat.)

Verfasserin / Verfasser:	Elisabeth Haller
Matrikel-Nummer:	0504862
Studienrichtung (lt. Studienblatt):	Chemie
Betreuerin / Betreuer:	Ao. Univ.-Prof. Mag. Dr. Michael Lämmerhofer

Wien, am 21.01.2011

Table of contents

Abstract (English)

This diploma thesis is dealing with the analysis of plasmid DNA isoforms (covalently closed circular, ccc; open circular, oc; linear, lin) and topoisomers. For this purpose suitable oc standard of two different plasmids (4.9 kbp and 15 kbp) had to be prepared initially. For preparation, optimized protocols (heat treatment for the 4.9 kbp plasmid or enzyme treatment for the 15 kbp plasmid) were developed for transforming supercoiled form into the open circular one. Subsequently, comparison of method validation for both plasmid samples of a novel support material, namely propylcarbamoyl quinine modified silica (5 µm, 100 Å, 150 x 4 mm ID), with the state-of-the-art method employing the DNA-NPR column (2.5 µm, 750 x 4.6 mm ID). The novel stationary phase offers several benefits compared to the commercial available DNA-NPR material, like better recovery for the oc form, separation of oc and ccc form, better peak performances and precisions. Moreover, the method validation for the 15 kbp plasmid was only successful using the new developed material but not with the DNA-NPR stationary phase. Further improvement of the PCQ modified material could be achieved when using 1.5 µm NPS silica particles as support. The NPS chromatographic material enabled successful validation except for the oc standard

Supplementary, two different in-process control samples were analyzed using an online 2D HPLC system to study the influence of fermentation duration on relative topoisomer abundances. In the first dimension a SRT-SEC column (5 µm, 1000 Å, 150 x 4 mm ID) was employed for purification of the sample from impurities. Subsequently, the analyte of the transferred sample fraction was injected online into the O-9-allylcarbamoyl-10,11-dihydroquinine modified stationary phase which provides selectivity for topoisomers. The change of linking number in the first few hours during fermentation process could be demonstrated.

Overall, new methods for pDNA analysis have been developed in the course of this diploma work which are supposed to be of great value in future plasmid research and quality control.

Abstract (German)

Diese Diplomarbeit beschäftigt sich mit der Analyse von Plasmid DNA Isoformen (superspiralisiert, ccc; offen zirkular, oc; linear, lin) und Topoisomeren. Dazu mussten zunächst oc Standards zweier Plasmide (4.9 kbp und 15 kbp) hergestellt werden. Die Transformation der superspiralisierten (ccc) Isoform in die Offen-zirkulare (oc) kann durch Temperaturbehandlung (4.9 kbp pDNA) oder durch Behandlung mit einem Enzym (15 kbp pDNA) erzielt werden, wobei jeweils ein optimiertes Protokoll entwickelt wurde. Anschließend wurden Methodenvalidierungen beider Plasmide mit zwei unterschiedlichen Säulenmaterialien durchgeführt. Die Validierungsergebnisse der Propylcarbamoyl Chinin Säule (5 μm, 100 Å, 150 x 4 mm ID), welche innerhalb der Arbeitsgruppe entwickelt und hergestellt wurde, wurde mit den Ergebnissen der laut aktuellen Stand der Wissenschaft für die Plasmidanalyse verwendeten DNA-NPR Chromatographiesäule (2.5 μm, 750 x 4.6 mm ID) verglichen. Die neu entwickelte stationäre Phase besitzt einige Vorteile im Vergleich zum kommerziell erhältlichen Material wie z.B. eine bessere Wiederfindung der oc Isoform, Auftrennung des oc und ccc Plasmids, bessere Peakperformance und Präzision. Darüber hinaus konnte eine erfolgreiche Methodenvalidierung des 15 kbp Plasmids mit dem neu entwickelten Material nicht aber mit der DNA-NPR Säule durchgeführt werden. Durch die Verringerung der Partikelgröße von 5 μm auf 1.5 μm (NPS Silika) konnte eine weitere Optimierung des PCQ modifizierten Materials erreicht werden. Mit den modifizierten NPS Micra Partikel konnte eine erfolgreiche Validierung der superspiralisierten und der linearen Isoform (4.9 kbp) durchgeführt werden.

Der Einfluss der Fermentationsdauer zweier verschiedener Realproben auf die relative Topoisomerenverteilung wurde mittels eines zweidimensionalen HPLC Systems untersucht. In der ersten Dimension befand sich eine Größenausschluss-Chromatographiesäule (5 μm, 1000 Å, 150 x 7.8 mm ID), welche zur Abtrennung der Verunreinigungen von der Probe diente. Anschließend wurde der Analyt (pDNA) in die O-9-Allylcarbamoyl-10,11-Dihydrochinin modifizierte stationäre Phase transferiert. Diese Säule ermöglichte eine Auftrennung der Topoisomere. Es konnte gezeigt werden, dass die größte Änderung der Linking Nr. beider Proben innerhalb der ersten Stunden des Fermentationsprozess erfolgt.

Summa summarum konnten neue Methoden für die pDNA Analyse entwickelt werden, welche auch für die weitere Forschung und Qualitätskontrolle auf diesem Gebiet von großer Bedeutung sein werden.

Objective and aims of this work

This diploma thesis deals with the separation and analysis of plasmids, which exist mainly in three basic isoforms: linear, open-circular and covalently-closed circular. Besides multimeric forms may exist. For there plasmid isoforms, methods for their chromatographic separation as well as analytical quantitation have been developed in this diploma work.

Structure and course of action of this thesis

The thesis can be structured in two main topics.

The first part of this paper focuses on the method development and the validation of the isoform separation of two different plasmids (pMCP1 4.9 kb and pGNA3 15 kb) employing two different chromatographic selectors and stationary phases, respectively. In both cases, a standard of the open circular isoform had to be prepared, whereby either thermal or enzymatic treatment of the supercoiled sample has delivered the desired open circular (oc) form. However, optimized standard protocols for both plasmids (4.9 kb and 15 kb) preparing their oc isoforms had to be developed. Furthermore two different weak anion exchangers have been compared as separation media: the commercially available Tosoh DNA-NPR column and the in-house produced and packed propylcarbamoyl quinine material. After method development and optimization, the standard validation parameters according to the ICH guidelines (precision, recovery, detection and quantitation limits) have been determined and calculated in order to characterize the analytical method and to enable an accurate comparison of both anion exchangers. The main problem making accurate and reliable analysis challenging is the selectivity between oc and the linear form. The key for their adequate resolution is expected to be the reduction of the particle size. Therefore, improvement in the separation performance of the quinine-modified silica seemed to be possible by decreasing the particle size of the support material (from 5 µm to 1.5 µm). Subsequently a validation of the smaller plasmid (pMCP1) was carried out with such smaller-sized particles in order to investigate the influence of the 1.5 µm non-porous (MICRA) material and for method characterization. Moreover, the buffers and the gradient method needed to be re-optimized to achieve an analysis time below 15 minutes including the washing and re-equilibration steps.

The second topic of this thesis deals with the distribution of the topoisomers of the ccc form. It had to be investigated how the fermentation duration influences the supercoiling of two different plasmids. Performed analysis used a two dimensional chromatographic setup to combine two different separation modes: size exclusion in the first dimension and anion exchange chromatography in the second dimension. Additionally, the concentration as well as the topoisomer distribution should be determinable within one single run in an automated manner without excessive sample preparation or handling steps between two subsequent chromatographic steps. The results are expected to explain whether the day time has an influence on topoisomer distribution and how long the fermentation should take place to obtain a maximum of supercoiling with the highest concentration.

1 Introduction

1.1 Historic background

In 1952, J. Lederberg discovered that bacteria contain ring-shaped, extra chromosomal DNA which he termed "plasmids". In the early 1990s, the usage of DNA vaccine against pathogens and tumor antigens *in vivo* were discovered. About 15 years ago, the first DNA vaccine studies in humans were carried out with an HIV candidate in the earliest phase of the clinical trial. Afterwards tests against cancer, influenza, malaria and hepatitis B were carried out (M. Kutzler, 2008). At present, about 18 percent of all vectors used in gene therapy trials are plasmidic DNA (The Journal of Gene Medicine, 2010). These facts confirm that treatment of diseases (e.g. cancer, acquired immunodeficiency syndrome AIDS, human immunodeficiency virus HIV, Malaria) based on gene therapy and vaccination with nucleic acids is a promising option to cure such genetic defects. Consequently, it is necessary to investigate the stability and to characterize those nucleic acid-based drug substances (Middaugh, 1998).

1.2 Basic knowledge about plasmid DNA (Schleef, 2001)

Plasmids are extrachromosomal, double-stranded deoxyribonucleic acid (DNA) molecules, which naturally exist in both, eukaryotic and prokaryotic cells (Schleef, 2001). Their size can vary from less than 1 to over 200 thousand base pairs (kilobase pairs, kbp). To afford a stable coexistence with their host cell, they are able to strictly control their replication. This process is autonomously and independent from their host chromosome, that is why they are also called replicons.

Plasmids can provide several advantages, for instance fixing nitrogen, encoding for antibiotics or degrading pollutants in bacteria. However they are not essential for bacterial growth. They are often compatible, which means that different plasmid types can coexist in the same bacteria cell. One of the most important feature of plasmids is their origin of replication (the so-called "*ori*V site"), where replication starts and which is responsible for the regulation of the copy number. There are two possibilities how plasmid host-to-host transfer can be realized: either by transformation or conjugation. Transformation means that the plasmids released from lysed cells are absorbed by surrounding cells through their cell wall, whereas

conjugation involves a transfer by direct cell-to-cell contact. To transform a species matching *oriV* sites (because of enzyme specificity) and a high enough copy number are necessary.

Application in molecular biology and genetic engineering

The most important function of plasmids is that they can be used as vectors and therefore transfer DNA into an organism. Also viruses, cosmids or phages can be used for such applications, but their utilization becomes less important. Plasmid vectors for therapy or vaccination, the size of which can be from less than 1 kb to more than 20 kb, contain two units: the *bacterial backbone* (origin of replication, selection markers) and the *transcription unit* (encoding the antigen under appropriate promoter control) (Schleef, 2001).

1.3 Topological structures of plasmids
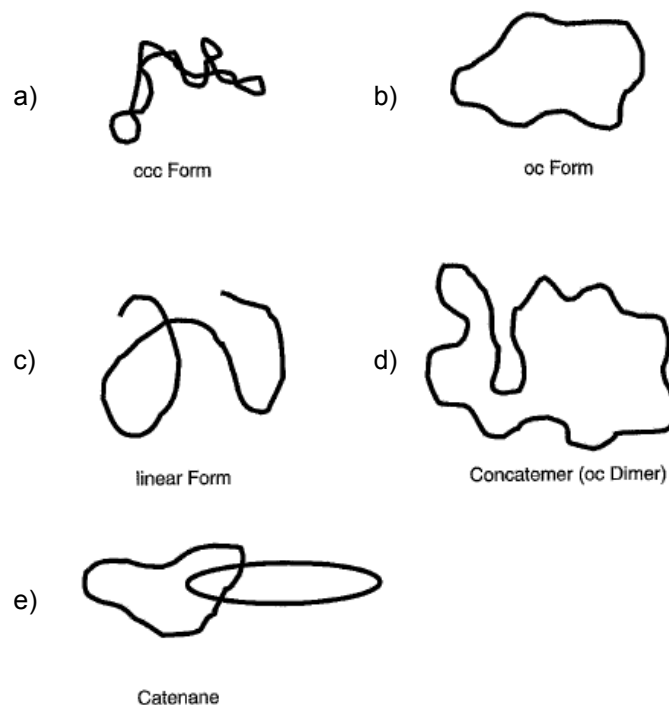
Figure 1: Topological structures of plasmid DNA (Schleef, 2001)

Fig. 1 shows the main five forms of plasmids. The first three pictures show monomer forms (a-c), whereas d) illustrates the structure of the oc dimer. The last one (e) describes two mechanically interlocked oc molecules.

Plasmids, which have an identical nucleotide sequence, appear in different shapes which differ in topology and size as seen in Figure 1. Only a dimer of one

isoform (d) is presented in this figure, but also the ccc and linear dimers have to be considered as well. In a bacterial cell, the most common form is the so-called ccc (covalently closed circular) form, which is usually negatively supercoiled. This form has a compact structure in which the DNA double-strand helix is wound around itself. One DNA strand can be nicked (breakage of one phosphodiester bond) as a result of mechanical stress, nucleases or UV irradiation. Consequently, the molecule relaxes and is less compact. This form is labelled as open circular (oc) or nicked plasmid. In the absence of agents altering the superhelicity, totally relaxed ccc form (without any supercoiling) can not be distinguished from the oc form. If both DNA strands are broken at the same position, linear DNA molecules are formed. All three isoforms can exist as equivalent oligomeric forms (concatemers) as well as dimeric plasmid molecules (Kutzler, 2008; Schleef, 2001).

For therapeutic applications, the most important isoform is the supercoiled plasmid molecule (ccc form), because it is believed to be most active and stable topological isoform.

Supercoiling of plasmids

In principle, ccc DNA is negatively supercoiled, which is the opposite rotation to the right-handed double helix structure. Therefore this type of DNA is underwound, which means that there are less helical turns than in relaxed or linear DNA and a torsional tension is created in the molecule (Schleef, 2001).


a)

b)

Relaxed state
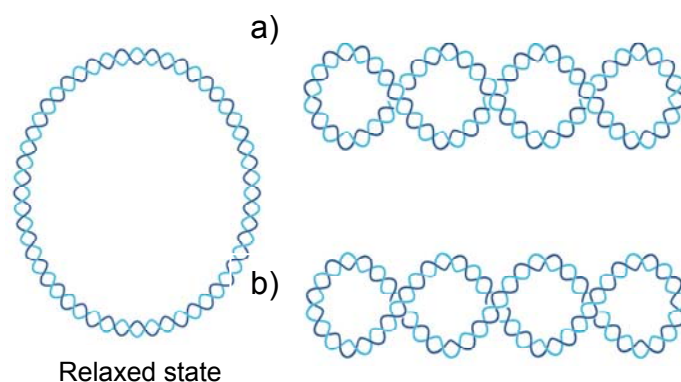
Figure 2: Illustration of positive and negative supercoiling (Travers, 2005)

The upper strand needs to be aligned with the lower DNA strand by rotation
< 180°, resulting in a positively supercoiling (+1) for counter-clockwise rotation
(a) and negatively supercoiling (-1) in the case of clockwise rotation (b)

Linking number Lk (Bates, 2005)

By the formation of 5'-3' phosphodiester bonds, linear double-stranded DNA can be closed and the linking number corresponds to the number of double-helical turns. For example, if the dsDNA is cut and rejoined after making a full 360° twist in one end, the linking number is one. Thus the Lk value is determined using the number and handedness of the crossovers of the two curves when projected onto a plane.
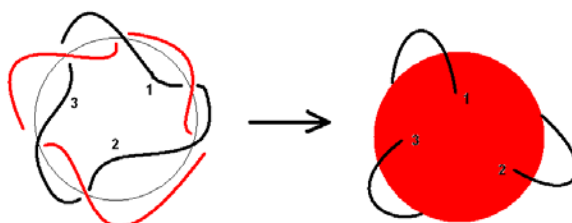

Figure 3: Visual Evaluation of the linking number (Bates, 2005)

Each crossing of one strand over the other a value of +1 or -1 can be assigned and the sum of the values is halved to give the linking number of the two DNA strands. Consequently, the Lk value has to be an integer.

$$Lk_m = \frac{N}{h} = \frac{N}{10.5}$$

Equation 1: Definition of the Linking number (Bates, 2005)

The number of double-helical turns is determined by the length of the DNA in base pairs (N) divided by the number of base pairs per turn of helix (h).

Different conditions, such as ionic strength, temperature and pH, influence the linking number hence the h^0 value is often used. Under standard conditions (0.2 M NaCl, pH 7.0, 37°C) it corresponds to 10.5 bp/turn (Bates, 2005). In general acceptance, the standard linking number of plasmids is positive based on their negative supercoiling.

In addition, the actual supercoiling of ccc plasmids has to be related to their hypothetically completely relaxed state (closure of a linear molecule into a planar circle without any torsional strain) Lk^0, resulting in the linking difference.

$$\Delta Lk = Lk_m - Lk^0$$

Equation 2: Calculation of the linking difference (Bates, 2005)

To compare different molecules, the specific linking number can be used, because the standard linking number Lk^0 is proportional to the number of bp. Instead of specific linking number, σ is also termed as superhelix density because it

describes the degree of supercoiling. Negative supercoiling ($\sigma < 0$) delivers values of $Lk < Lk^0$.

$$\sigma = \frac{Lk - Lk^0}{Lk^0} = \frac{\Delta Lk}{Lk^0}$$

Equation 3: Specific linking difference (Bates, 2005)

The specific linking difference is related to the
number of base pairs. Therefore, also plasmids
with different sizes are comparable.

The change of the conformation without breaking one or both strands does not influence the linking number. Hence, supercoiled plasmids which can only be distinguished because of their different linking numbers are called **topoisomers**.

Twist (Tw) and Writhe (Wr)

The twist (Tw) describes the coiling of individual strands around each one another and therefore the number of bp per helical turn h is altered. The second important term is the writhe (Wr) which is defined by the superhelical turns in space. The sum of both geometric values results in the linking number.

$$\Delta Lk = \Delta Tw + \Delta Wr$$

Equation 4: Definition of the linking number

The linking number is invariant, therefore any change in the twist must cause
an equal and opposite change in the writhe of the molecule.
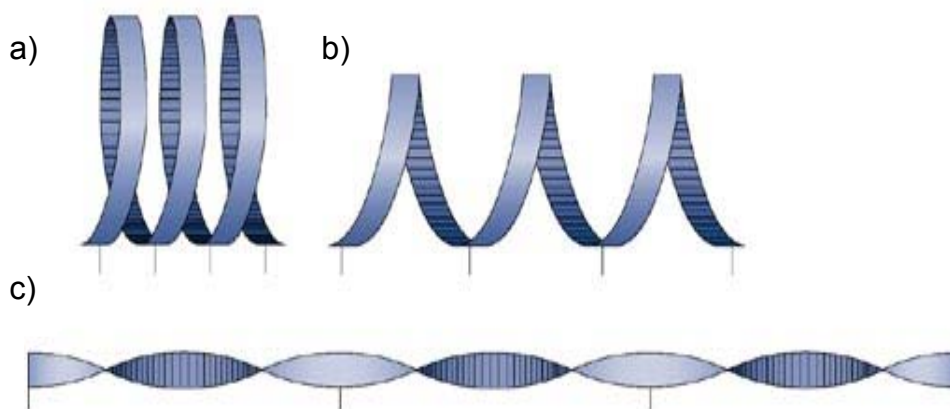
Figure 4: Visualization of the twist and writhe (Cozzarelli, 2006)

a) Wr~-3, Tw~0 b) writhe decreases, twist increases c) Wr~0, Tw~-3

As it is obvious from the picture above, those two parameters (twist and writhe) have a huge influence on the overall size of the molecule. Therefore analyses, in which the size of the analyte is important for the separation, are very useful for determination of the DNA topology.

Influence of environmental conditions on the topology

The availability of positively charged ions to neutralize the negatively charged backbone of the DNA and a change in the temperature can affect the helical repeat and hence the twist. (Bates, 2005) The higher the concentration of counter ions is the more tightly wound the helix becomes. This results in an increase of twist. In addition, increasing the temperature occurs an unwinding of the DNA helix and the linking number is decreasing. For instance in *E.coli* bacteria, the degree of negative supercoiling increases as the temperature increases (Schleef, 2001).

Statistic distribution of topoisomers (Bates, 2005)

Depew and Wang and Pullyblank et al. investigated 1975 the Gaussian distribution of relative concentrations of topoisomers (intensity evaluation on agarose gel) of DNAs. The most intense band corresponds to the most stable topoisomer with Lk^0. Considering the Hooke's Law ($G_{(Lkm)}=K\omega^2$) and the standard thermodynamic equation ($\Delta G=-RT\ln K$), following equation results.

$$\underbrace{\frac{1}{\Delta Lk}\ln\frac{[LK_x]}{[Lk_m]}}_{y} = -\frac{K}{RT}\underbrace{\Delta Lk}_{x} - \frac{2K\omega}{RT}$$

Equation 5: Correlation of the elastic constant and the angular (Bates, 2005)

By plotting ΔLk against the left term of the equation, a linear relation can be observed. Thus K and ω can be determined, because the slope of the line is –K/RT and the y-intercept -2Kω/RT
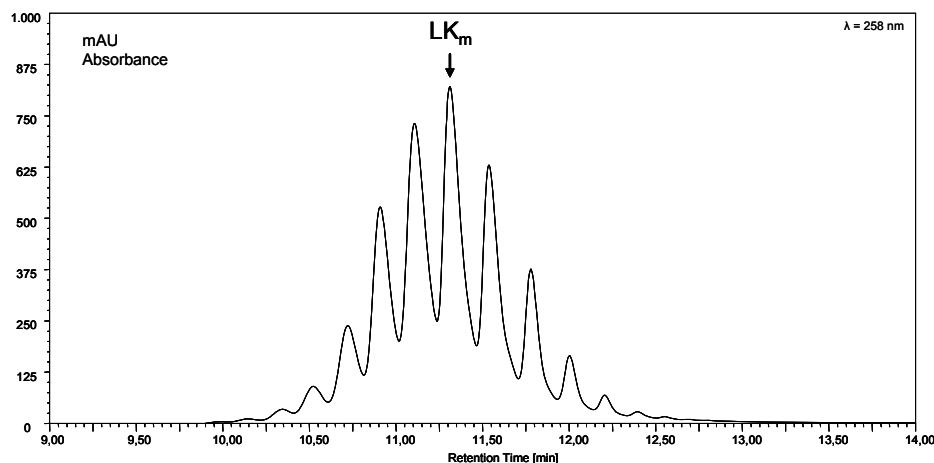
Figure 5: Example for the Gaussian distribution of topoisomers

2D chromatographic setup (SEC-AIEX) of 4.9 kbp plasmid:
Method description:
1st dimension: SRT SEC-1000 (150 x 7.8 mm ID) 5 µm, 1000 Å at room temperature, isocratic elution with 0.1 M NaCl, 1 mM EDTA, pH 7.5, flow rate: 2 mL/min, collection time: 1.35 – 2 minutes
*2nd dimension:*O-9-allylcarbamoyl-10,11-dihydroquinine (150 x 4 mm ID) on Daiso 5 µm, 120 Å, at 60°C, gradient elution 0-73% buffer B in 11 minutes (buffer A: 50 mM phosphate, pH 7.2, buffer B: 50 mM phosphate⁻, 0.6 M NaCl, 10% IPA, pH 7.2) flow rate: 1 mL/min

Topoisomers can be visualized either with an appropriate HPLC method or with agarose gel electrophoresis.

DNA intercalators and their impact on the DNA structure

In the structure of DNA, the aromatic bases are stacked over each other in the interior of the molecule and stacked over each other in the helix axes causing gaps between adjacent bases. Within these gaps the bases can form hydrophobic or electrostatic interactions with staining agents. Intercalating substances are aromatic planar molecules, such as ethidium bromide. EtdBr is very toxic and may be carcinogen, thus alternatives like minor-groove binding Sybr dyes are advertised. However, details of mutagenic and toxicity are still lacking.
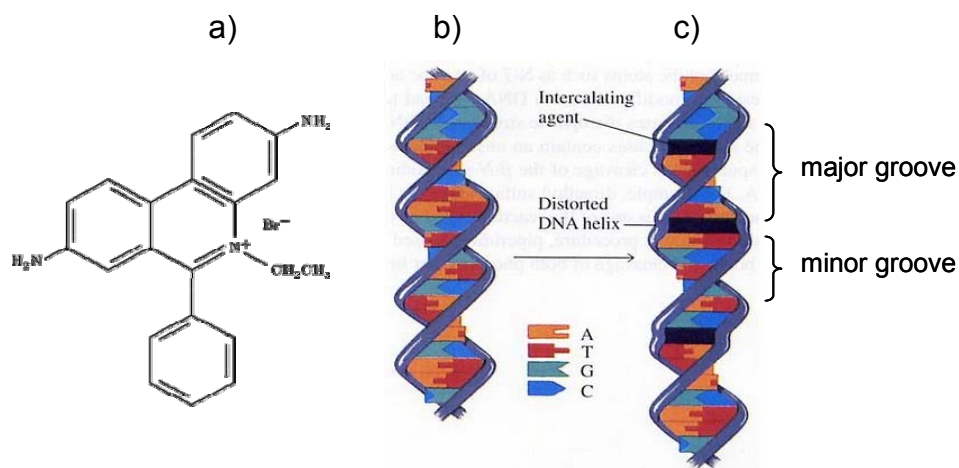
Figure 6: Ethidium bromide as intercalating dye (http://sandwalk.blogspot.com)

Molecular structure of ethidium bromide (a), untreated DNA (b) and the
impact of intercalation on the twist of the DNA helix (c)

When the intercalator is added to the DNA sample, it stretches and unwinds the DNA helix (26° per molecule EtdBr). The binding of intercalating agents is proportional to the specific linking number σ. Upon addition of EtdBr, the initially negatively supercoiled DNA reduces the twist and hence increases the writhe (Bates, 2005). Thereby, it is possible to determine σ by dye titration and analysis by agarose gel electrophoresis. By increasing the EtdBr concentration the DNA molecule becomes fully relaxed and at last positively supercoiled (Schleef, 2001). Intercalation does not only increase the adjacent base pair distance but also induces local conformation changes in the backbone (M. Mahut, PhD thesis (2010) *University of Vienna*).

Influence of enzymes

In the 1970s, the application of restriction enzymes (so-called topoisomerases) to produce certain DNA topologies was discovered. Those topoisomerases are able to cut one or both DNA strands, consequently they cause a relaxation of the molecule. Additionally, they can control the equilibrium between topoisomers, resulting in a distribution centered at Lk^0 (Bates, 2005).

The two most important enzymes, which can alter the linking number, are the topoisomerase I (Topo I; Wang, 1971), and topoisomerase II or gyrase (Topo II; Dean et al. 1983). Topo I can introduce single-strand breaks hence the supercoiling is decreased consecutively until removed. Topo II is able to introduce double-strand

breaks and usually introduces higher supercoiling. It also can create as well as resolve DNA knots, depending on its type. Both enzymes regulate the degree of supercoiling because of their contrasting properties.

2 Plasmid manufacturing

The interest in gene therapy and DNA vaccines is constantly increasing which requires efficient manufacturing processes from the host bacteria, often Escherichia coli. Biopharmaceutical plasmid production has to be done considering the regulatory guidelines set by the European Medicines Agency (EMEA), which stipulate that animal-derived materials have to be omitted throughout the process and fully defined media has to be favoured.

2.1 Biotechnological production of pDNA

The production process of plasmids can be classified in three different parts.

1. Up-stream processing (construction and selection of appropriate expression vectors and production organisms)

2. Fermentation process (optimisation of the conditions)

3. Down-stream processing (isolation and purification steps)

The first two steps have the most impact in the process stream regarding the impurities and the contaminants (Kelley and Hatton 1991). To obtain highly purified ccc plasmid several impurities and host cell constituents (gDNA, RNA, proteins, small molecular weight nucleic acids, …) have to be removed in the course of the manufacturing process i. e. during downstream processing.
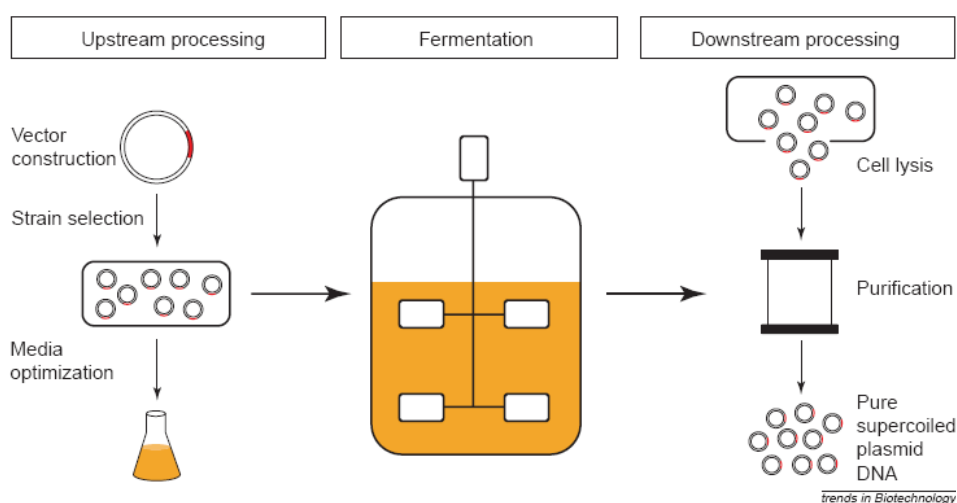

Figure 7: Illustration of the three stages of pDNA process development

(Ferreira, 2000)

1   Upstream process

The choice of bacterial strain and therefore its genetic sequence affects the plasmid quality as well as its yield. Cultivation of Escherichia coli are most commonly used for the production of plasmid DNA whereby the quality of the DNA is mainly influenced by the host strain (Werner, 2002). To improve the reproducibility and the yield, appropriate nutrient and oxygen levels (yeast extracts or peptones) as well as the temperature has to be optimized.

2   Plasmid fermentation

Initially, a process delivering a high amount of predominately supercoiled plasmid from bacterial cell has to be developed. The fermentation process which starts with inoculation takes place in bioreactors in industrial scale under optimum conditions (temperature, pH, nutrients)

3   Downstream processing

Alkaline cell lysis

At the end of fermentation the plasmid DNA is present in the intracellular space. Downstream processing starts with the alkaline disintegration of bacterial cell which is necessary to release plasmids and was firstly described by Birnboim and Doly in 1979. Different modes like chemical, physical or mechanical methods for the homogenisation of bacterial cells are feasible. The method of choice is the chemical one due to the sensitivity of plasmids to hydrodynamic shear forces (mechanical stress would reduce the yield) (Werner, 2002). To prevent the plasmid of damages caused by DNase (desoxyribonucleases) and shear forces, EDTA is added to protect the cell wall by chelating divalent cations. As chemical reagent, sodium dodecylsulfate (SDS) is used affecting a breakage of the bilayer membrane and the denaturation of proteins at an alkaline pH. Thus, by adding SDS plasmid DNA is released and remains in solution whereas host proteins and genomic DNA precipitate. Afterwards the solution has to be neutralized (usually with 3M potassium acetate) whereby nucleic acids, cDNA and proteins precipitate because the refolding is inhibited due to their size. The sc plasmid can simply be separated using centrifugation.

During the fermentation process also oc and linear plasmids are generated thus the best harvesting time has to be defined (ratio between the plasmid forms are

dependent from the fermentation time). In addition, the optimum ratio of lysis buffer per g biomass has to be investigated to enhance the amount of sc plasmid (Werner, 2002). After the fermentation, the resulting biomass has to be cooled down to prevent further degradation of the sc pDNA (Werner 2000, Schleef 2001). Only about 3% of bacterial cell lysate consists of plasmidic DNA thus plasmids with low copy number have to be concentrated at first (Stadler, 2004).

2.2   Purification

Achievement of pharmaceutical grade quality plasmidic DNA (sc) has to be separated from all other impurities using chromatographic operations. Different modes for the separation can be used, like affinity, ion-exchange, hydrophobic interactions, and size exclusion. (Schleef, 2001) However, removal of RNA can be performed either enzymatically (RNase), using chromatographic methods (SEC: RNA and proteins are permeating into intraparticulate pore spaces while pDNA elutes in the exclusion volume) or selective precipitation using Ca^{2+}, NH_4^+, Mg^{2+}(Thatcher et al. 1999, Ferreira 1999, Bhikhabhei 2001) or polyethylene glycol (Horn 1995). Bacterial chromosomal DNA which is much larger and less supercoiled can be removed by selective precipitation (Mihăsan, 2007) due to its topological difference to ccc pDNA. Using a HIC or IEX step, also smaller molecules can be eliminated (Stadler, 2004). The covalently closed form is the most appropriate for therapeutic applications (Food and Drug Administration; Middaugh, 1998) thus purification is absolutely essential.
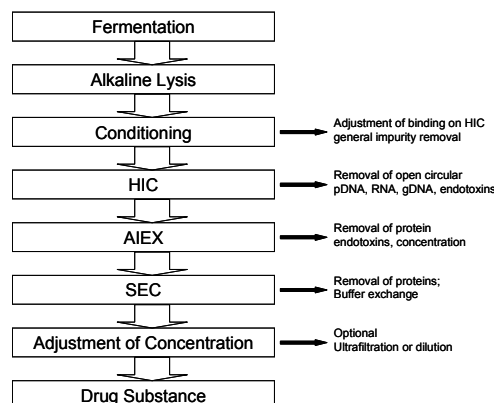

Figure 8: Flow-scheme of the purification process of manufacturing pharmaceutical grade pDNA (Urthaler, 2005)

For purification of plasmid DNA a chromatographic combination using hydrophobic interaction (HIC) (Diogo et al., 2000) as a capture step followed by anion exchange chromatography (AIEX) (Eon-Duval & Burke, 2004) as intermediate step and finally size exclusion (SEC) (Horn et al., 1995) for polishing was established. Carrying out this procedure the resulting product consists of more than 95% of supercoiled plasmid DNA (drug substance) (Werner, 2002). Furthermore, this three step column system provides fast and automatable, reliable and low cost purification process.

3 Analysis of plasmid structures (AGE, HPLC, CGE)

(Bates, 2005)

Plasmids are produced in bacterial cells, mainly in Escherichia coli bacteria. Consequently, impurities such as proteins, RNA, genomic DNA and endotoxins have to be removed using anion exchange (Colpan et al. 1999; Bussey et al. 1998), reversed phase (Green et al., 1997) or size exclusion chromatography (Horn et al., 1995). After discovering their application for gene therapy or DNA vaccination, additional requirements concerning purity and topological distribution have to be fulfilled. According to the guidelines set by the regulatory authorities like Food and Drug Administration (FDA) in the United States or European Medicines Agency (EMEA), plasmid therapeutics must have a characterized content of at least 90% ccc form. Therefore several techniques were developed for purification as well as a reliable and accurate determination of the purity. The analysis method guarantees a separation of different plasmids, of different topologies of the same plasmid as well as the determination of impurities.

3.1 Capillary gel electrophoresis (CGE)

For analyzing different plasmids and their structures, capillary gel electrophoresis is another powerful tool (Schmidt et. al, 1999). In principle, the separation mechanism is the same as for agarose gel electrophoresis differing only in the dimensions of the separation compartment in which the separation takes place. CGE describes separation within filled thin capillaries (50-100 µm ID) with a liquid polymer solution, usually polyacrylamide or derivatized cellulose. To analyze a DNA sample, it has to be injected into the capillary after which a certain voltage is applied to the capillary ends. As a result of the charged analytes, they migrate towards the electrode, whereby the shape and the topology of the analyte mainly affect the separation. Thus the migration order is ccc > lin > oc and monomers elute earlier than dimers of the same isoform (ccc monomer > ccc dimer > lin monomer > lin dimer > oc monomer > oc dimer). This order is independent from the plasmid size and simplifies identification. This effect indicates that the migration order is mainly influenced by the compactness and by the molecular size of the analyte.
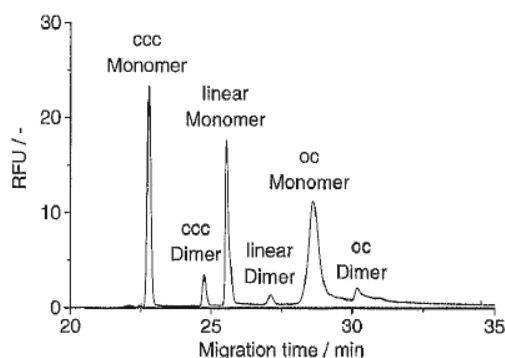
Figure 9: CGE electropherogram of pUC19 plasmid DNA (2.9 kb) (Schleef, 2001)

Liquid gel matrix: hydroxypropylmethylcellulose (HPMC)

CGE quantifies different isoforms fast and reliable in an automatable system. Hence CGE can be used for routine analysis to establish the plasmid DNA form distribution. Furthermore, CGE provides a higher resolution, sensitivity and selectivity than AGE. However, this type of electrophoresis does have a number of disadvantages like lack of robustness, poor reproducibility and low sample loading.

3.2   Agarose gel electrophoreses (AGE)

Agarose gel electrophoresis is the most common method to determine the distribution of isoforms and topoisomers of one plasmid. The separation is mainly based on size, geometric form and the charge of analyte.

Practically, an electric field has to be applied to a uniform gel, which is characterized by a certain sized mesh network of agarose. The negatively charged DNA, which stems from the sugar phosphate groups in the backbone, migrates from the cathode to the positively charged anode. The mesh size of the gel and the applied voltage are the reason for the faster migration of compact and highly charged supercoiled monomer than open circular pDNA. Hence the size, the compactness and the charge of the analytes are important criteria, which enable the separation. The resulting bands in the agarose gel may be assigned to different plasmid sizes and topologies, like supercoiled, linear or the open-circular form. However, visualisation of the DNA can not be done directly but either before or after the electrophoretic run by usage of an intercalating dye. It has to be considered that when added prior to the separation to both the gel and the buffer this additive influences the separation, the migration velocity and therefore the migration order of the different geometric-shaped DNA.

AGE is sensitive to changes in ionic strength (buffer composition), gel concentration, temperature, dye concentration and changes in the electric field, thus the single bands have to be identified correctly with an internal standard such as a DNA ladder or a certain topological standard. Therefore it is very important that the operating conditions are not changed if the results should be comparable. Consequently, it is very important to use the same buffer (usually TAE Tris-Acetate-EDTA or TBE Tris-Borate-EDTA) for preparing the gel and for the electrophoretic run to prevent a change of the migration because of the difference in the ion strength.

As general assumption, the linear form has the greatest migration velocity, followed by the negatively supercoiled form and the open circular form. If the ccc is highly supercoiled its migration can be eventually faster than the linear form. Furthermore, monomers migrate faster than dimers due to their size. These conclusions are only true, if the intercalating dye is added after the electrophoresis only for visualisation purposes or if the added amount is under a critical concentration at which the migration order is changed. In general, the resolution of the different plasmid structures in agarose gel electrophoresis and the separation of oc monomer and ccc dimer suffer with increasing plasmid size and increasing temperature.

The concentration of pDNA can be evaluated by densitometric quantification of the fluorescence intensity at 366 nm (maximum fluorescence of the DNA-EtdBr complex). This is a very sensitive method, but it is limited to a maximum of 2 µg plasmid guaranteeing sufficient resolution between the isoforms and sharp bands. Additionally low concentrations of impurities can not be observed anymore and a resolution problem appears with respect to oc monomer and ccc dimer structures (Schleef, 2001).

In conclusion AGE has a lot of advantages and disadvantages (like long analysis time), but nevertheless it is still one of the most important methods for determination of the purity and homogeneity of plasmid samples.
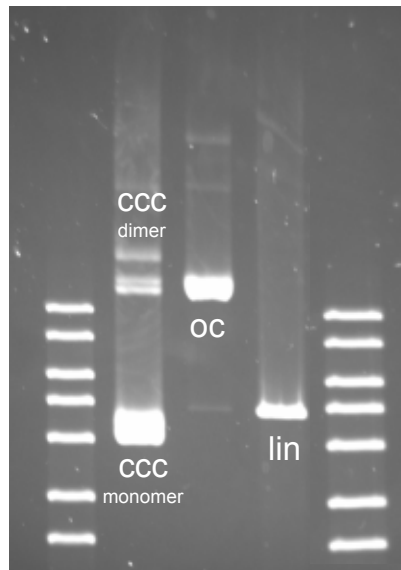
Figure 10: Separation of the different isoforms of pMCP1 (banding pattern)

The gel contains 0.8% of agarose and the running buffer consists of 1x TBE buffer. For the run 200 Volt for 2 hours are applied. Afterwards, staining with Sybr gold® (provided from Invitrogen) was performed

3.3 High performance liquid chromatography (HPLC)

For industrial applications it is important to have short analysis times with good and robust separation. That is why high performance liquid chromatography is the method of choice. Depending on the interactions between the analyte and the stationary phase different working modes in HPLC are possible: Reversed Phase (RP), Ion Pair (IPC), Anion Exchange (AIEX) and Size Exclusion Chromatography (SEC). Nowadays nearly all chromatographic methods for detection of plasmid DNA are based on the anion exchange principle which is obvious for negatively charged biomolecules. To improve the method for the individual application, different parameters concerning the stationary phase can be optimized such as particle size (Huber, 1998), porous or nonporous particles and the nature of the support material (based on silica, methacrylate or organic monoliths). Using macroporous silica based supports the limiting factor is the slow mass transport within the stationary phase resulting in broad peaks, low sample recovery and long analysis times. This can be solved with micropellicular packing material, which decreases the surface due to its non-porosity and therefore gain the enhancement of separation efficiency as a result of acceleration of mass transport due to elimination of intraparticulate pore diffusion. Additionally, lower amounts of selector are immobilized on the stationary phase. Thus the best compromise between the available surface and the particle size has to

be found. Furthermore, the separation can be influenced by additional interactions such as hydrophobic forces (HIC) or intercalation if appropriate functionalities are bound to the support. Silica based supports are very polar because of their terminal OH groups and even after modification of the surface they are still present in a lower content. Thus also hydrogen bonds are possible. If they have to be suppressed, the silica support has to be end capped resulting in steric hindering of Si-OH groups (for example derivitization of accessible silanol groups with hexamethyldisilazane).

Concerning the mobile phase, parameters such as pH value, ionic strength and buffer type have to be optimized. Also organic additives (e.g. isopropanol as hydrophobic suppressor), cationic additives (Zhdanov, 2002) (for example spermidine or spermine, which are highly charged and thus they compact pDNA), chaotropic agents (like urea) or chelating agents (Ca^{2+}, Mg^{2+}, EDTA) (Burda, 1997) can improve the resolution of the plasmid-containing sample. Considering compacted DNA it may stick to some anion exchange materials like Tosoh DNA-NPR or even hardware (glass frits, metal frits) and clog the column. Thus additives have to be used carefully.

By working with DNA samples it also has to be considered that at a pH above 4 the net charge of the molecule is negative and therefore anion exchange chromatography (AIEX) can be used. Silica based supports are only stable below a pH of 8 hence only a limited pH range is suitable for this application.
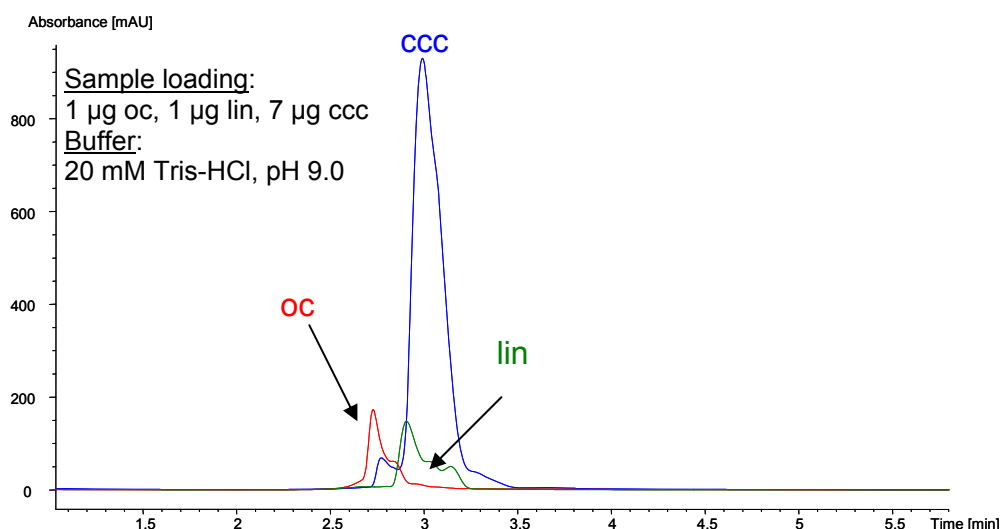
Figure 11: Chromatogram of 4.9 kbp plasmid with AIEX

Column: Tosoh DNA-NPR, ligand: DEAE
(750 x 4.6 mm ID, 2.5 µm)
Elution: buffer A: 20 mM TrisHCl, pH 9.0,
buffer B: A + 1M NaCl, 50-75% buffer B in 5 min
Column temperature: 25°C
Flow rate: 1 mL/min

As it can be seen in Figure 11, only the ccc and oc isoform can be separated but the ccc and linear form are co-eluting. The selectivity of the ligand of the stationary phase is not sufficient for this separation and an appropriate selector has to be developed in order for the chromatographic system to be more powerful and robust. Several ligands have already been developed to separate all isoforms but more selective commercially available stationary phases for this application are still in development. The commonly most often used stationary phase is the Tosoh DNA-NPR employing a diethylaminoethyl (DEAE) ligand. However, some drawbacks have been observed with this column including besides insufficient selectivities between isoforms a poor recovery in particular the oc form.

Using high performance liquid chromatography, advantages like short analysis times, robustness, simple handling and automation (no need for qualified personnel) can be provided. Furthermore, an upscaling of the method for industrial purposes is possible.

To sum up, high performance liquid chromatography is the most promising method for characterization of plasmid DNA.

4 Method development and Validation

To enable separation of plasmid isoforms and thus validation, a novel material (propylcarbamoyl quinine) have been developed in house.

Validation of an analytical procedure means to demonstrate that the procedure is suitable for its intended purpose. Before starting the validation, the physical properties of the analyte have to be investigated and preliminary tests have to be performed in order to find the best conditions of the analytical method.

By performing such a validation, important parameters like precision or repeatability (experimental variance of determinations), accuracy (recovery experiments), specificity, detection limit (LOD), lower and upper quantitation limit (LLOQ, ULOQ) and the linearity range have to be determined. Based on these parameters, a good prediction about the suitability of this method for the quantitation determination of a predefined analyte can be given. To get values for these parameters as good as possible, each single method (stationary phase, mobile phase, elution conditions) has to be optimized.

This thesis focuses on improving an HPLC method for the separation of different plasmid isoforms, thus the following text is focused on chromatographic techniques.

At first, the choice of selector and stationary phase, respectively, is the most important part by improving an HPLC method, because it decides which interactions enable separation, resolution and elution of the analyte. As plasmidic DNA has a negatively charged phosphate backbone the usage of an AIEX system is obvious. Furthermore non porous silica based support is used because the plasmids have a high molecular weight (5-15 kDa). That is why they are not able to diffuse into pores and interactions between the analyte and the stationary phase are only possible at the surface of the particles.

Characterization of the Propylcarbamoyl quinine material

Propylcarbamoyl quinine (PCQ) covalently linked to silica (see Figure 12) was used as stationary phase based on the studies of M. Mahut (PhD thesis (2010) *University of Vienna*). The main function of this ligand immobilized onto porous silica (100 Å, 5 µm) is to enable a hydrogen bond-mediated electrostatic interaction mechanism by protonation of basic tertiary amine of the quinuclidine and

simultaneously H-bonding at the quinine carbamate with the plasmid DNA. Thus, the molecular recognition principle can be classified as chemoaffinity principle and is not merely an ion-exchange process. Experimental evidence for this assumption is provided by a series of structural variations of the ligand and structure-selectivity relationships based on these experiments (M. Mahut, PhD thesis (2010) *University of Vienna*).

The residual silanol groups are negatively charged, resulting in an amphoteric character of the material. To reduce the impact of repulsive Coulomb forces, those silanol residues are partly derivatized with hexamethyldisilazane giving trimethylsilyl(TMS)-endcapping. At this point it should be added that the mesopores (100 Å) are not accessible for the plasmid and thus the support behaves like a nonporous material for the plasmid separation.

In earlier studies, our working group with M. Mahut found out that a certain distance (four atom spacer) between the two H-donor groups of the quinuclidine and the carbamate is necessary for a successful separation of the isoforms. This result can be explained by considering the topology and size of the ligand. In addition, the negative charges of each isoform are different considering their accessibility to the stationary phase which results in different binding strengths enabling a separation.
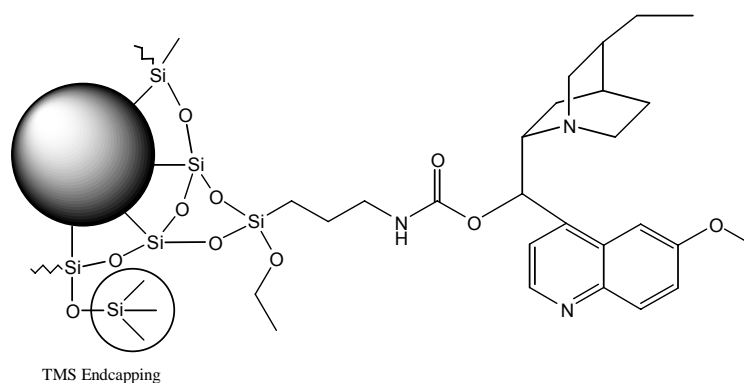

Figure 12: Molecular structure of Propylcarbamoyl-Quinine ("PCQ")

Elution of adsorbed DNA can be achieved either by increasing the pH or the salt concentration. An increase of the pH affects the stability range of the silica support and the analyte. Thus a suitable pH range from 6.5 to 8 is chosen.

Moreover, the Coulomb force, one of the strongest and long-ranged interaction, as well as hydrophobic interactions can influence the separation. The resolution and the peak capacity of the isoforms can be improved by exploiting the influence of

intercalators on DNA or by suppressing hydrophobic interactions through the addition of organic modifiers like 2-propanol (IPA) (Huber, 1998).

For exploiting the present forces in the best way, the ligand as well as the analyte has to be studied very well. This enables an optimum of separation with pre-defined parameters such as separation material and analyte.

The PCQ column, which was used for the validation measurements, is prepared and packed in-house (column dimension: 150 x 4 mm ID).

Characterization of the Tosoh Bioscience DNA-NPR material

TSKgel DNA-NPR columns from Tosoh Bioscience are packed with non-porous particles (2.5 µm) hydrophilic polymer beads (hydroxylated methacrylic polymer) modified with a weak anion exchanger (ligand: DEAE - diethylaminoethylgroups).
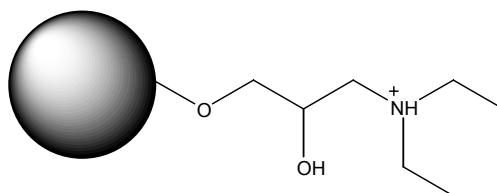

Figure 13: Molecular structure of the weak anion exchanger (DEAE)

This support material can be used in the pH range between 2 and 12 (pK_a=11.2). Compared to columns packed with porous particles and the same ligand functionality, TSKgel DNA-NPR columns have a low binding capacity (5 mg BSA/mL). To gain a high efficiency separation of plasmids, the column dimensions are optimized (750 x 4.6 mm ID). For the protection of the column a small guard column can be used. The housing material consists of stainless steel in both the separation and the guard column.

Concerning the elution of the analyte the composition of the mobile phases as well as the gradient follows standard protocols employing NaCl-gradient elution (see Figure 14).
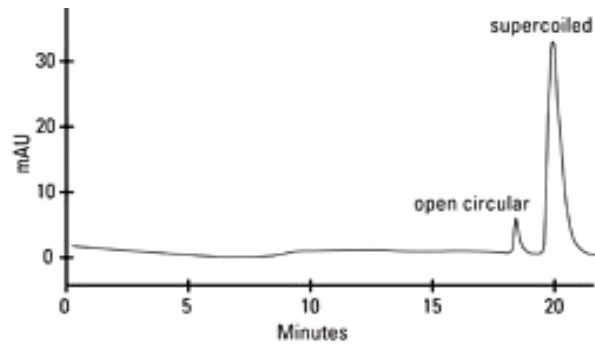
Figure 14: Plasmid analysis with TSK gel DNA-NPR column

(http://www.separations.us.tosohbioscience.com)

Column: TSKgel DNA-NPR (750 x 4.6 mm ID)
Sample: pUC19 plasmid
Elution: buffer A: 20 mM Tris-HCl, pH 9.0, buffer B: A +
      1M NaCl, 50-65% buffer B in 10 column volumes
Flow rate: 1 mL/min
Detection: UV at 260 nm

As seen above, only the open circular and the supercoiled pDNA are detected but no linear form. The column is not able to separate the linear isoform at certain mobile phase and gradient conditions which is a disadvantage of this system. Nevertheless it is the most important material in plasmid separation because the open circular isoform is the most common impurity by the production of plasmids.

5 Method validation for pMCP1 with propylcarbamoyl quinine modified silica

Performing method validation, standards of each isoform have to be analyzed, whereby a representative oc standard has to be prepared.

5.1 Manufacturing of oc standards

There are two possibilities to gain the oc form out of the ccc form: either to expose the DNA to temperature or to use an enzyme. The enzyme (Nt.BstNBI) catalyzes a single-strand nick from 3' end of its nucleotide recognition (5'-GAGTC-3' respectively 3'-CTCAG-5', with single strand break four bases beyond the 3' side of the recognition sequence) (New England Biolabs). As a result each molecule has a different number of nicks. The natural open circular form is relaxed due to only one cut. In contrast, the oc form prepared with an enzyme can have several cuts depending on its base sequence.

5.2 Preparation and verification of the oc standard

In the case of the **pMCP1** there are 10 possible cuts within its sequence, therefore different types of open circular forms exist. The fact that the natural as well as the enzymatic produced oc show the same retention time on PCQ modified silica support material indicates that there is not enough selectivity to distinguish between the two forms and therefore these conditions do not enable separation. So it is assumed that both, the enzymatic and the natural open circular form have the same chromatographic behaviour on the PCQ stationary phase. However, the plasmidic sample (buffer: 20 mM Tris-HCl, pH 7.5) was treated with temperature only in the absence of the enzyme to avoid additional nicks. Without any heating, only a negligible amount of supercoiled pMCP1 was transformed to the open circular form even when the sample was stored over the weekend at room temperature. Subsequently, the sample was exposed to higher temperature whereby an exposition to 55°C for 24 hours was best to gain the highest yield of open circular form avoiding transformation to the linear form. To control the ratio between the isoforms (ccc-oc-lin) and to estimate the concentration, the samples are injected into a HPLC system (see Figure 15)

Table 1: Optimized experimental protocol

Temperature [°C]	Incubation time [h]
55	24
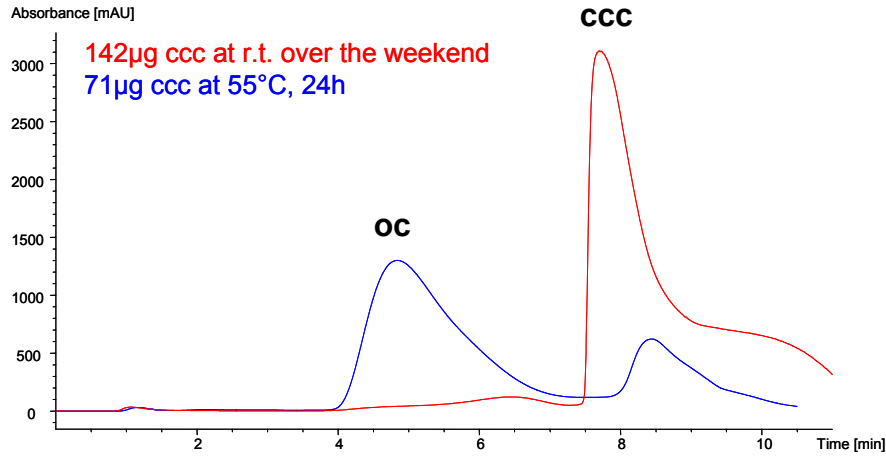
Figure 15: Preparation of the open circular isoform (pMCP1)

Column: Propylcarbamoyl quinine PCQ (5 µm, 100 Å,
   150 x 4 mm ID)
Elution: buffer A: 50 mM phosphate, pH 7.2, buffer B: A + 20%
   IPA pH 7.9, 0-100% buffer B in 15 min
Column temperature: 60°C
Flow rate: 0.7 mL/min

To gain the generated open circular isoform in pure form, the oc peak was isolated chromatographically on an analytical 150 x 4 mm ID PCQ column by injecting six times a sample volume of 100 µL ($c_{origin,pMCP1}$ = 2.84 µg/µL). Afterwards the volume is reduced in a stream of nitrogen. The concentration of the oc sample was determined by comparing the absorbance with those of a calibration set with known concentration. Therefore an empty union was used instead of a chromatographic column and the samples were eluted with an isocratic elution with a flow rate of 0.7 mL/min.
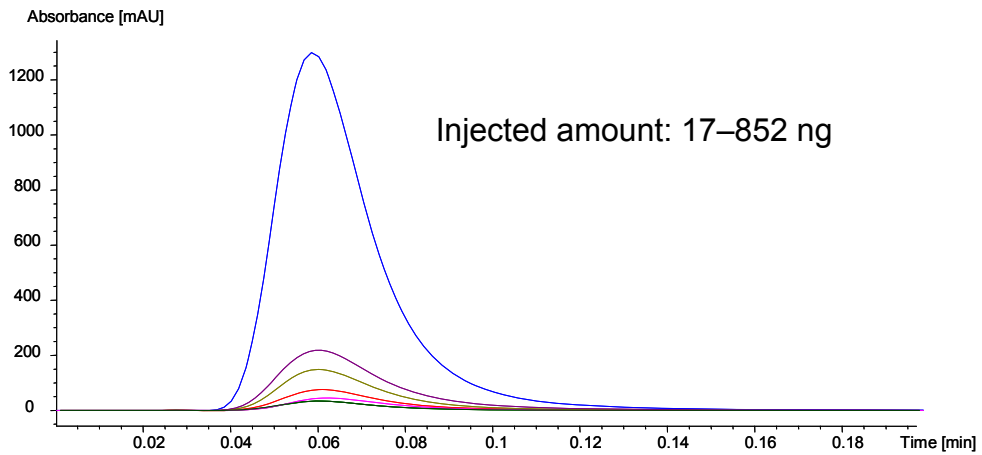
**Figure 16: Absorbance of different amounts of ccc form monitored without column**
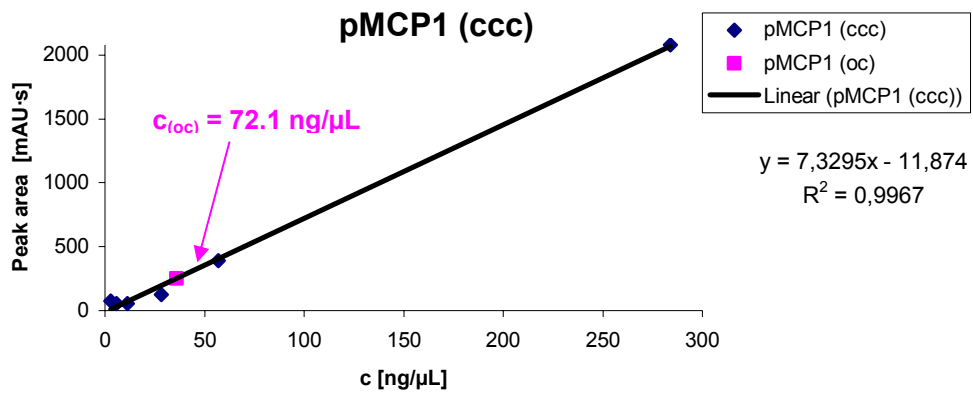
Figure 17: Calibration curve of ccc form

Table 2: Calibration curve and the calculation of the oc-concentration

concentration [ng/µL]	injected amount [ng]	peak area [mAU·s]
284.0	852.0	2079.0
56.8	170.4	391.1
28.4	85.2	124.6
11.4	34.1	55.1
5.7	17.0	55.7
oc sample		
72.1	216.4	503.2

The concentration of the prepared oc standard was determined to be 72.1 ng/µL

In addition the identity of the isolated oc sample was verified with AGE.
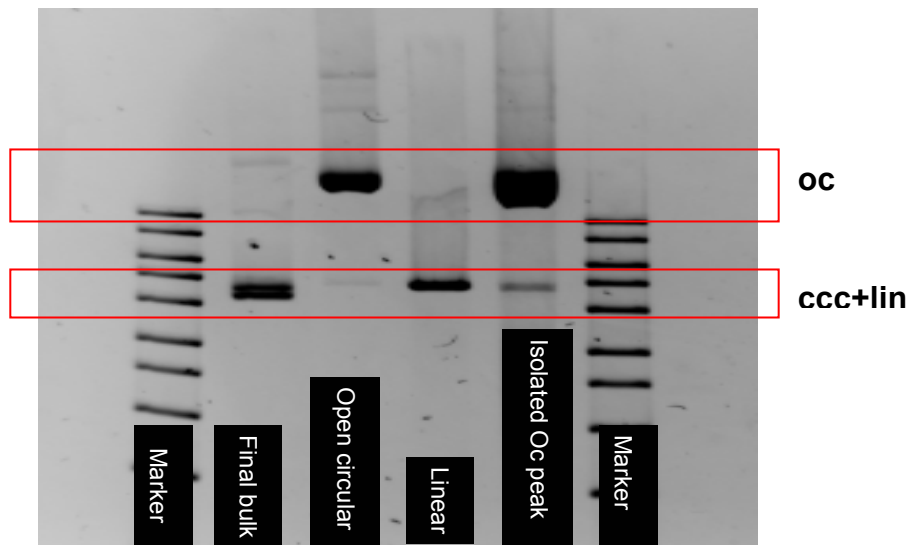
Figure 18: Agarose gel for the verification of the oc standard

0.8% agarose, 1x TBE buffer, applied voltage: 200 V for 2 hours,
Staining: 2 µL EtdBr (10 mg/mL)

The agarose gel reveals one prominent band which can be identified as the open circular form by comparing with standards. The additional band with lower intensity can be assigned to a negligible impurity of the linear form. Furthermore, the linear and the ccc form can not be distinguished, although by adding EtdBr to the gel a separation between the linear and the ccc can be obtained.

Method validation for two different plasmids (pMCP1, pGNA3) with two different stationary phases (propylcarbamoyl quinine modified silica, TSKgel DNA-NPR material) concerning the International Conference on Harmonisation guideline for analytical procedures (ICH guideline) was performed.

6 Method validation for pMCP1 with Propylcarbamoyl quinine modified silica

For confirming the application of the PCQ modified stationary phase for a 4.9 kb plasmid, method validation was performed.

6.1 Equipment and Instruments

The validation measurements are performed using an Agilent 1200 rapid resolution system equipped with a binary pump, a thermostated autosampler (cooled to 4°C) and a diode array UV detector (DAD). All buffer solutions are filtered by a glass filtration unit (Millipore) through a 0.22 µm nylon filter before using.

6.2 Method Information

An AIEX-LC method was developed for the separation and quantification of the ratio of supercoiled, open circular and linear form of pDNA. The gradient with the best results was used:

Column: Propylcarbamoyl quinine on Kromasil (5 µm, 100 Å)
          TMS endcapped (150 x 4 mm ID)
Buffer A: 50 mM phosphate, pH 7.2
Buffer B: 50 mM phosphate, pH 7.9, 20% IPA
0 to 100% buffer B in 15 minutes
Column temperature: 60°C
Flow rate: 0.7 mL/min

DNA can simply be spectrophotometrically quantified by its maximum absorbance at 258 nm whereby 360 nm was used as a reference wavelength. It should be guaranteed that samples do not contain RNA which also absorbs in this region. The purity of double-stranded DNA from protein can be estimated by the 258 nm/280 nm absorbance ratio, which should be between 1.8 and 2.0, because the maximum absorbance for the majority of proteins is at 280 nm (Middaugh, 1998).

6.3   Results and evaluation

Each concentration was measured at least two times in series and the measurements were done starting from the lowest to the highest injected amount to avoid a carry over.

Linearity Range

The linearity range is the concentration range of the calibration function where the signal linearly increases with the concentration. For analytical purposes it is desirable to have a wide linear range.

a. Chromatograms
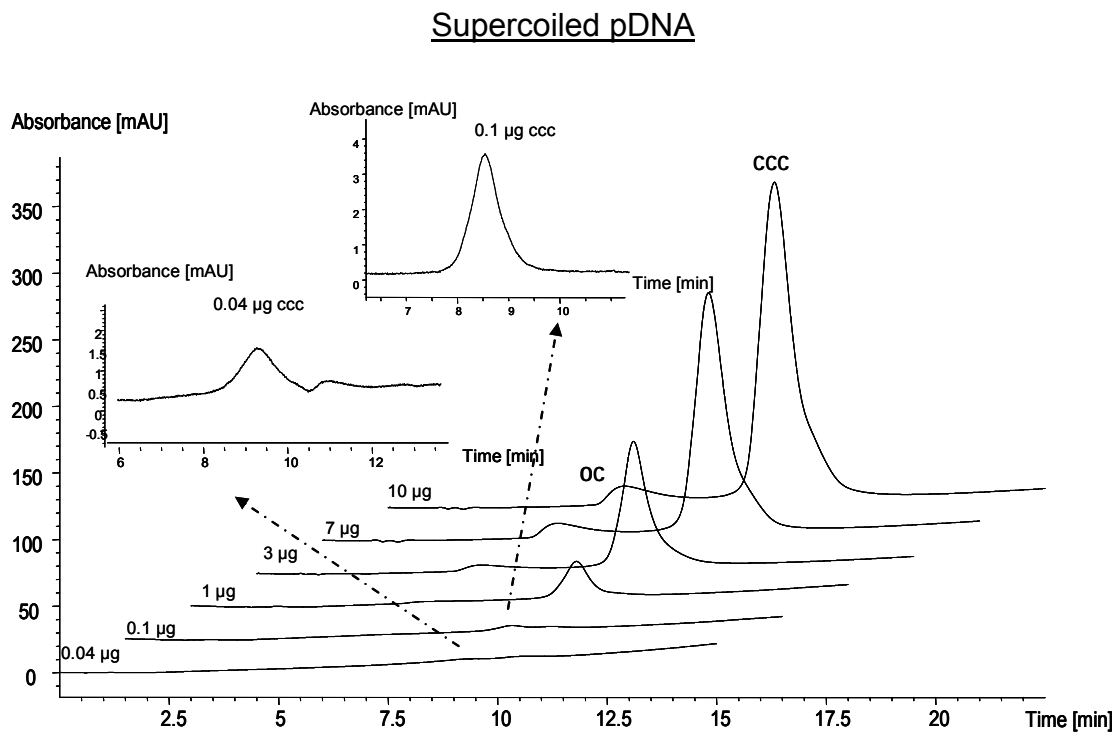
Supercoiled pDNA

Figure 19: Stacked chromatograms of the supercoiled isoform (0.04-10 µg pDNA)
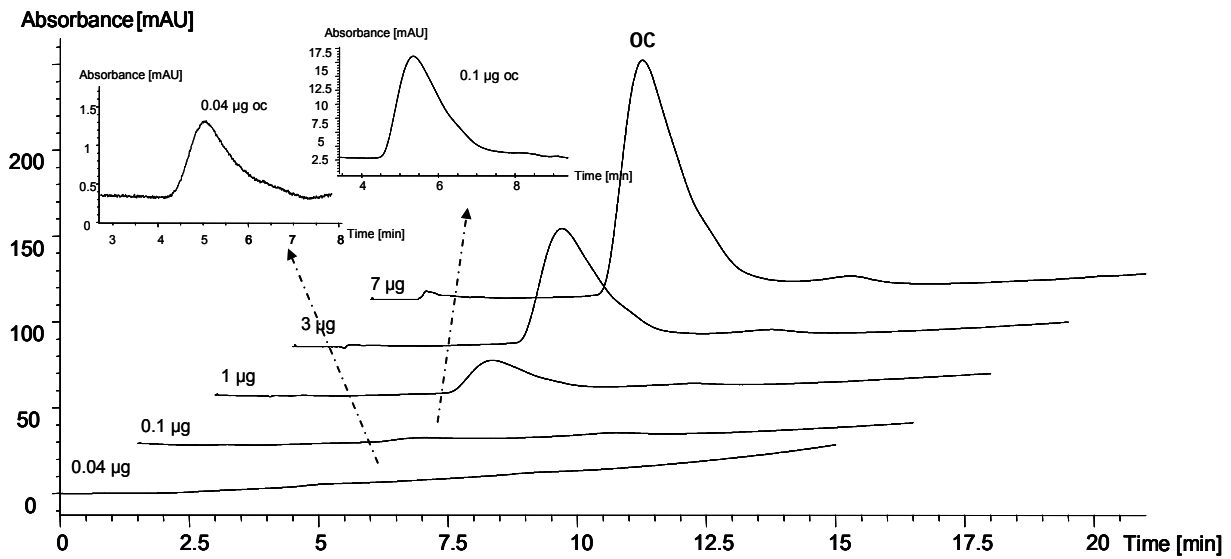
## Open circular pDNA

Figure 20: Stacked chromatograms of the open circular isoform (0.04-7 µg)

Linear pDNA
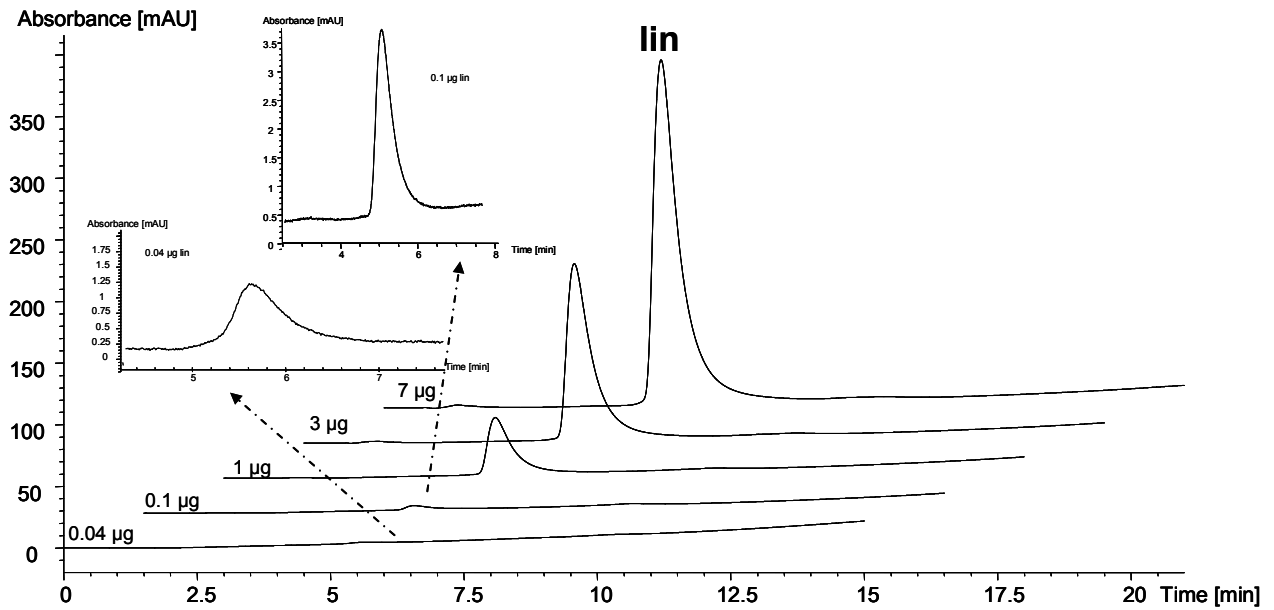
Figure 21: Stacked chromatograms of the linear isoform (0.04-7 µg)

In Figure 19-21, chromatograms with increasing injected amounts within the linearity range for each isoform can be seen.

b. Calculated calibration curves:

If a carry-over phenomenon occurred because of insufficient cleaning steps in-between or irreversible adsorption, the noise was assumed to be the peak area of the blank at the same retention time as the isoform and was subtracted from the peak area signal of the plasmid.

Table 3: Results of the supercoiled plasmid

Sample	Inj. amount [µg]	1st measurement		2nd measurement	
		t_R [min]	A [mAU·s]	t_R [min]	A [mAU·s]
ccc	*0.001*	*8.644*	*11.3*	*8.884*	*14.6*
	0.01	*9.188*	*8.2*	*9.189*	*7.8*
	0.02	*9.29*	*321.4 outlier*	*9.288*	*285. outlier*
	0.04	9.288	42.3	9.262	40.1
	0.1	8.796	70.2	8.793	83.9
	1	8.792	1046.1	8.831	1130.5
	3	8.639	3773	8.638	3802.4
	7	8.821	8027.8	8.812	8363.5
	10	8.821	11464.5	8.84	11436

Based on the calibration curve which is illustrated in Figure 22 it is obvious that a dilution error occurred during the preparation of 0.02 µg plasmid which has therefore to be eliminated in the calibration. According to the results given in Table 3 and in Figure 22, the response is linear in the concentration range from 0.04 to 10 µg plasmid DNA.

1st measurement

$y = 1149.4x + 20.805$
$R^2 = 0.999$

2nd measurement

$y = 1157.9x + 63.088$
$R^2 = 0.9985$
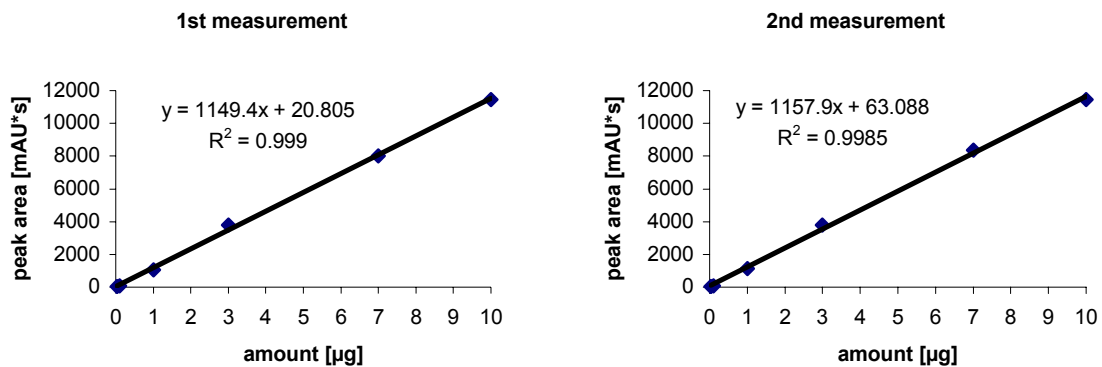
Figure 22: Calibration curve of the ccc isoform (0.04-10 µg plasmid)

Table 4: Results of the open circular plasmid

Sample	Inj. amount [µg]	1st measurement		2nd measurement	
		t_R [min]	A [mAU·s]	t_R [min]	A [mAU·s]
oc	0.001	5.0	2.1	5.0	2.3
	0.01	5.224	6.8	5.228	6.5
	0.04	5.197	44.3	5.178	54.8
	0.1	5.406	104.9	5.401	127
	1	5.429	1406.5	5.337	1436.3
	3	5.327	5174.6	5.328	5246
	7	5.27	10732.1	5.264	10794.8
	10	5.227	18819.7	5.238	18891.9

Comparing peak areas of 7 and 10 µg plasmid, the higher concentrated sample can be estimated as an outlier. The linearity range of the oc form extends from 0.04 to 7 µg oc plasmid.

1st measurement

$y = 1554.8x + 28.398$
$R^2 = 0.9963$

2nd measurement

$y = 1562x + 51.555$
$R^2 = 0.996$
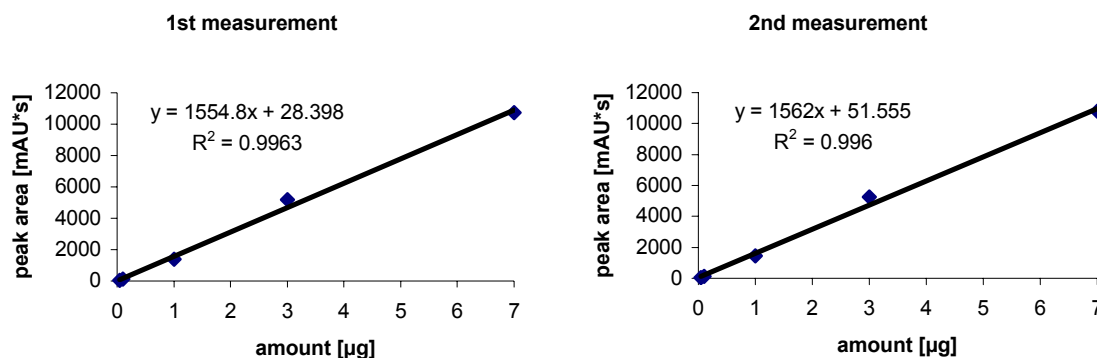
Figure 23: Calibration curve of the oc isoform (0.04 – 7 µg plasmid)

Table 5: Results of the linear plasmid

Sample	Inj. amount [µg]	1st measurement		2nd measurement	
		t_R [min]	A [mAU·s]	t_R [min]	A [mAU·s]
lin	0.001	5.039	1.8	5.012	3.2
	0.01	5.062	11	5.042	10.2
	0.02	5.719	67.4	5.631	57.4
	0.04	5.608	44.5	5.608	37.3
	0.1	5.055	99.6	5.063	102.1
	1	5.085	1421.9	5.083	1421.2
	3	5.058	4324.8	5.044	4260.7
	7	5.193	9839.8	5.179	9858
	10	5.163	15455.2	5.161	15459.3

The linear relation between concentration and peak area exists from 0.04 to 7 µg. The 0.02 µg plasmid sample delivered higher peak areas compared to 0.04 µg which

has therefore to be eliminated in the calibration curve to obtain the lowest coefficient of determination.

1st measurement

$y = 1410.8x + 2.7767$
$R^2 = 0.9998$

2nd measurement

$y = 1412.3x - 10.654$
$R^2 = 1$
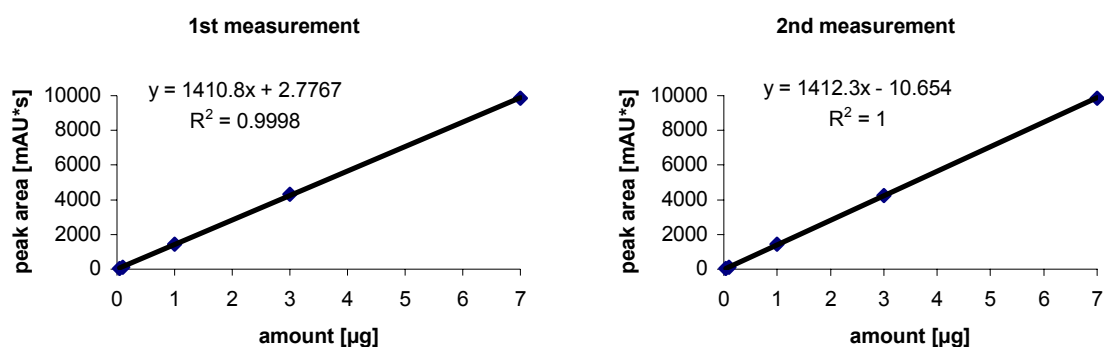
Figure 24: Calibration curve of the lin isoform (0.04-7 µg plasmid)

The similarity of both calibration curves (first and second measurement) for all measurements indicates the high repeatability of those chromatographic results. Moreover, the high degree of linearity is represented through R^2 values greater than 0.99 for all three isoforms in the specified range. These results show that the main issue is the recovery of the open circular form (lowest correlation coefficient). It can be adsorbed at the steel frits, at the fibreglass in the column filter sandwich or irreversibly at the stationary phase. To remove the DNA from the support material a sanitizing step with sodium hydroxide would be advantageous but impossible due to limited pH stability. Thus cleaning was carried out with 3 M sodium chloride.

Determination of the precision (repeatability)

The precision of an analytical procedure expresses the closeness of agreement between a series of measurements obtained from multiple sampling of the same sample under the same operating conditions over a short interval of time. (ICH-Q2(R1), 1994) For the mathematical calculation, the relative standard deviation is used (standard deviation related to the average value in percent.

3 µg of each isoform of pMCP1 were injected 6 times in series with the PCQ-column and the precision (peak area and retention time) was calculated. The values ranged from 0.6 to 1.5% evaluating the peak areas and from 0.06 to 0.32% evaluating the retention time whereby the oc form delivered the lowest precision.

Table 6: Calculated precision (peak area) (n=6; 3 µg injected)

		Peak area [mAU·s]
Supercoiled	**Average value [mAU·s]**	3808.5
	Standard deviation [mAU·s]	21.6
	Relative standard deviation	**0.6%**
Open circular	**Average value [mAU·s]**	5199.9
	Standard deviation [mAU·s]	43.6
	Relative standard deviation	**0.8%**
Linear	**Average value [mAU·s]**	4352.7
	Standard deviation [mAU·s]	66.7
	Relative standard deviation	**1.5%**

Table 7: Calculated precision (retention time) (n=6; 3 µg injected)

		Retention time [min]
Supercoiled	**Average value [min]**	8.78
	Standard deviation [min]	0.01
	Relative standard deviation	**0.07%**
Open circular	**Average value [min]**	5.27
	Standard deviation [min]	0.07
	Relative standard deviation	**1.25%**
Linear	**Average value [min]**	5.20
	Standard deviation [min]	0.00
	Relative standard deviation	**0.06%**
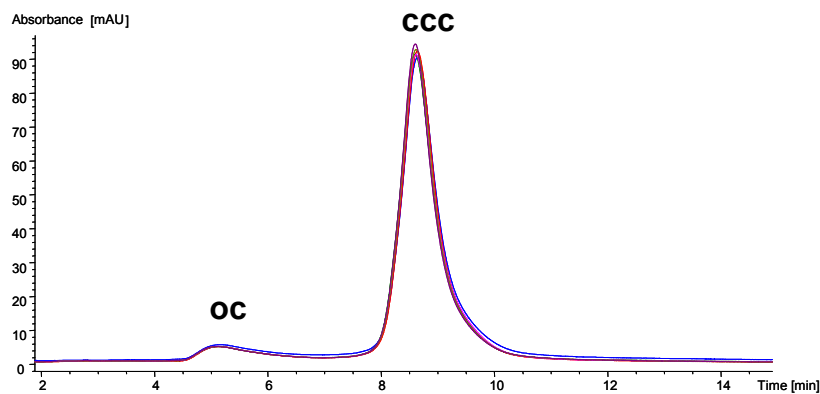
Figure 25: Chromatograms of precision measurements (3 µg) of ccc plasmid
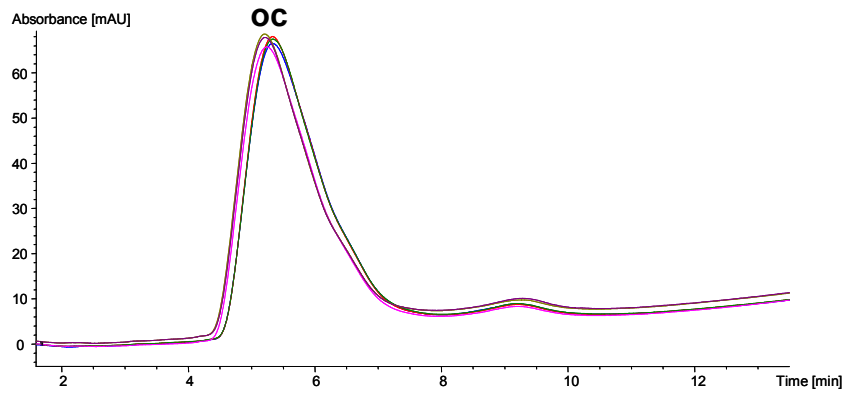
**Figure 26: Chromatograms of precision measurements (3 µg) of oc plasmid**
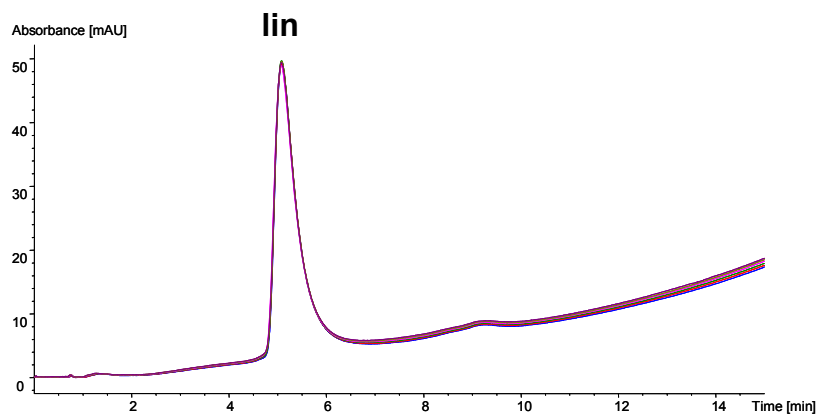
Figure 27: Chromatograms of precision measurements (3 µg) of lin plasmid

As can be seen in Figure 25-27 the propylcarbamoyl quinine modified silica material showed good peak performances and repeatabilities for ccc, oc and linear isoform.
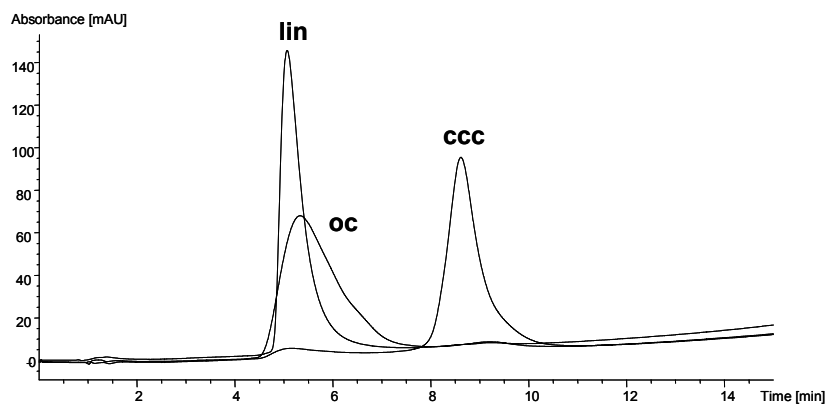

Figure 28: Comparison of ccc, oc and lin isoform (each 3µg)

The comparison of chromatograms of all three isoforms illustrates that there is a good selectivity between the oc and the ccc form, but the open circular and the linear

isoform could only be partial separated due to their similar retention. However, isoforms can influence each other when coexisting resulting in a slight shift of retention time enabling determination.

Determination of the Recovery of the open circular isoform

Insufficient recovery of the oc form is one of the startcomings of state-of-the-art plasmid analysis in AIEX chromatography. Hence it is an important method characteristics for assessment of its performance. Thus, for one purpose recovery was determined as the percentage of the peak areas of the open circular isoform was related to the peak areas of the linear isoform with the same concentration (0.1 µg, 1 µg, 3 µg, 7 µg pDNA). The use of the linear plasmid as reference is based on the fact that it is not irreversibly adsorbed at any part in the HPLC system contrary to the oc isoform and therefore the entire amount of DNA can be recovered in the chromatogram.

The average recovery of the oc pDNA related to the linear isoform in a concentration range from 0.1 µg to 7 µg DNA was **112 ± 9%** (1st measurement: 108 ± 9%, 2nd measurement: 115 ± 9%), whereas the precision measurements delivered a recovery of **119 ± 2%**. Compared to currently employed HPLC methods the recovery of this new method was greatly improved

Table 8: Summary of calculated recoveries

Recovery

Concentration rage:	1st measurement	2nd measurement	Average value
0.1 to 7 µg	108 ± 9%	115 ± 9%	**112 ± 9%**
3µg (precision measurements)	**119 ± 2%**		

Determination of the Limit of Detection / Limit of Quantification

The Limit of detection and quantification are important values to describe the concentration limits of a method.

Limit of Detection (LOD)

The detection limit of an individual analytical procedure is the lowest amount of analyte in a sample which can be detected but not necessarily quantified as an exact value. The LOD can be determined either by visual evaluation or by the usage of an

acceptable signal to noise ratio of 3 to1. Determination of the signal-to-noise ratio is performed by comparing measured signals (peak area at the same retention time) from samples with known low concentrations of analyte with those of blank samples and establishing the minimum concentration at which the analyte can be reliably detected. (ICH-Q2(R1), 1994)

Lower Limit of Quantification (LLOQ)

The quantification limit of an individual analytical procedure is the lowest amount of analyte in a sample which can be quantitatively determined with suitable precision and accuracy. (ICH-Q2(R1), 1994) The LLOQ is determined as the signal which is 10 times higher than the noise.

Comparing peak areas, values for LOD and LLOQ of the isoforms were located between two measurements, thus the concentrations had to be calculated using the calibration curve.

Table 9: Summary of LOD (S:N = 3:1) and LLOQ (S:N = 10:1)

	LOD [µg injected on column] based on S:N=3:1	LLOQ [µg injected on column] based on S:N=10:1
Supercoiled isoform	0.15	0.65
Open circular isoform	0.02	0.06
Linear isoform	0.04	0.05

As can be seen in Table 9 the LOD is about 0.02 to 0.15 µg and the LLOQ between 0.04 and 0.1 µg pDNA.

Upper Limit of Quantification (ULOQ)

The ULOQ is the highest amount of analyte that can be quantified with adequate precision and accuracy. The highest injected amount which is still in the linearity range of the open circular and linear isoform is 7 µg. The highest injected amount for the covalently closed circular isoform was 10 µg which was still in the linear range of the calibration curve. Thus the ULOQ of ccc pDNA is assumed to be 10 µg.

Determination of Impurities

The impurities present in the supercoiled sample are detected determining the content of open circular and linear DNA using spiked samples.
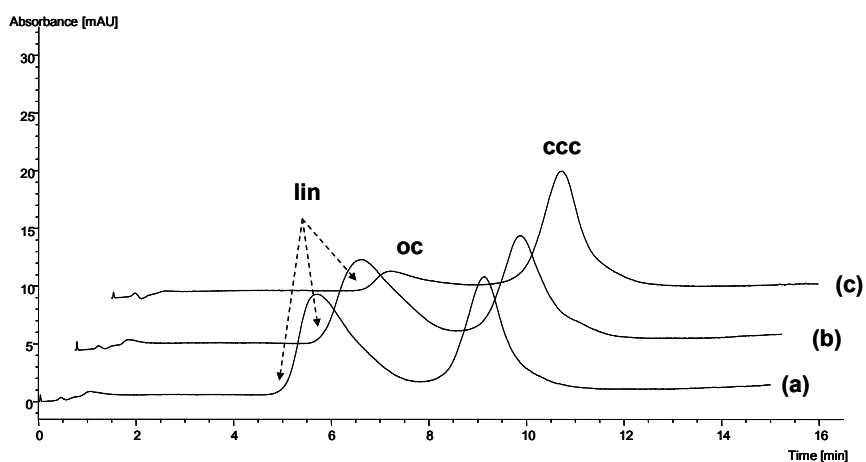
Figure 29: Chromatograms of different spiked samples

    a)   sample no 1: 0.5 µg ccc, 0.5 µg oc, 0.05 µg lin

    b)   sample no 2: 0.5 µg ccc, 0.5 µg oc, 0.01 µg lin

    c)   sample no 3: 0.5 µg ccc, 0.05 µg oc, 0.01 µg lin

As it can be seen above, impurities of 0.06 µg (11%) of oc and lin form can be still detected in the presence of 0.5 µg supercoiled plasmid. Additionally, the calculated peak area ratio was compared with the recovered ratio.

Table 10: Comparison of injected and recovered peak ratio

Sample no.	Injected amount on column	Recovered ratio of peak areas
1	47.6% (ccc) 52.4% (oc+lin)	47.8% (ccc) 52.2%(oc+lin)
2	49.5% (ccc) 50.5%(oc+lin)	50% (ccc) 50% (oc+lin)
3	87.7% (ccc) 12.3% (oc+lin)	89.3%(ccc) 10.7%(oc+lin)

As it can be seen in Table 10, the recovered peak area ratios match perfectly with the injected amounts.

Table 11: Calculation of impurities using calibration curves

Sample no	Spiked impurities	Calculated impurities	Recovery
1	0.5 µg ccc	0.44 µg ± 9.2% (ccc)	88% (ccc)
	0.55 µg oc+lin	0.47 µg ± 9.5% (oc+lin)	85.5% (oc+lin)
2	0.5 µg ccc	0.40 µg ± 9.9% (ccc)	80% (ccc)
	0.51 µg oc+lin	0.39 µg ± 10% (oc+lin)	76.5% (oc+lin)
3	0.5 µg ccc	0.38 µg ± 10%(ccc)	76% (ccc)
	0.06 µg oc+lin	0.05 µg ± 45% (oc, lin)	93.3% (oc+lin)

The concentration of impurity was recalculated using the peak area and the related calibration curve (Figure 22-Figure 24) to demonstrate the suitability of the validation.

Furthermore, the recovery of supercoiled form existing in the spiked sample related to the calibration curve of the validation was **81 ± 6%**. Furthermore the calculation of the recovery of the other two isoforms was quite difficult because they were not separated respectively differentiation between them was not possible because of the relative low amount of linear besides the oc form. Therefore the both isoforms were calculated together resulting in a recovery of **85 ± 8%**.

7 Method validation for pMCP1 with TSK-Gel® DNA-NPR

The 4.9 kb plasmid had to be validated with the commercial available DNA-NPR stationary phase.

7.1 Equipment and Instruments

The same system as for validation with the PCQ column was used (see chapter 6 Method validation for pMCP1 with Propylcarbamoyl quinine modified silica page 32)

7.2 Method Information

The following method was used was.

> Column: TSK-Gel® DNA-NPR (750 x 4.6 mm ID, 2.5 µm)
>
> Buffer A: 20 mM Tris-HCl, pH 9.0
>
> Buffer B: 20 mM Tris-HCl, 1M NaCl, pH 9.0
>
> 50 to 75% buffer B in 5 minutes
>
> 50% buffer B for 0.5 minutes for re-equilibration
>
> Column temperature: 25°C
>
> Flow rate: 0.7 mL/min

The plasmidic DNA was quantified with a UV diode array detector at 258 nm whereby 360 nm was used as reference wave length.

7.3 Results and evaluation

Each sample (0.001–7 µg pDNA) was measured at least two times in series and the measurements were done from the lowest to the highest injected amount to avoid a carry over.

Linearity Range

In Figure 30-32 chromatograms of ccc, oc and lin isoform are represented with increasing sample injections. While the ccc form provides reasonable peak shape over the entire studied concentration range, oc and lin forms reveal poor peak shapes with splitted peak. Also the linear range is narrower for oc and lin form (see Table 12-14). Overall the performance in terms of linearity appears to be worse than for the measurements with PCQ.

a. Chromatograms:

All chromatograms were measured with increasing injected amounts to minimize carry over phenomena. The isoforms were analyzed in following order: ccc, oc, lin.

<u>Supercoiled pDNA</u>
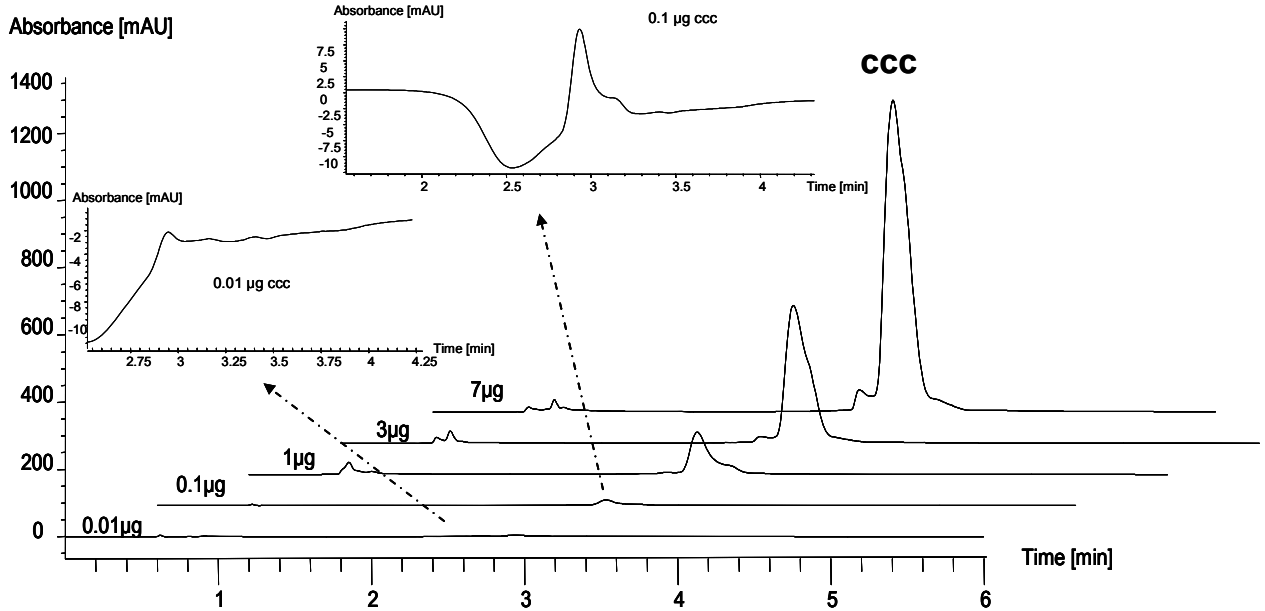
Figure 30: Stacked chromatograms of the supercoiled isoform (0.01-7 µg)
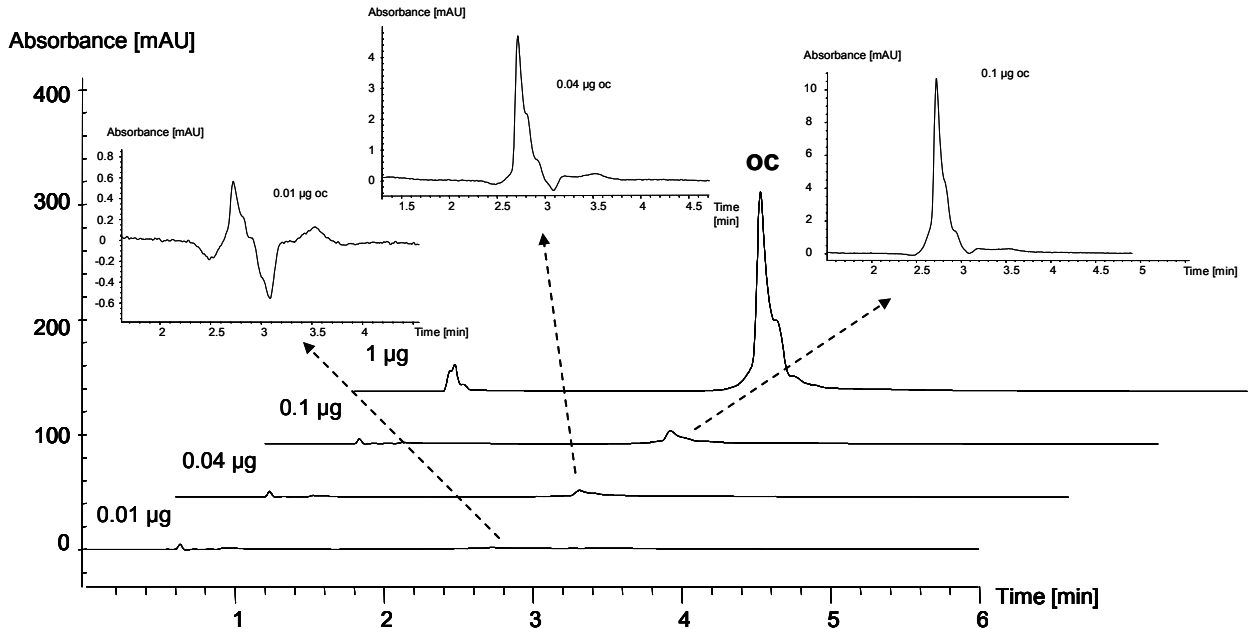

Figure 31: Stacked chromatograms of the open circular supercoiled isoform (0.01-1 µg)
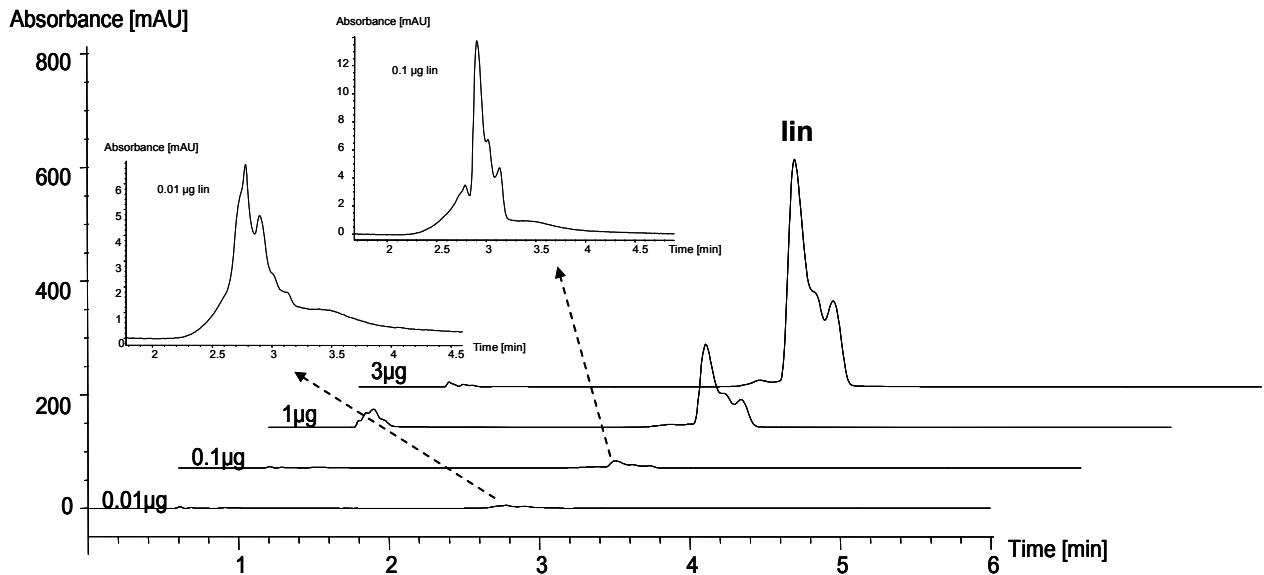
Figure 32: Stacked chromatograms of the linear isoform (0.01-3 µg)

Figure 30-32 illustrate the linear relation between the peak area and injected amount for ccc, oc and lin isoform.

b. Calculated calibration curves:

For determination of the linearity range for each isoform the linear relation between the peak area and injected amount was evaluated.

Table 12: Results of the supercoiled plasmid

Sample	Inj. amount [µg]	1st measurement		2nd measurement	
		t_R [min]	A [mAU·s]	t_R [min]	A [mAU·s]
ccc	0.001	3.201	2.1	3.20	2.9
	0.01	2.94	15.9	2.94	14.7
	0.1	2.932	119.5	2.93	124.0
	1	2.927	1040.4	2.93	1033.6
	3	2.952	3633.4	2.95	3636.4
	7	3.007	8574.6	2.99	8824.3
	10	2.983	13544.8	-	-

The injected amounts 0.001 and 10 µg supercoiled plasmid had to be excluded because they are beyond the linear dependence of the signal on the concentration. Thus, the linearity range extends from 0.01 to 7 µg plasmid.
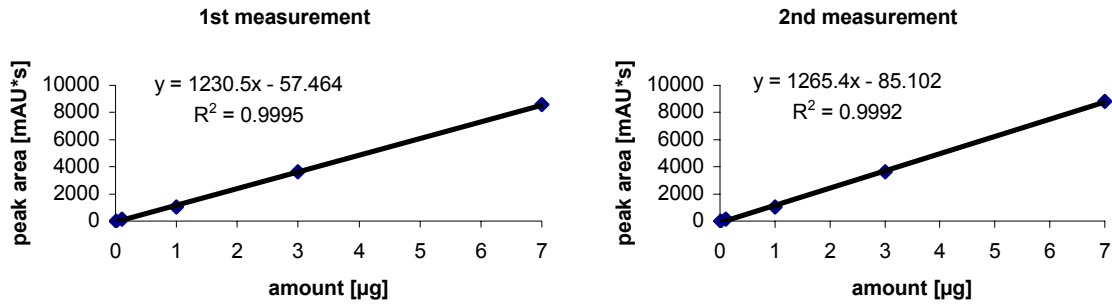
Figure 33: Calibration curve of the ccc-isoform (0.01-7 µg plasmid)

Table 13: Results of the open circular plasmid

Sample	Inj. amount [µg]	1st measurement		2nd measurement	
		t_R [min]	A [mAU·s]	t_R [min]	A [mAU·s]
	0.001	2.71	1.24	2.72	1.01
	0.01	2.72	3.18	2.72	3.41
	0.04	2.714	24.32	2.73	26.63
Oc	0.1	2.72	58.82	2.73	80.02
	1	2.73	838.50	2.73	852.85
	3	2.79	1870.48	2.80	1903.01
	7	2.84	2112.7	2.82	2681.1
	10	2.80	4933.5	-	-

As it can be seen in Table 13 and Figure 34, the response (peak area) of the injected amounts from 0.01 to 1 µg behave in a linear way thus this concentration range it can be assumed to be the linearity range.
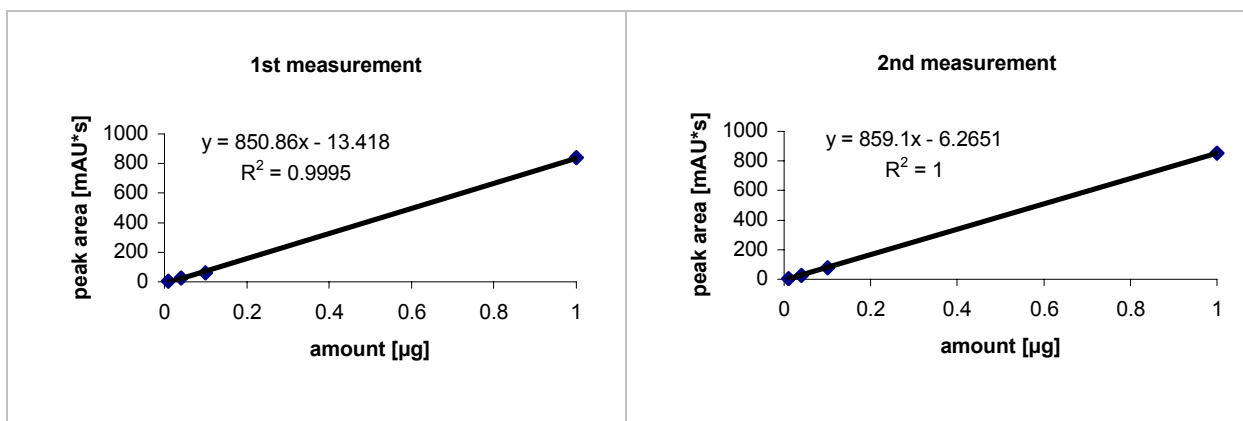
Figure 34: Calibration curve of the oc-isoform (0.01-1 µg plasmid)

Table 14: Results of the linear plasmid

Sample	Inj. amount [µg]	1st measurement		2nd measurement	
		t_R [min]	A [mAU·s]	t_R [min]	A [mAU·s]
lin	0.001	2.93	9.31	2.92	8.74
	0.01	2.92	9.38	2.92	12.39
	0.1	2.90	37.84	2.90	38.33
	1	2.91	944.10	2.90	928.97
	3	2.90	3088.87	2.90	3207.21
	7	2.98	6300.03	2.97	6295.18
	10	2.96	10623.3	2.96	10508.3

In the range from 0.01 to 3 µg injected plasmid, the resulted peak area corresponds linearly to the amount.

1st measurement

$y = 1040.6x - 49.198$
$R^2 = 0.9992$

2nd measurement

$y = 1080.4x - 63.415$
$R^2 = 0.9981$
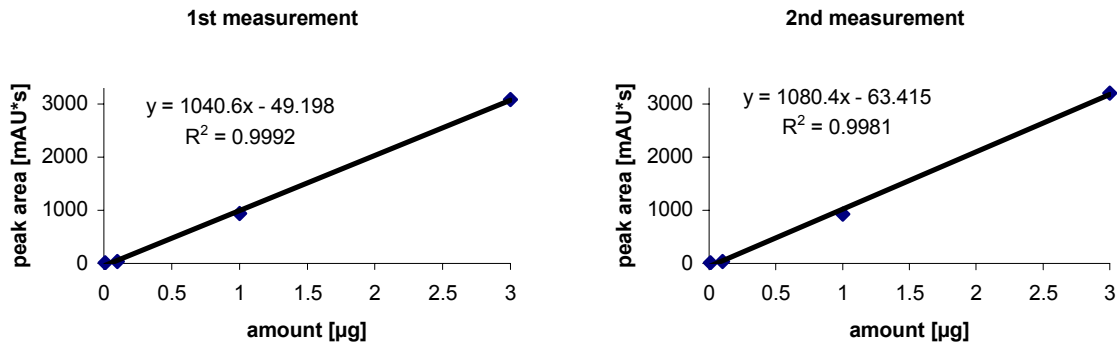
Figure 35: Calibration curve of the lin isoform (0.01-3 µg plasmid)

Determination of the precision (repeatability)

For the definition of precision see page 34.

3 µg of each isoform of pMCP1 were injected 6 times with the DNA-NPR-column and the precision concerning both peak area and retention time was calculated. Precision was between 0.8 and 6.4% concerning the peak area with the highest imprecision for the oc form and 0.2 to 1% concerning the retention time.

Table 15: Calculated precision (peak area) (n=6; 3 µg injected)

		Peak area [mAU·s]
Supercoiled	**Average value [mAU·s]**	3591.2
	Standard deviation [mAU·s]	28.2
	Relative standard deviation	**0.8%**
Open circular	**Average value [mAU·s]**	1847.7
	Standard deviation [mAU·s]	119
	Relative standard deviation	**6.4%**
Linear	**Average value [mAU·s]**	3113.5
	Standard deviation [mAU·s]	64.2
	Relative standard deviation	**2.1%**

Table 16: Calculated precision (retention time) (n=6; 3 µg injected)

		Retention time [min]
Supercoiled	**Average value [min]**	2.95
	Standard deviation [min]	0.03
	Relative standard deviation	**0.98%**
Open circular	**Average value [min]**	2.72
	Standard deviation [min]	0.01
	Relative standard deviation	**0.20%**
Linear	**Average value [min]**	2.90
	Standard deviation [min]	0.01
	Relative standard deviation	**0.30%**
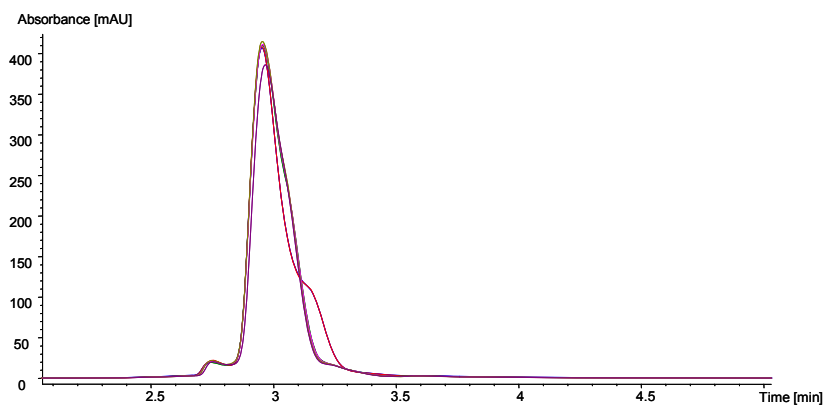
Figure 36: Chromatograms of precision measurements (3 µg) of ccc plasmid
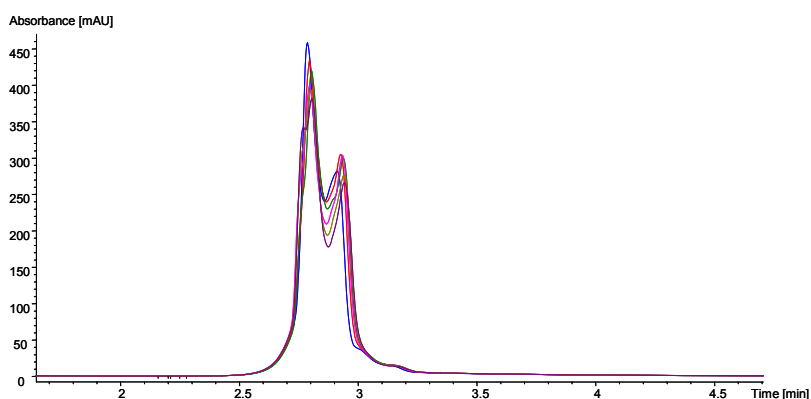
Figure 37: Chromatograms of precision measurements (3 µg) of oc plasmid
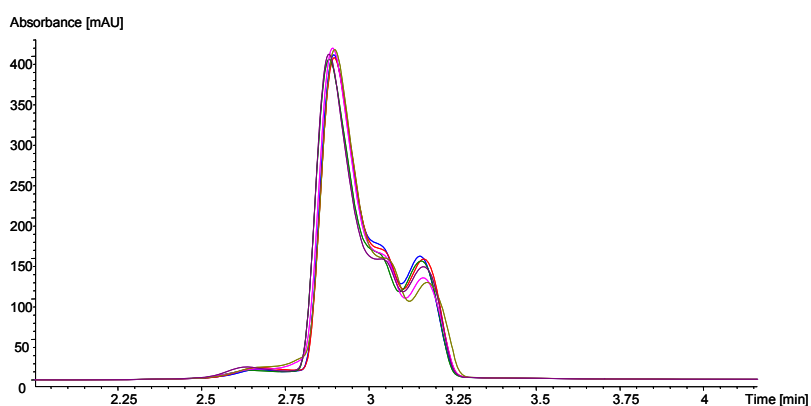
Figure 38: Chromatograms of precision measurements (3 µg) of lin plasmid

Figure 36-38 show the repeatability of the used method as well as the poor peak shape (splitted peaks). Furthermore, by comparing the retention times of linear and ccc form, it is obvious that they coelute as a result of insufficient selectivity.

Determination of the Recovery of the open circular isoform

To determine the recovery, the peak areas over the concentration range of 0.01 µg to 3 µg pDNA are compared to those of the linear isoform. The average recovery of the oc pDNA related to the linear isoform in a concentration range from 0.01 µg to 3 µg DNA is **60 ± 28%** (1st measurement: 61 ± 29%, 2nd measurement: 60 ± 28%), whereas the precision measurements (at 3 µg) deliver **51 ± 6%** recovery.

Table 17: Summary of calculated recoveries

	Recovery		
Concentration rage:	1st measurement	2nd measurement	Average value
0.01 to 3 µg	61 ± 29%	60 ± 28%	**60 ± 28%**
3 µg (precision measurements)	**51 ± 6%**		

Determination of the Limit of Detection / Limit of Quantification

Irreversibly adsorbed analyte can cause an absorption signal which has to be subtracted from the measured signal. This additional peak area was set as blank value or so-called noise.

Limit of Detection (LOD)

For the definition of Limit of Detection (LOD) see page 37.

Lower Limit of Quantification (LLOQ)

For the definition of Lower Limit of Quantification see page 38.

As can be seen from Table 18, the LOD is about 0.3 to 0.4 µg and the LLOQ between 0.04 and 0.1 µg on column for all isoforms.

Table 18: Summary of LOD (S:N = 3:1) and LOQ (S:N = 10:1)

	LOD [µg on column] Based on S:N=3:1	LLOQ [µg on column] Based on S:N=10:1
Supercoiled pDNA	0.3	0.7
Open circular pDNA	0.3	0.7
Linear pDNA	0.4	1.5

The values for both limits had to be calculated using the calibration curves for each isoform, because the limits were located between two injected amounts: 0.1 - 1 µg for ccc and oc and 1 - 3 µg linear form.

Upper Limit of Quantification (ULOQ)

For the definition of Upper Limit of Quantification (ULOQ) see page 38.

The ULOQ is determined by the highest injected amount which is still in the linear range. Hence the ULOQ of the supercoiled isoform corresponds to 7 µg, of the open circular isoform to 1 µg and of the linear isoform to 3 µg.

8 Comparison of method performance of propylcarbamoyl quinine modified silica and TSK-Gel® DNA-NPR material

8.1 Results: Summary and Comparison

The novel method for pDNA analysis based on the PCQ column is supposed to replace the state-of-the-art method employing the DNA-NPR column if the method characteristics outperforms the one of the better. Hence, the results of the method validations are summarized and compared again.

Linearity Range

In Table 19 above, an overview of the linearity ranges of PCQ respectively DNA-NPR for each isoform is given.

Table 19: Comparison of linearity ranges and coefficient of determination

	PCQ	DNA-NPR
ccc	0.1 – 7 µg R² 0.9985	0.01 – 7 µg R² 0.9994
oc	0.04 – 7 µg R² 0.9962	0.01 – 1 µg R² 0.9998
lin	0.04 – 7 µg R² 0.9999	0.01 – 3 µg R² 0.9987

The data show that the linearity range is equal or slightly wider for DNA-NPR. However, the possible sample loading of plasmid DNA of the new propylcarbamoyl quinine modified silica is higher compared to the commercial available column. Thus the chromatographic material is more suitable for semi-preparative applications.

Peak area and retention time precision

Six measurements of 3 µg plasmid (ccc, oc, lin) were performed with both columns and compared in Table 20.

Table 20: Comparison of peak area precision (n=6; 3µg injected)

	PCQ	DNA-NPR
ccc	0.6%	0.78%
oc	0.8%	6.4%
lin	1.5%	2.1%

Table 21: Comparison of retention time precision (n=6; 3µg injected)

	PCQ	DNA-NPR
ccc	0.07%	0.98%
oc	1.25%	0.20%
lin	0.06%	0.30%

The precision represents the variation of the signal (peak area or retention time) at a certain amount of pDNA. As can be seen from Table 20 and Table 21 the PCQ material yielded better precisions than the DNA-NPR material. This conclusion applies for all three isoforms, especially for the oc isoform being the most prominent and critical impurity.

Recovery of oc isoform (related to the linear isoform)

In following table, the recoveries of the PCQ and DNA-NPR column are illustrated.

Table 22: Comparison of oc recovery

PCQ	DNA-NPR
112 ± 9% (0.1-10 µg)	60 ± 28% (0.01-3 µg)
119 ± 2% (3 µg)	51 ± 6% (3 µg)

The recovery of the oc isoform is better in the case of the PCQ material compared to the DNA-NPR. A part of the oc form, when injected onto the Tosoh material, does not elute from the column under the chosen conditions. With DNA-NPR the recovery was only ~ 60% in the concentration range from 0.01 – 3 µg and ~ 50% at 3µg injections, while the recovery was quantitative with the PCQ column was between 112 and 119%.

Sensitivity

The detection limit (LOD) and the quantification limit (LOQ) were determined according to the signal to noise ratio 3:1 and 10:1.

Table 23: Comparison of LOD, LLOQ and ULOQ (µg pDNA injected on column)

		PCQ	DNA-NPR
ccc	LOD	0.15 µg	0.3 µg
	LLOQ	0.65 µg	0.7 µg
	ULOQ	10 µg	7 µg
oc	LOD	0.02 µg	0.3 µg
	LLOQ	0.06 µg	0.7 µg
	ULOQ	7 µg	1 µg
lin	LOD	0.04 µg	0.4 µg
	LLOQ	0.05 µg	1.5 µg
	ULOQ	7 µg	3 µg

As it can be seen from Table 23, the detection and quantification limits were better using the PCQ than the DNA-NPR column. Thus using the modified quinine silica material, lower amounts and therefore lower contents of impurities can be detected and quantified. Based on these results it may be concluded that the quinine material shows better performance in impurity determinations of plasmidic DNA.

8.2   Conclusion

The in-house produced and packed quinine modified column should be favoured for analytical purposes based on the results above. It is evident that the quantification performance as well as the selectivity is slightly better compared to the TSK® gel DNA-NPR column. With the better, only a slight separation of oc and ccc form can be seen in the chromatogram of spiked samples. Nevertheless, the Tosoh DNA-NPR can not separate the lin and ccc isoform which is the biggest disadvantage.

In sharp contrast, the PCQ phase shows large separation factors both between oc and ccc as well as between linear and ccc forms. However, the linear and oc form coelute in case of the 4.5 kbp plasmid of pMCP1. Hence, the determined impurity represents the summ of oc and lin form. All those parameters confirm that for validation of smaller plasmids (molecular size around 5 kb) the new, self-prepared material has a greater benefit.

9 Method validation for pGNA3 with propylcarbamoyl quinine modified silica

9.1 Preparation and verification of the oc standard

In the case of the **pGNA3** (14.9 kbp), a treatment of different temperatures (35 to 55°C) for different time periods (up to 65 hours) was carried out but without satisfying results. In a first set of experiments there was almost no transformation of ccc to the oc isoforms, whereas in a second set of experiments a mixture of different forms or fragments of DNA arose from the supercoiled isoform resulting in a broad peak. To avoid degradation of the DNA, 55°C was found to be the highest temperature which should be used for the oc preparation.
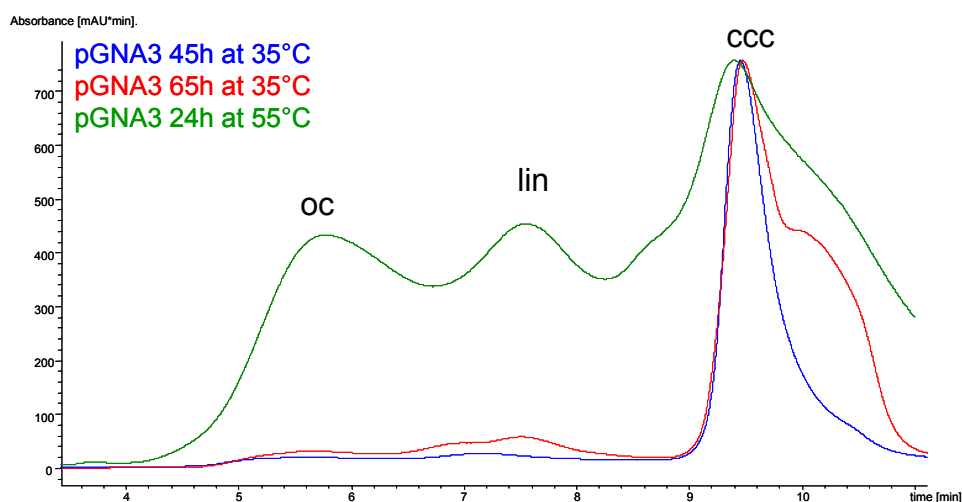
Figure 39: Chromatogram of different temperature treated ccc pGNA3

Column: propylcarbamoyl-quinine PCQ (based on Kromasil, 100 Å, 5 µm)
Column dimension: 150 x 4 mm ID
Buffer A: 50 mM phosphate, pH 7.2, Buffer B: A + 20% IPA, pH 7.9, 0-100%
buffer B in 15 min, column temperature: 60°C, flow rate: 0.7 mL/min

Due to the lack of success with temperature induced nicking, an enzymatic reaction for producing the open circular isoform was used. Because of the base sequence there are 21 possible cuts when using the Nt.BstNBI enzyme (see page 28), which results in a diversity of open circular isoforms. When using this enzyme it is necessary to find the optimum of incubation time and enzyme units per µg ccc pDNA to be sure that the transformation to the oc isoform is completed. To produce an open circular isoform similar to the natural one with one single strand break the

digestion has to be incomplete; otherwise several nicks in the DNA strain would occur.

Definition of one unit: "One unit is defined as the amount of enzyme required to digest 1 µg T7 DNA (substrate for assaying the activity because of the proximity of GAGTC sequences) in 1 hour at 55°C in a total reaction volume of 50 µL" (http://www.neb.com).

To stop this reaction the enzyme has to be inactivated. Therefore either the solution has to be heated to 80°C for 20 minutes or by adding EDTA. The higher the incubation temperature, the more fragments are produced hence the prepared sample has to be purified. All parameters concerning this enzymatic reaction have to be optimized for each molecule because it depends on the molecule size and its sequence. The NE buffer 3 (100 mM NaCl, 50 mM Tris-HCl, 10 mM $MgCl_2$, 1 mM Dithiothreitol, pH 7.9) provided from New England Biolabs ensures optimal activity (100%) of the enzyme.

Test series with 0.01, 0.1 and 1 Unit enzyme per µg pDNA and with different incubation times (1-10 min) at 40°C were carried out. The enzymatic reactions were stopped with 10 mM EDTA and afterwards checked with AGE. It was observed that 1 Unit enzyme per µg DNA and 1 minute incubation time are the best choice, because the entire supercoiled plasmid is changed to the open circular isoform and only a little amount of linear plasmid is generated. Subsequently, the mixture (1 U/µg pDNA, ccc pDNA, NE buffer 3) was incubated for 1 minute at 40°C by using a thermo mixer (Eppendorf) and then the enzymatic reaction was stopped by adding 10 mM EDTA. The successful generation of open circular plasmid was verified with AGE and then isolated with HPLC (PCQ, 150 x 4 mm ID column).

Table 24: Summary of test series

Unit enzyme/ µg pDNA	Incubation time [min]	Temperature [°C]	EDTA (c=10 mM)
0.01	1	40	75 µL
0.01	5	40	75 µL
0.01	10	40	75 µL
0.1	1	40	75 µL
0.1	5	40	75 µL
0.1	10	40	75 µL
1	1	40	75 µL
1	5	40	75 µL
1	10	40	75 µL

Figure 40: Chromatogram after the enzymatic reaction

Column: Propylcarbamoyl quinine PCQ (based on Kromasil, 100 Å, 5 µm)
Column dimension: 150 x 4 mm ID
Buffer A: 50 mM phosphate, pH 7.2, Buffer B: A + 20% IPA, pH 7.9, 0-100%
buffer B in 15 min, column temperature: 60°C, flow rate: 0.7 mL/min

Peak areas used for the calibration curve were monitored without column because of irrelevant retention times. The signals from the calibration standards (ccc) were compared with the signal of the oc form concluding its concentration. However, ccc form was used as standards because of its good recovery.
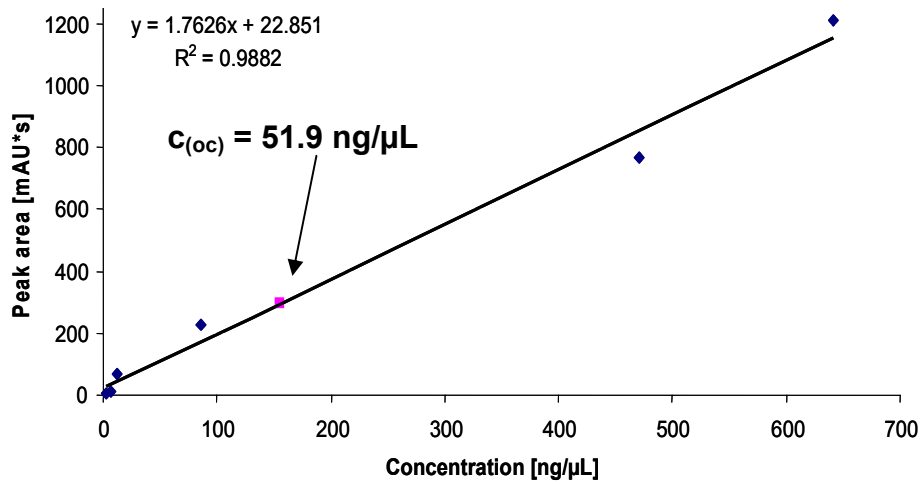
Figure 41: Calibration curve of ccc form (pGNA3)

Table 25: Calibration curve and the calculation of the oc concentration

Concentration [ng/µL]	Injected amount [ng]	Peakarea [mAU*min]
214	642	1210.5
157	471	692.2
28.5	85.6	106.4
4.3	12.8	51.1
2.1	6.4	13.9
oc sample		
51.9	156.0	297.2

As can be seen in Figure 41 and Table 25 a concentration of 51.9 ng/µL oc plasmid based on the ccc isoform calibration curve was determined.
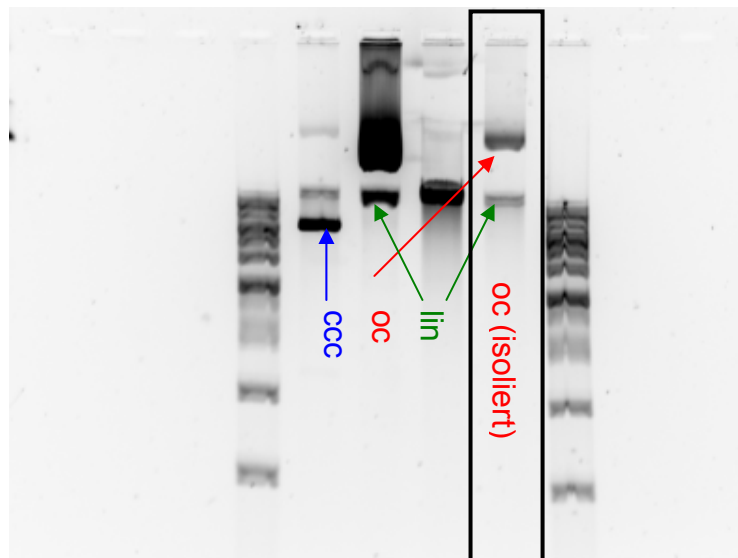
Figure 42: Agarose gel for the verification of the oc standard

0.75% agarose, 1x TBE buffer, applied voltage: 120V for 3 hours,
Staining: 20µL Sybr gold® (provided from Invitrogen) in gel

Figure 42 depicts the AGE gel of the isolated oc standard. It can be seen that the prepared oc standard contains no supercoiled pDNA and only a small amount of the linear isoform. As a result, the conditions used for the enzymatic reaction (1U/µg pDNA, 1 min at 40°C) were confirmed to be practicable.

9.2 Equipment and Instruments

The same system as for the previous validation was used (see chapter 6 Method validation for pMCP1 with Propylcarbamoyl quinine modified silica page 32).

9.3 Method Information

For the separation of the isoforms the standard gradient for propylcarbamoyl quinine modified silica material was used:

Column: Propylcarbamoyl quinine on Kromasil 5 µm
100 Å, TMS endcapped
Buffer A: 50 mM phosphate, pH 7.2
Buffer B: 50 mM phosphate, pH 7.9, 20% IPA
0 to 100% buffer B in 15 minutes
Column temperature: 60°C
Flow rate: 0.7 mL/min

The plasmidic DNA was quantified with a UV diode array detector at 258nm. As reference wave length, 360 nm was used.

9.4 Results and evaluation

Amounts from 0.001 to 10 µg pDNA were measured whereby each measurement was repeated at least once.

Linearity Range

Increasing quantities of each plasmid isoform were injected (see Figure 43-45) and the resultant peak areas plotted against the injected amount to obtain calibration functions as shown in Figure 46-48). The range where this calibration function is linear was determined and the results are given in Table 26-28). As can be seen from Figure 44, the oc form splits into two peaks and for the calibration function the peak

area of the sum of these two peaks was utilized. Linear ranges were found between 0.04 – 10 µg (ccc, lin) and 0.01 – 3 µg (oc). It is also seen that the repeatability of the calibration function is satisfactory.

a. Chromatograms
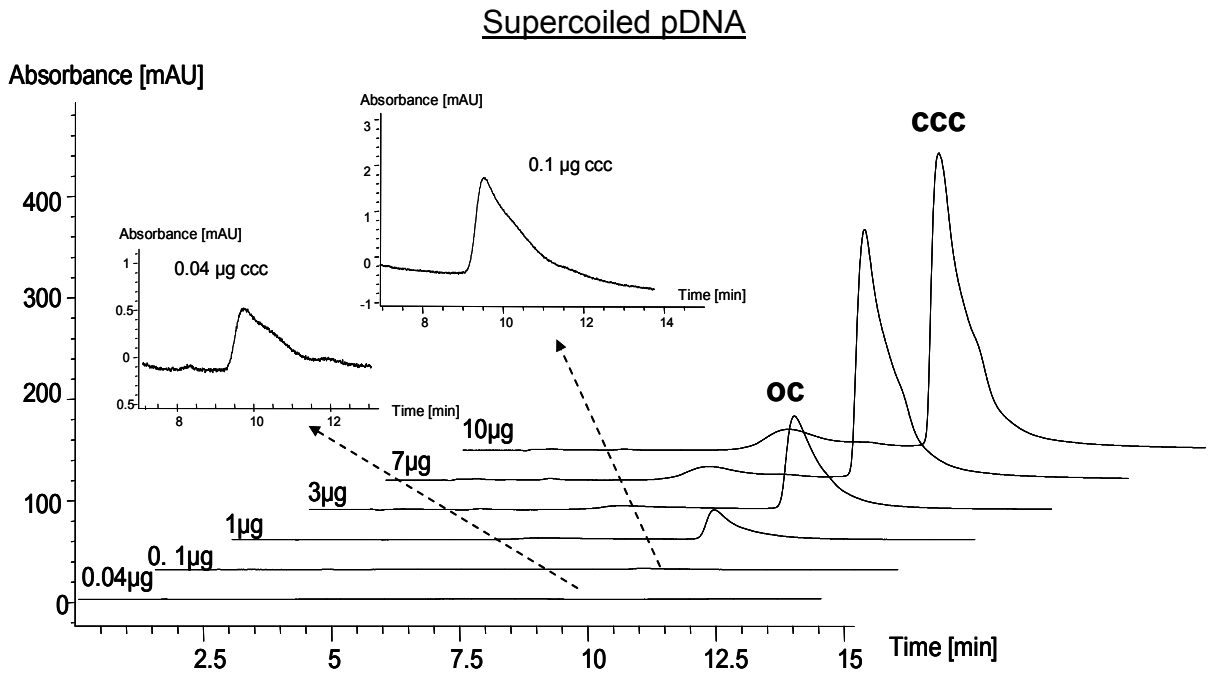
Supercoiled pDNA

Figure 43: Stacked chromatograms of the supercoiled isoform (0.04-10 µg pDNA)
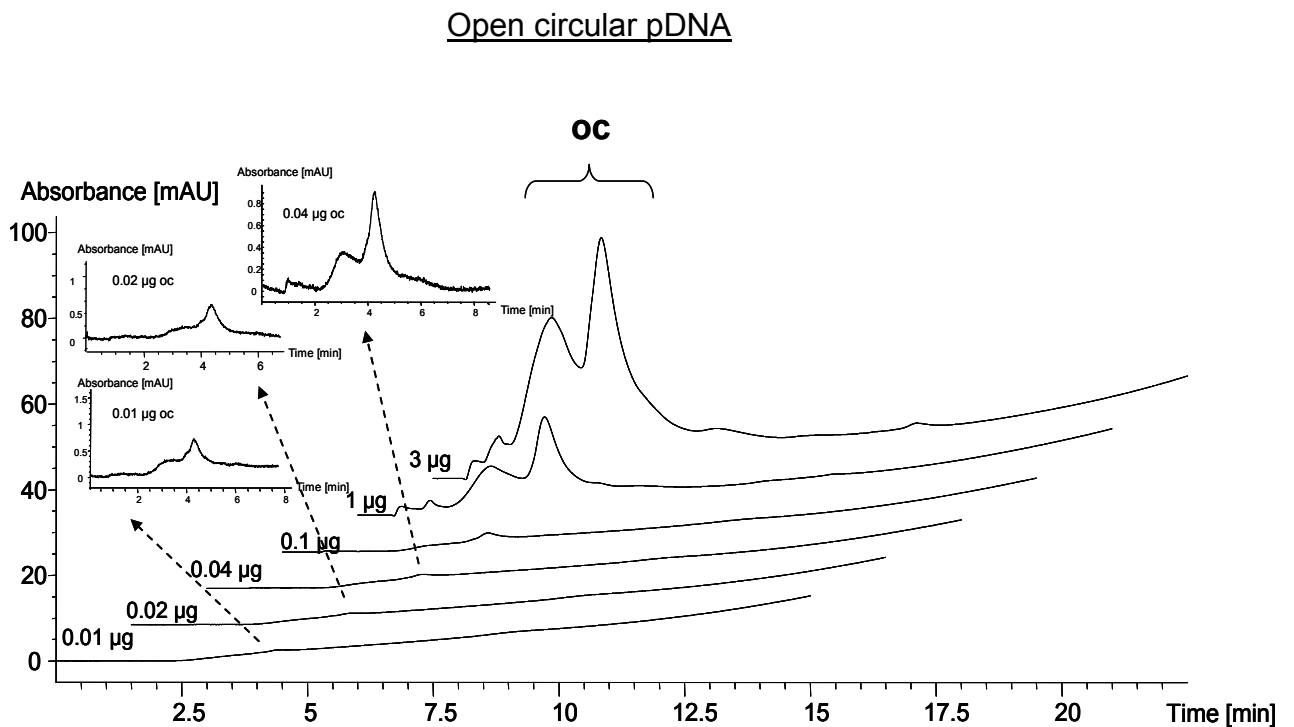
Open circular pDNA

Figure 44: Stacked chromatograms of the open circular isoform (0.01-3 µg pDNA)

Linear pDNA
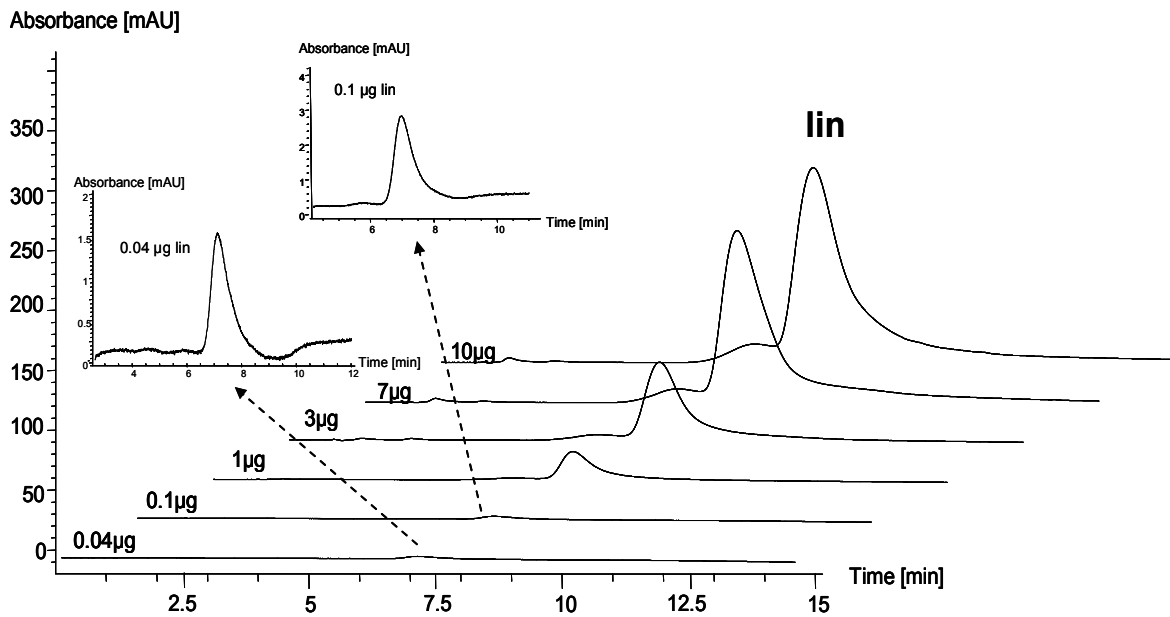
Figure 45: Stacked chromatograms of the linear isoform (0.04-10 µg pDNA)

In Figure 43-45 the linear correlation between the injected amount and resulting peak area can be seen for each isoform, whereby low concentrations are enlarged.

b. Calculated calibration curves

The linearity ranges were calculated by plotting peak areas against injected amounts. The concentration range with minimal coefficient of determination was determined.

Table 26: Results of the ccc plasmid

Sample	Inj. amount [µg]	1st measurement		2nd measurement	
		t_R [min]	A [mAU·s]	t_R [min]	A [mAU·s]
ccc	0.001	-	-	-	-
	0.01	9.72	25.1	9.69	23.8
	0.02	9.56	35.2	9.53	333
	0.04	9.49	51.1	9.56	40.6
	0.1	9.55	134.6	9.50	121.4
	1	9.4	1366.1	9.40	1373.6
	3	9.46	4302.2	9.45	4361.1
	7	9.33	10615.6 outlier	9.33	11080.9 outlier
	10	9.28	13395.9	9.26	13555.6
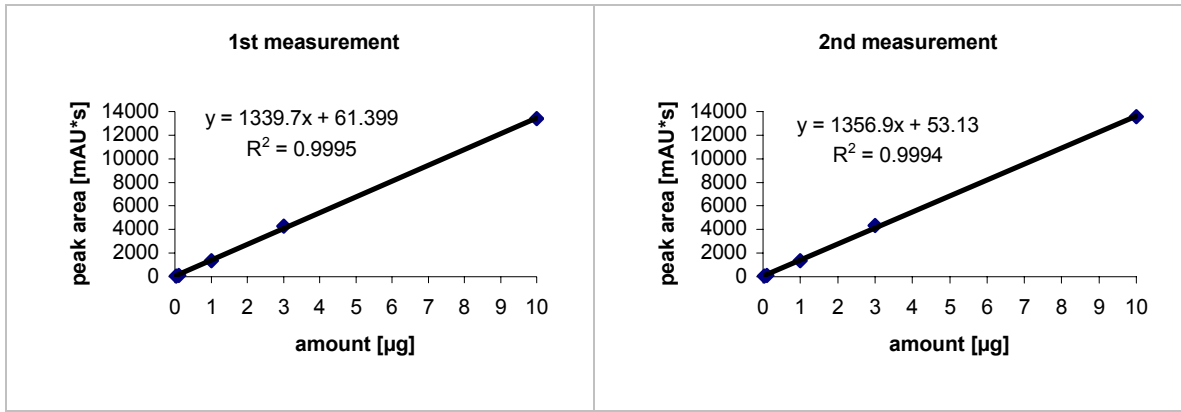
Figure 46: Calibration curve of the ccc-isoform (0.04-10 µg plasmid)

Table 27: Results of the oc plasmid

Sample	Inj. amount [µg]	1st measurement		2nd measurement	
		t_R [min]	A [mAU·s]	t_R [min]	A [mAU·s]
	0.001	-	-	-	-
	0.01	4.41	14.9	4.34	10.8
	0.02	4.29	13.5	4.36	14.7
	0.04	4.23	42.4	4.22	51.9
oc	0.1	4.08	103.2	4.04	103.3
	0.3	2.69	206.9	2.59	209.5
	1	3.72	1535.3	3.65	1533.57
	3	3.35	5188.6	3.15	5452.5
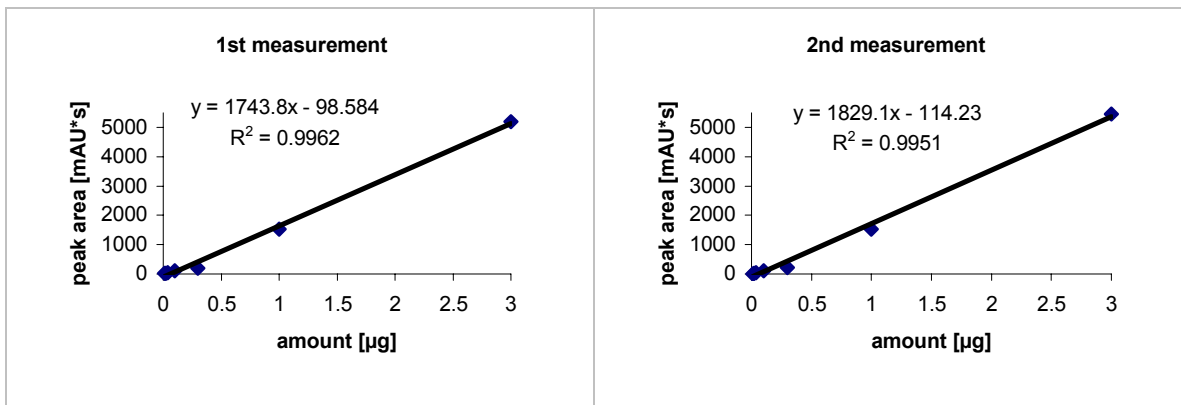
Figure 47: Calibration curve of the oc-isoform (0.01-3 µg plasmid)

Table 28: Results of the lin plasmid

Sample	Inj. amount [µg]	1st measurement		2nd measurement	
		t_R [min]	A [mAU·s]	t_R [min]	A [mAU·s]
lin	0.001	-	-	-	-
	0.01	7.13	141.2	7.11	81.5
	0.02	7.13	125.9	7.13	96.1
	0.04	7.03	97.2 outlier	7.03	66.4
	0.1	7.05	105.4	7.04	105.3
	1	7.09	1311.2	7.13	1345.1
	3	7.31	4147.1	7.37	3980
	7	7.33	8492.5	7.32	8282.5
	10	7.34	12750.3	7.37	12788.1
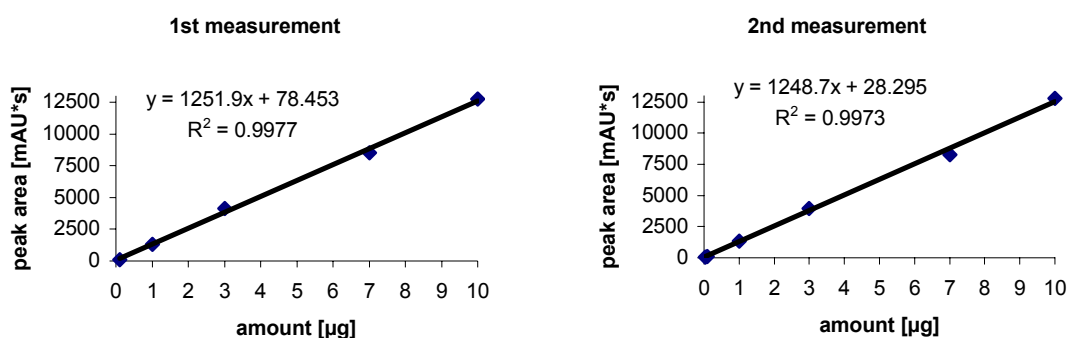
Figure 48: Calibration curve of the lin-isoform (0.04-10 µg plasmid)

In Figure 46-48 the resulting calibration curves are represented.

Determination of the precision (repeatability)

For the definition of precision see page 34.

0.1 µg of the lin and oc isoform and 3 µg of the ccc isoform were injected 6 times into the quinine modified silica column and the precision of the peak area and the retention time was calculated. Determined precisions between 0.7 and 6.9% using peak areas and 0.20 and 0.41% using retention times indicate an adequate repeatability, especially for ccc and linear isoform. The largest imprecision was found for the oc form which in any way is the most critical isoform.

Table 29: Calculated precision (peak area) (n=6; 0.1 resp. 3 µg injected)

		Peak area [mAU·s]
Supercoiled pDNA	**Average value [mAU·s]**	4312.4
	Standard deviation [mAU·s]	29.3
	Relative standard deviation	**0.7%**
Open circular pDNA	**Average value [mAU·s]**	97.0
	Standard deviation [mAU·s]	6.7
	Relative standard deviation	**6.9%**
Linear pDNA	**Average value [mAU·s]**	103.6
	Standard deviation [mAU·s]	2.6
	Relative standard deviation	**2.5%**

Table 30: Calculated precision (retention time) (n=6; 0.1 resp. 3 µg injected)

		Retention time [min]
Supercoiled pDNA	**Average value [min]**	9.43
	Standard deviation [min]	0.02
	Relative standard deviation	**0.20%**
Open circular pDNA	**Average value [min]**	3.99
	Standard deviation [min]	0.07
	Relative standard deviation	**1.86%**
Linear pDNA	**Average value [min]**	7.05
	Standard deviation [min]	0.03
	Relative standard deviation	**0.41%**
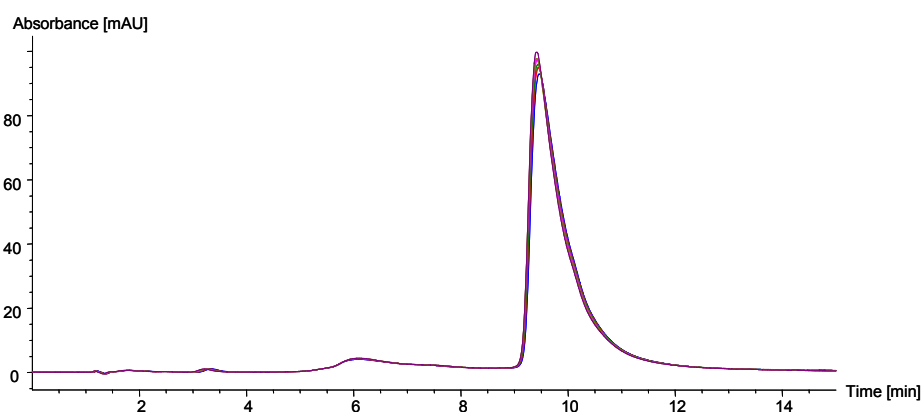
Figure 49: Chromatograms of precision measurements (3 µg) of ccc plasmid
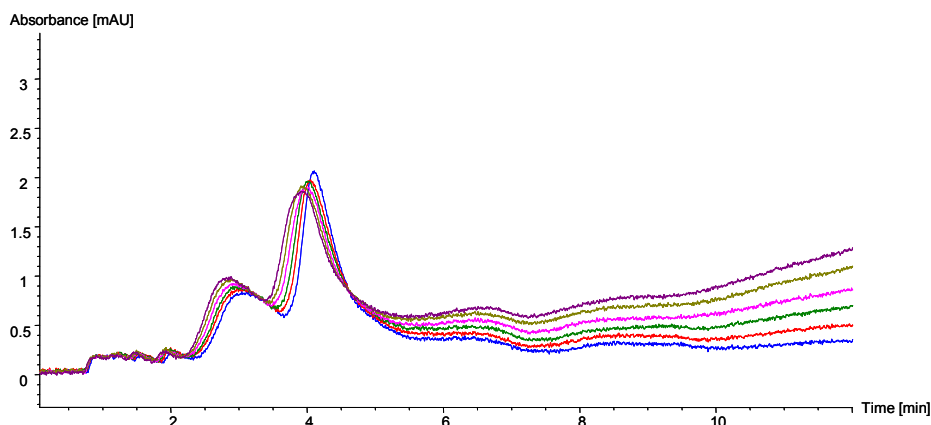
Figure 50: Chromatograms of precision measurements (0.1 µg) of oc plasmid
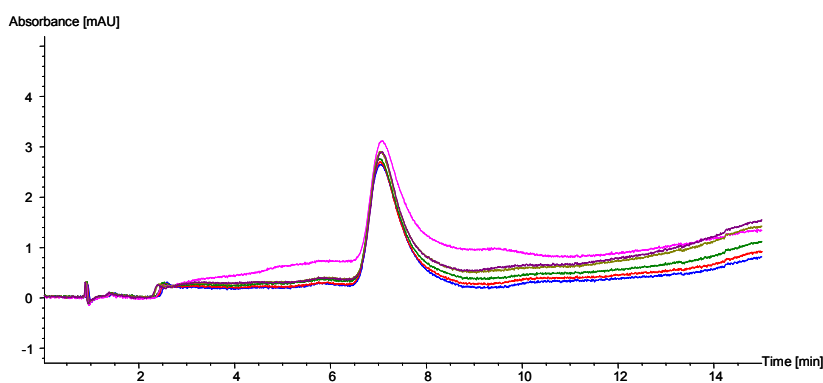
Figure 51: Chromatograms of precision measurements (0.1 µg) of lin plasmid

These chromatograms (Figure 49-51) show that all three isoforms are separated from each other. However, it is very difficult to assign the open circular plasmid which shows two main peaks to a certain peak. There is no proof if both peaks belong to the open circular plasmid, but the agarose electrophoresis showed that there is just one isoform in this sample. One explanation for this phenomenon could be that they both have the open circular shape but different nicking in their DNA strands as a result of the enzymatic treatment. Another possibility would be that sample is not pure and it still contains fragments or other impurities eluting approximately at the same time, being not detectable by the used AGE method.

By comparing peak areas of the oc form with the other isoforms it can be seen that they are too low. Thus either a dilution error or an error during the concentration determination of the oc standard occurred. One explanation would be, that the standards (ccc) for determination of concentration of the oc standard were too concentrated causing an imprecisely result for the oc-sample.

Furthermore the propylcarbamoyl quinine column broke down during the validation hence the test series of linear and supercoiled pDNA were measured with

a new column (same batch stationary phase). For comparing the columns, all three isoforms were injected and they all showed the same retention time in both columns. As a consequence, only the open circular isoform was measured with the "old" column whereas the "new" column was used for the other two isoforms.

Determination of the Recovery of the open circular Isoform

The average recovery of the oc pDNA related to the linear isoform in a concentration range from 0.04 µg to 3 µg DNA is **102 ± 31%** (1st measurement: 96 ± 38%, 2nd measurement: 107 ± 23%), whereas the precision measurements (at 0.1 µg) deliver a recovery of **91 ± 10%**.

Table 31: Summary of calculated recoveries

Recovery

Concentration rage:	1st measurement	2nd measurement	Average value
0.04 to 3 µg	96 ± 38%	107 ± 23%	**102 ± 31%**
0.1 µg (precision measurements)	**91 ± 10%**		

Determination of the Limit of Detection / Limit of Quantification

Both parameters, Limit of detection and quantification are important values to describe the suitability of a method for a certain concentration range.

Limit of Detection (LOD)

For the definition of Limit of Detection (LOD), see page 37.

Lower Limit of Quantification (LLOQ)

For the definition of Lower Limit of Quantification (LLOQ), see page 38.

Table 32: Summary of LOD (S:N = 3:1) and LOQ (S:N = 10:1)

	LOD [µg injected on column] Based on S:N=3:1	LLOQ [µg injected on column] Based on S:N=10:1
Supercoiled pDNA	0.02	0.04
Open circular pDNA	0.01	0.02
Linear pDNA	0.01	0.04

As can be seen in Table 32 the LOD is between 0.01 (oc, lin) and 0.02 µg (ccc) and the LLOQ between 0.02 (oc) and 0.04 µg (ccc, lin).

Upper Limit of Quantification (ULOQ)

For the definition of Upper Limit of Quantification (ULOQ), see page 38.

The ULOQ of the supercoiled and the linear isoform corresponds to 10 µg whereas the upper limit of the open circular isoform is 1 µg.

Determination of Impurities

For measuring impurities, the amount of open circular and linear DNA in the presence of the supercoiled isoform is detected.
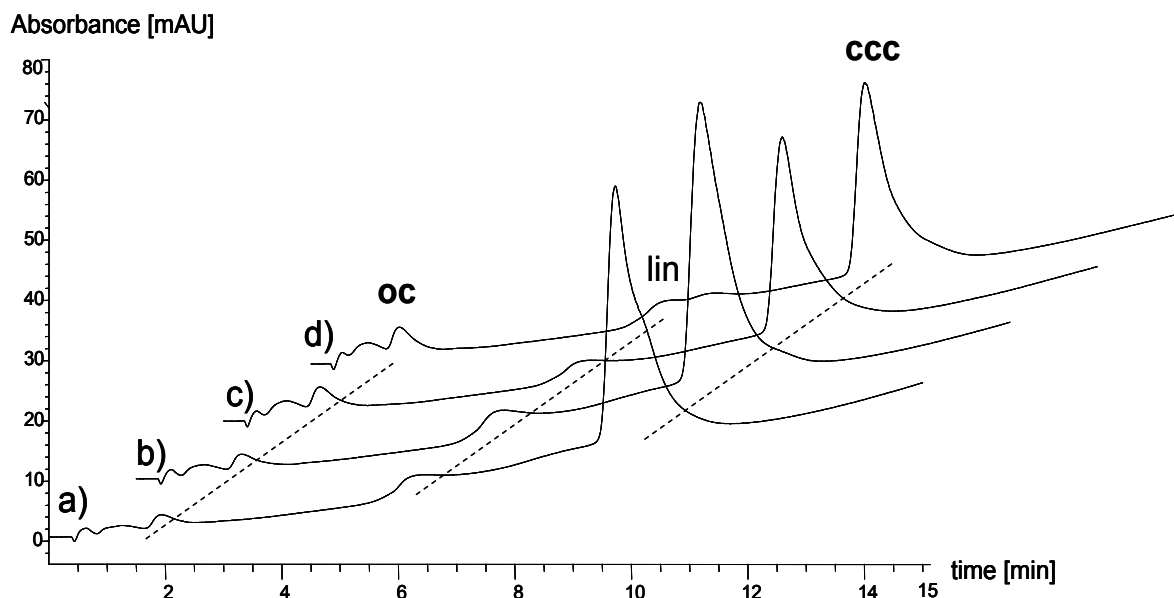
Figure 52: Chromatograms of different spiked samples

a) sample no 1: 0.1 µg oc, 2 µg ccc
b) sample no 2: 0.2 µg oc, 2 µg ccc
c) sample no 3: 0.27 µg oc, 1.33 µg ccc
d) sample no 4: 0.27 µg oc, 1.33 µg ccc, 0.2 µg lin

As it can be seen in Figure 52 even 5% oc impurity can be detected next to supercoiled pDNA. However, in Table 33 the recovered impurities calculated from peak ratio of isoforms is compared with the spiked impurities. It can be seen that the linear isoform is prominent in each sample and that the oc could be recovered satisfactory in all spiked samples.

Table 33: Comparison of spiked and recovered impurities (peak ratio)

Sample no	Spiked impurities	Recovered impurities
1	5% oc	7% oc
		8% lin
2	10% oc	5.1% oc
		8.5% lin
3	17% oc	12% oc
		8% lin
4	15% oc	13% oc
	11% lin	14% lin

Furthermore, enlargement of chromatogram d (Figure 53) shows that there are always two overlapping peaks at $t_R \approx 6$ min. Both peaks have an UV DNA spectrum. One explanation for this phenomenon could be that a small amount of natural oc form was formed which had a similar retention time to the linear form.
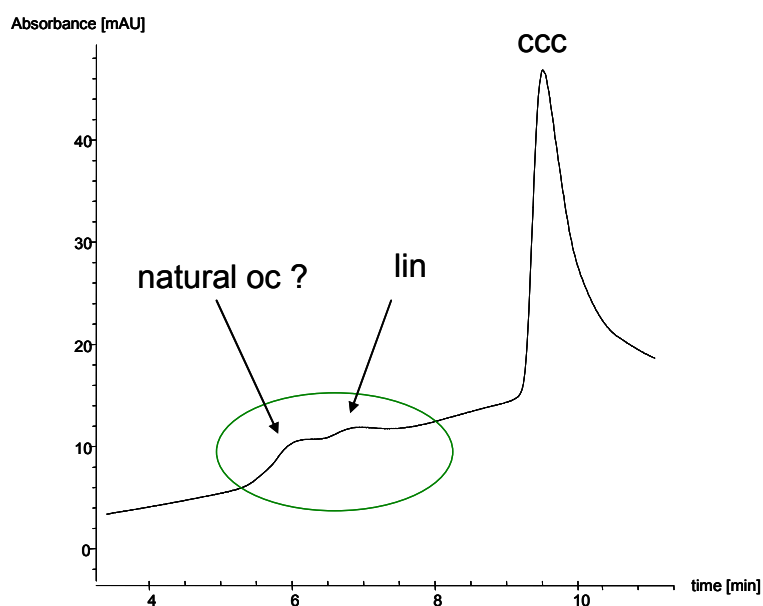
Figure 53: Enlargement of chromatogram d

Figure 53 shows that there are two overlapping peaks whereby the second one represents the spiked linear isoform. It is obvious that the first peak is the natural oc because this peak is present in nearly every supercoiled plasmid (pGNA3) sample and shows similar retention behaviour as the linear isoform. On the contrary the isolated, enzymatically produced oc isoform has significantly less retention on the PCQ modified silica support.

Furthermore, the recovery was calculated using the calibration curves for each isoform.

Table 34: Calculation of impurities using calibration curves

Sample no	Spiked impurities	Calculated impurities	Recovery
1	2 µg ccc	1.1 µg ± 0.6% ccc	55% ccc
	0.1 µg oc	0.2 µg ± 4.3% oc	200% oc
		0.07 µg ± 43% lin	-
2	2 µg ccc	1.3 µg ± 0.6% ccc	65% ccc
	0.2 µg oc	0.2 µg ± 3.6% oc	100% oc
		0.1 µg ± 28.6% lin	-
3	1.33 µg ccc	0.9 µg ± 0.5% ccc	68% ccc
	0.27 µg oc	0.24 µg ± 2.4% oc	89% oc
		0.05 µg ± 60% lin	-
4	1.33 µg ccc	0.85 µg ± 0.5% ccc	64% ccc
	0.27 µg oc	0.25 µg ± 2.2% oc	93% oc
	0.2 µg lin	0.12 µg ± 25% lin	60% lin

As it can be seen above, the recovery was ~63% for the supercoiled isoform and about 121% for the open circular isoform. Moreover, linear isoform was present in each spiked sample.

10 Method validation for pGNA3 with TSK-Gel® DNA-NPR

The measurements are performed using the same conditions as for the validation of the pMCP1 but there was no elution of the open circular isoform. This isoform is the most important impurity when working with supercoiled pDNA hence this column can not be employed for this study. Nevertheless, method validation of ccc and linear form was performed using DNA-NPR material provided from Tosoh Bioscience.
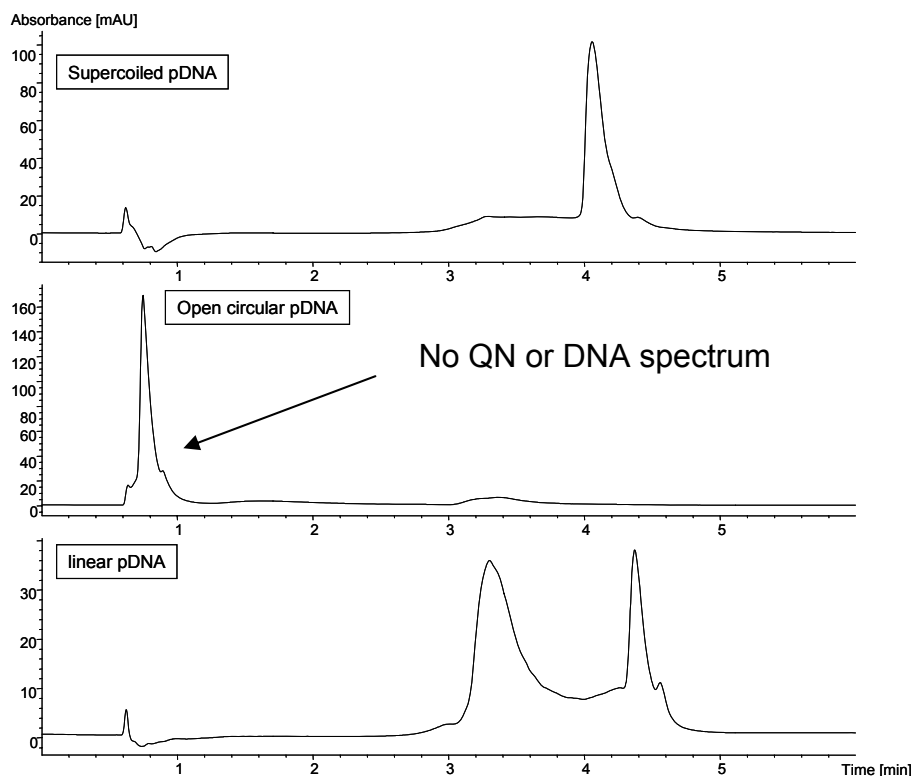
Figure 54: Comparison of the chromatograms of all different isoforms

(each 1 µg pDNA)

10.1 Preparation of the oc standard

For this method validation, the same self-prepared oc standards as for the method validation with PCQ material (see Method validation for pGNA3 with propylcarbamoyl quinine modified silica , page 56) was used.

10.2 Equipment and Instruments

The same system as for the previous validation was used (see chapter 6 Method validation for pMCP1 with Propylcarbamoyl quinine modified silica page 32).

10.3 Method Information

Plasmid samples were analyzed using following method:

Column: TSK-Gel® DNA-NPR (750 x 4.6 mm ID, 2.5 µm)

Buffer A: 20 mM Tris-HCl, pH 9.0

Buffer B: 20 mM Tris-HCl, 1M NaCl, pH 9.0

50 to 75% buffer B in 5 minutes

50% buffer B for 0.5 minutes for re-equilibration

Column temperature: 25°C

Flow rate: 0.7 mL/min

The plasmidic DNA was quantified with a UV diode array detector at 258nm. As reference wave length 360 nm was used.

10.4 Results and evaluation

Amounts from 0.1 to 3 µg plasmidic DNA were measured and evaluated.

10.5 Linearity range

Chromatograms of linear and supercoiled plasmid were measured using increasing quantities from 0.1 to 3 µg pDNA and the linear relation of injected amounts and resulting peak areas was determined. Both isoforms (ccc, lin) showed a linear correlation over the entire concentration range (0.1 – 3 µg).

a. Chromatograms
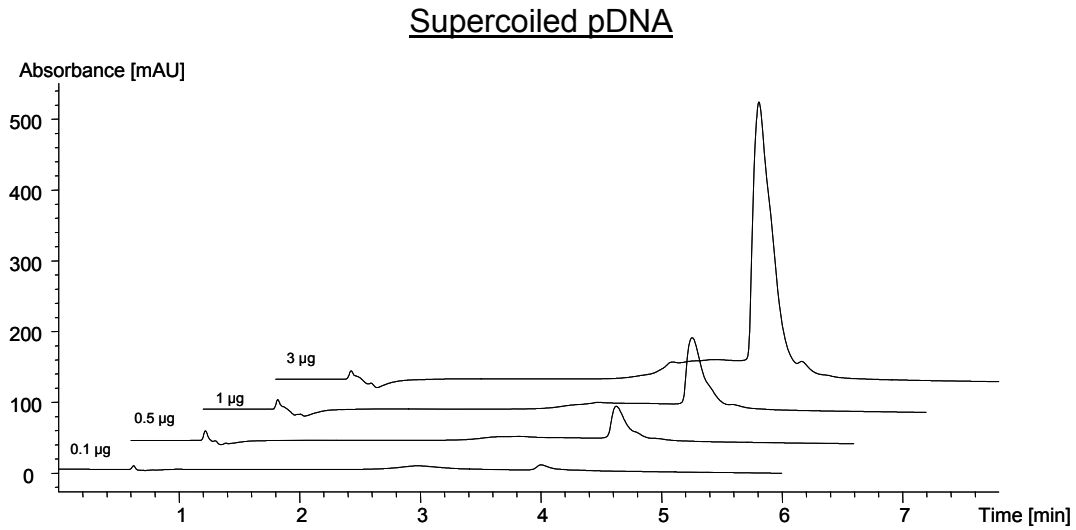
Supercoiled pDNA

Figure 55: Stacked chromatograms of the supercoiled isoform (0.1-3 µg)

Linear pDNA
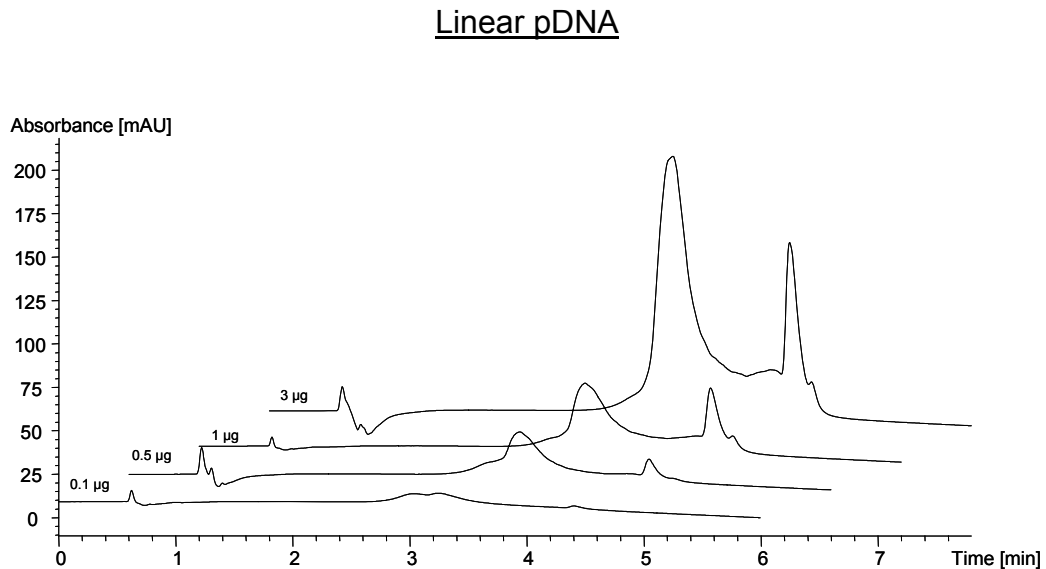
Figure 56: Stacked chromatograms of the linear isoform (0.1-3 µg)

Figure 55 and Figure 56 illustrate the change of the absorption signal with increasing injected amount. Both figures illustrate the poor peak performance (splitted peaks) in particular lin isoform.

b. Calculated calibration curves

Table 35: Results of the ccc plasmid

Sample	Inj. amount [µg]	1st measurement		2nd measurement	
		t_R [min]	A [mAU·s]	t_R [min]	A [mAU·s]
ccc	0.1	4.0	72	4.0	74.5
	0.5	4.0	444	4.0	456
	1	4.1	969	4.1	698 outlier
	3	4.0	4053	4.0	4188

1st measurement

$y = 1406.1x - 232.56$
$R^2 = 0.9925$

2nd measurement

$y = 1461.4x - 205.65$
$R^2 = 0.9992$
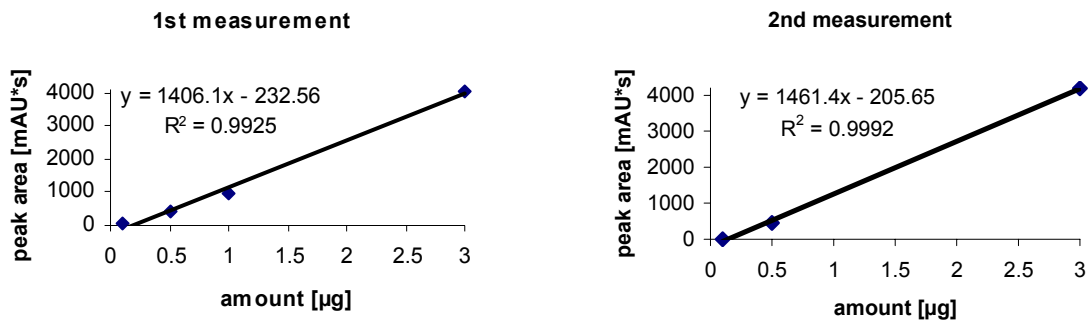
Figure 57: Calibration curve of the ccc isoform (0.1-3 µg plasmid)

Table 36: Results of the lin plasmid

Sample	Inj. amount [µg]	1st measurement			2nd measurement		
		t_R [min]		A [mAU·s]	t_R [min]		A [mAU·s]
lin	0.1	3.25	4.40	62	3.25	4.41	80
	0.5	3.34	4.44	770	3.34	4.44	775
	1	3.30	4.37	1420	3.29	4.36	1438
	3	3.45	4.45	4688	3.44	4.45	4624

1st measurement

$y = 1588.4x - 91.626$
$R^2 = 0.9991$

2nd measurement

$y = 1559.5x - 64.229$
$R^2 = 0.9994$
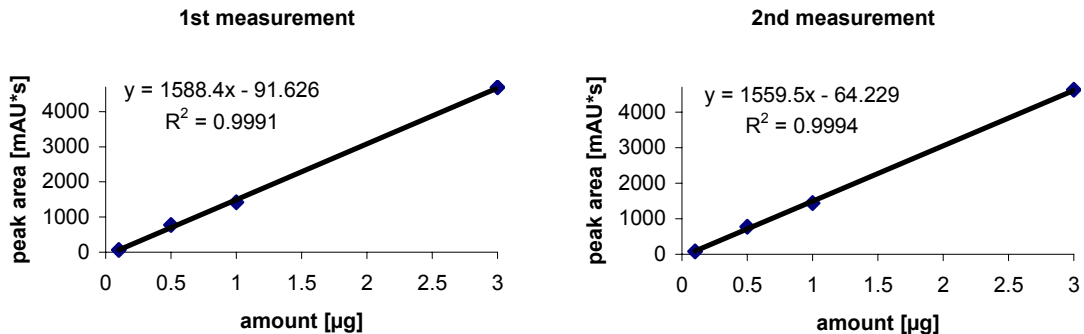
Figure 58: Calibration curve of the lin isoform (0.1-3 µg plasmid)

As it can be seen in Figure 57 and 59 the peak areas increase linearly by increasing injected amounts, thus the measured concentration range from 0.1 to 3 µg can be assumed to be the linearity range for both isoforms (ccc, lin).

Determination of the precision (repeatability)

For the definition of precision see page 34.

1 µg of the lin and 3 µg of the ccc isoform were injected 3 times into DNA-NPR column and the precision of the peak area and the retention time was calculated.

Precision was between 0.9 and 2.3% evaluating peak areas and 0 and 21% for using retention time for calculation. The results are not significant due to only two precision measurements.

Table 37: Calculated precision (peak area) (n=3; 1 resp. 3 µg injected)

		Peak area [mAU·s]
Supercoiled pDNA	**Average value [mAU·s]**	4120.5
	Standard deviation [mAU·s]	95.5
	Relative standard deviation	**2.3%**
Linear pDNA	**Average value [mAU·s]**	1429.0
	Standard deviation [mAU·s]	12.7
	Relative standard deviation	**0.9%**

Table 38: Calculated precision (retention time) (n=3; 1 resp. 3 µg injected)

		Retention time [min]
Supercoiled pDNA	**Average value [min]**	4.0
	Standard deviation [min]	0
	Relative standard deviation	**0%**
Linear pDNA	**Average value [min]**	3.30 resp. 4.37
	Standard deviation [min]	0.01 resp 0.01
	Relative standard deviation	**0.21 resp. 0.16%**

In Table 38, two different retention times were used for calculation of precision of linear isoform due to its splitted peak.
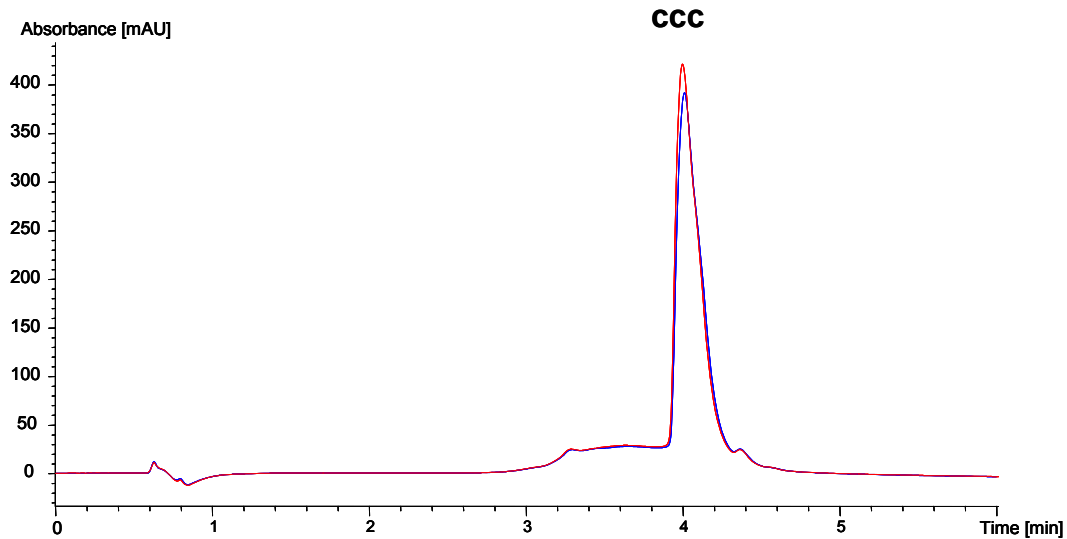
Figure 59: Chromatograms of precision measurements (1 µg) of ccc plasmid
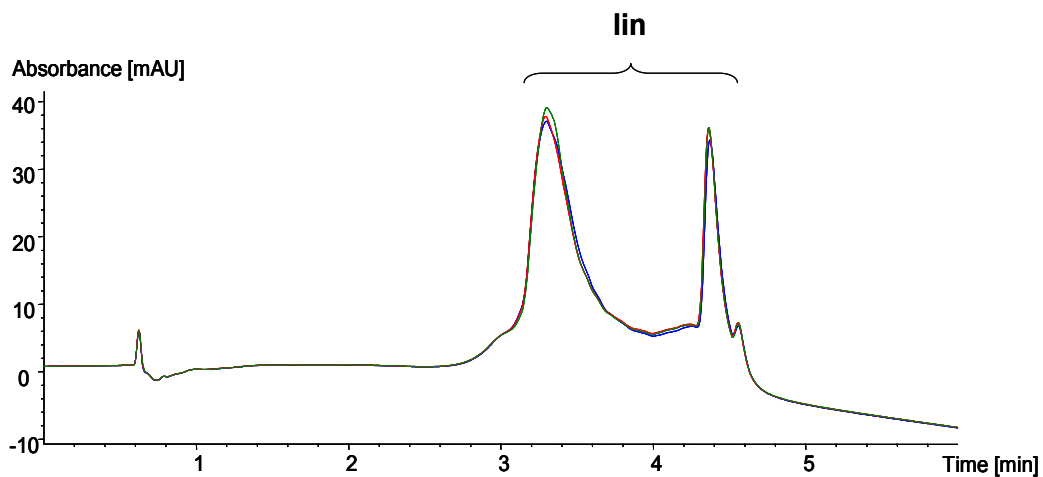
Figure 60: Chromatograms of precision measurements (1 µg) of lin plasmid

Overlaid chromatograms of precision measurements of both isoforms illustrate the high precision of the method validation. Nevertheless, the oc form which is the most critical isoform could not be eluted from the column.

Determination of the Limit of Detection / Limit of Quantification

The limit of quantification for the ccc and linear plasmid was represented by the lowest injected amount 0.1 µg respectively. To obtain more precisely values for LOD and LLOQ further measurements of lower concentrations ought to be measured.

Limit of Detection (LOD)

For the definition of Limit of Detection (LOD), see page 37.

Lower Limit of Quantification (LLOQ)

For the definition of Lower Limit of Quantification (LLOQ), see page 38.

Table 39: LLOQ (S:N = 10:1)

	LLOQ [µg injected on column] Based on S:N=10:1
Supercoiled pDNA	0.1
Open circular pDNA	-
Linear pDNA	0.1

Upper Limit of Quantification (ULOQ)

For the definition of Upper Limit of Quantification (ULOQ), see page 38.

The ULOQ of the supercoiled and the linear isoform is 3 µg, which was the highest injected amount.

The results of the method validation for pGNA3 with a DNA-NPR column demonstrate that this method is able to validate the supercoiled and the linear form but it is not useful for the oc form. It has to be considered, that the oc form can arise from the ccc form and is therefore the most critical impurity while working with plasmids. Thus the method validation has to be modified to gain an elution of the oc form. However, the LOQ of supercoiled and linear isoform is 0.1 µg and the linearity range was between 0.1 and 3 µg for both. In addition the ccc plasmid has a good peak performance whereby the linear isoform is splitted into two main peaks.

11 Method validation for pMCP1 with propylcarbamoyl quinine modified non porous MICRA

MICRA NPS phase (1.5 µm) based on non porous silica is a possibility to improve the resolution as well as the analysis time. Compared to porous silica, the MICRA material has a smaller surface area (< 3 m^2/g) and therefore lower selector loading which decreases the retention. Macromolecules like biopolymers (DNA, proteins, peptides) or polymers have a low diffusion coefficient thus moving inside the pores takes a long time. Therefore non porosity of the support material accelerates the mass transfer resulting in higher efficiency of the column. Consequently the analysis time can be shortened because it is possible to work at higher flow rates without significant efficiency loss.

As a consequence of lower content of selector, the MICRA support material is more acidic compared to the 5 µm material. Thus the pH gradient has to be relocated at lower values.

Based on previous knowledge, separation of plasmid isoforms is improved using MICRA silica material. The objective of this part of the work was the detailed elucidation of this stationary material and its characterisation by method validation for the pMCP1 plasmid.
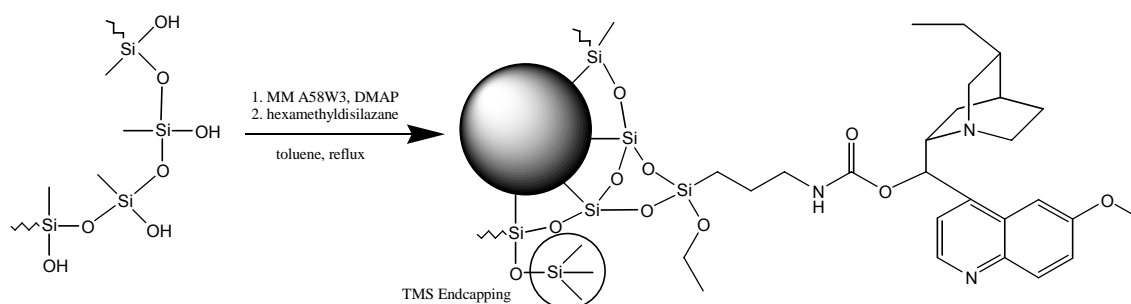
Figure 61: Reaction scheme for the synthesis of the MICRA PCQ column

The non-porous silica (NPS MICRA ®) PCQ material (particle size 1.5 µm) was made in-house and then packed into stainless steel columns (dimension 33 x 4.6 mm ID) by Bischoff Chromatography Leonberg. A selector coverage of approximately 19 µmol/g was calculated from elemental analysis data.

Each three columns were packed with endcapped and non-endcapped particles (endcapping with hexamethyldisilazane).

11.1 Method development

First, it was aimed of an improvement of the separation of all three isoforms by optimizing various parameters like pH gradient, ionic strength of the buffers (phosphate concentration), content of organic modifier (IPA), column temperature and the flow rate. Furthermore the influence of silanol endcapping and the effect of using stainless steel frits instead of glass wool were studied.

The major problem while working with the MICRA based material was the limited lifetime of the columns as a result of ligand bleeding. On average about 20 sample injections per column were possible. Subsequently, there was no retention of the analytes anymore.

Dependence of pH value

Initially the standard method as employed before (Method validation for pMCP1 with Propylcarbamoyl quinine page 32) was tested.

- Method 1

> Buffer A: 50 mM phosphate, **pH 7.2**
>
> Buffer B: 50 mM phosphate, **pH 7.9**, 20% IPA
>
> 0 to 100% buffer B in 15 minutes
>
> Column temperature: 60°C
>
> Flow rate: 0.7 mL/min

Table 40: Detailed cleaning steps

short cleaning step
(3 times)

%B	t [min]	flow rate [mL/min]
0	0	1
0	1	

long cleaning step & re-equilibration

%B	t [min]	flow rate [mL/min]
50	0	0.7
100	0.5	
100	2	
0	2.2	
0	7.5	

If not stated otherwise, for cleaning of the column after each injection, the conditions and the sequence (3 times the short method and subsequently one single long cleaning step) specified above were used.

The plasmids were not retained with method 1 and eluted with t_0, accordingly a lower pH range (pH 7.0 to 7.6) was used for following experiments.

- Method 2

> Buffer A: 50 mM phosphate, **pH 7.0**
>
> Buffer B: 50 mM phosphate, **pH 7.6**, 20% IPA
>
> 0 to 75% buffer B in 10 minutes
>
> Column temperature: 60°C
>
> Flow rate: 0.7 mL/min

By reducing the analysis time, the pH values in channel A and B and shortening of the gradient from 15 to 10 minutes the following chromatogram was observed.
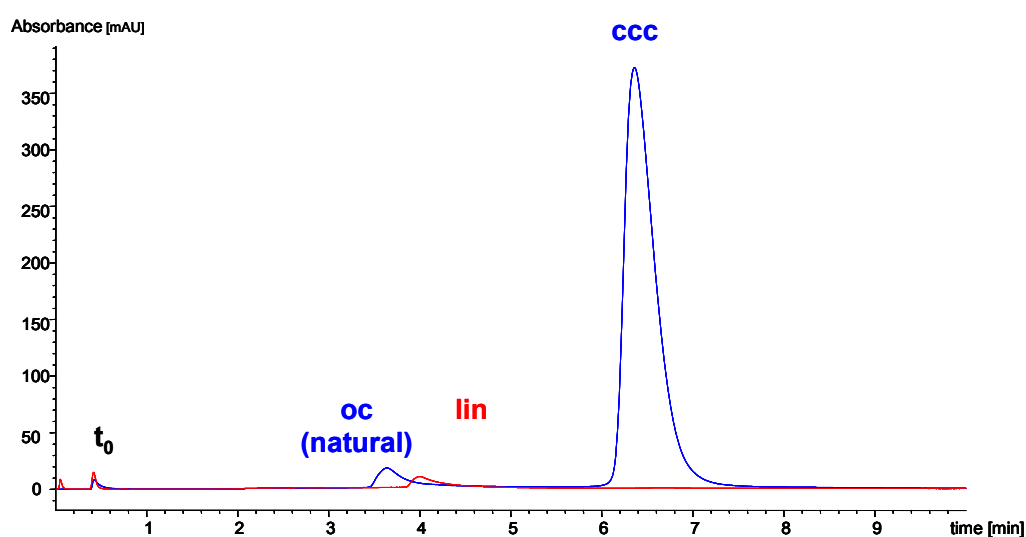
Figure 62: Chromatogram of pMCP1 plasmid (lin, ccc)

Column: Micra NPS PCQ with endcapping, HETP/dp=8.91
(33 x 4.6 mm ID)

As it can be seen in Figure 62 all plasmid isoforms are sufficiently retained and excellent separation between the open circular and the supercoiled pDNA forms can be achieved. Moreover, it is remarkable that the PCQ modified MICRA based stationary phase shows same selectivity between the oc and linear isoform.

Dependence of ionic strength

Besides the pH of the buffers also the influence of the ionic strength was studied. Therefore, the three phosphate concentrations (in the range of 10 mM to 50 mM phosphate) for both buffers and the same elution gradient are compared.

0 to 75% buffer B in 10 minutes

Buffer A: **x** mM phosphate, pH 7.0

Buffer B: **x** mM phosphate, pH 7.6, 20% IPA

Flow rate: 0.7 mL/min
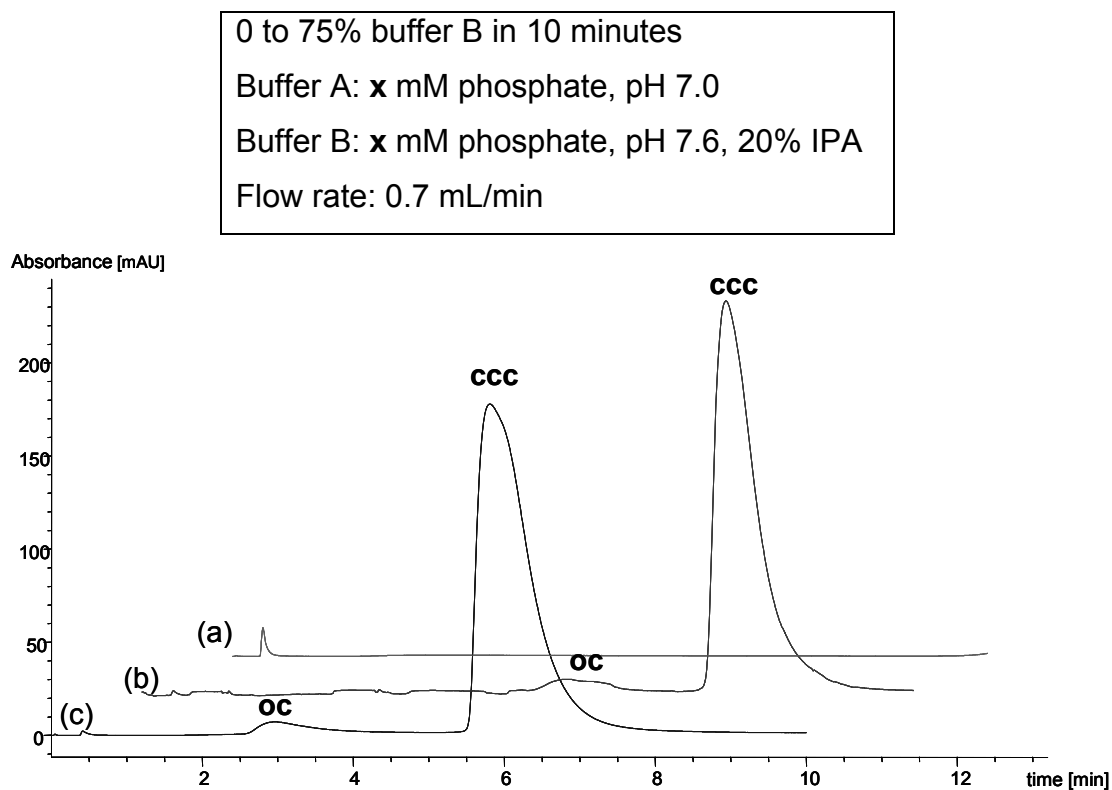
Figure 63: Stacked Chromatograms of ccc pDNA (4.9 kb) with

different phosphate buffers

Column: Micra NPS PCQ without end-capping, HETP/dp=16.04
Column dimension: 33 x 4.6 mm ID
x=**10 mM** phosphate (a) x=**20 mM** phosphate (b) x=**30 mM** phosphate (c)

Figure 63 confirms the influence of the phosphate buffer on the migration time of the plasmid DNA. The phosphate groups can displace the DNA molecules which are interacting with the stationary phase hence the retention time decreases (according to an anion-exchange mechanism). If only a low concentrated phosphate buffer (10mM) is used, no elution of the supercoiled isoform can be observed. Furthermore Figure 63 shows that with phosphate concentrations above 20 mM the retention times are still in a convenient range. Moreover the selectivity between oc and ccc form is not negatively impacted by higher buffer concentrations.

Thus for further measurements with the Micra PCQ based material, phosphate concentrations above 20 mM phosphate are recommendable.

Dependence of column temperature

To investigate the effect of the temperature on the selectivity and retention times, supercoiled pDNA (4.9 kb) was analyzed at different column temperatures in the range from 40°C to 60°C.

Buffer A: 30 mM phosphate, pH 7.0

Buffer B: 30 mM phosphate, pH 7.6, 20% IPA

0 to 75% buffer B in 10 minutes

Flow rate: 0.7 mL/min
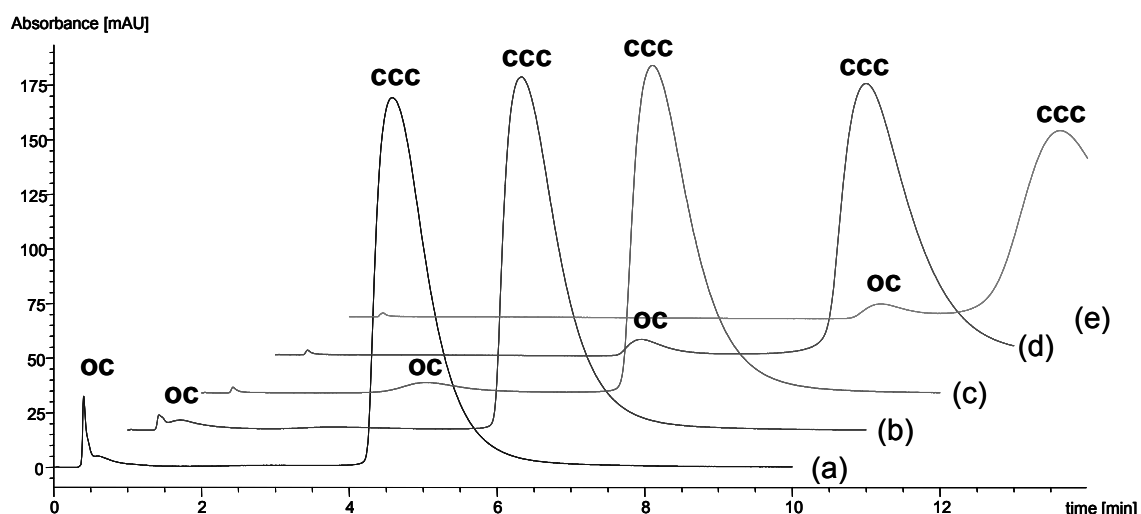
**Figure 64: Influence of the temperature on chromatograms**

Column: Micra NPS PCQ without end-capping, HETP/dp=16.04
Column dimension: 33 x 4.6 mm ID
different column temperatures:
60°C (a), 55°C (b), 50°C (c), 40°C (d), 30°C (e)

This chromatogram shows the variation of the temperature has a great influence on selectivity and may lead to substantial reduction of the analyzing time.

Table 41: Retention time of supercoiled plasmid as a function of the temperature

temperature [°C]	t_R(ccc) [min]	t_R(oc) [min]	α
60	4.58	0.41 (t_0)	-
55	5.33	0.41 (t_0)	-
50	6.11	3.03	2.17
40	8	4.96	1.67
30	9.6	7.2	1.35

Temperature dependence of the retention time
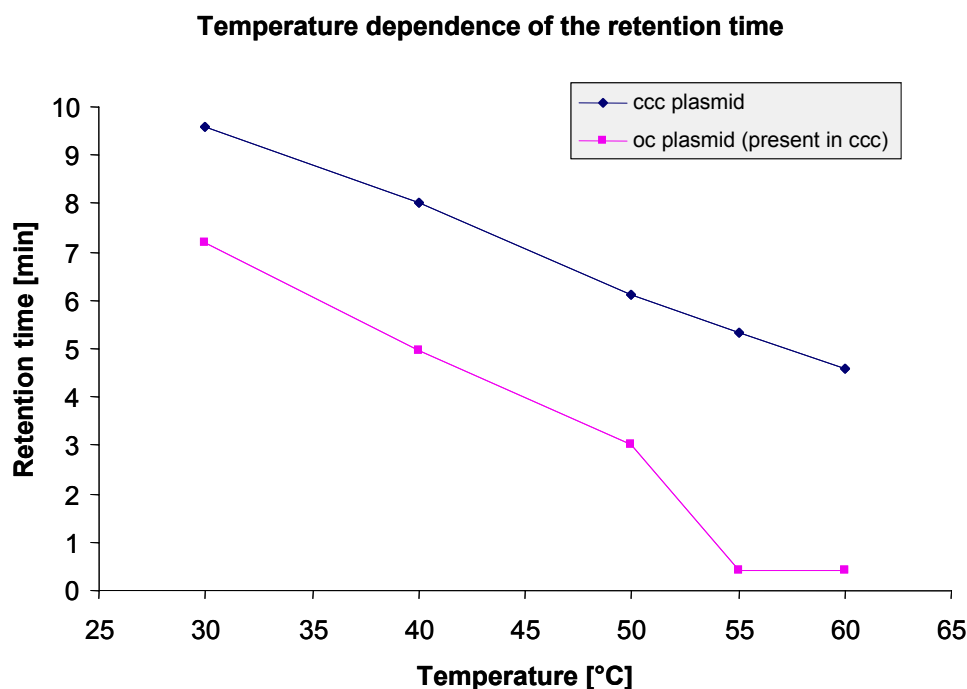
Figure 65: Retention time versus temperature

It can be seen (Figure 64, Figure 65 and Table 41) that an increasing temperature negatively affects the migration of both, ccc and oc form. The best selectivity is, however, achieved with a column temperature of 50°C i.e. at higher temperatures.

Previous works of our group (M. Mahut, diploma thesis, *University of Vienna*) showed the inverse effect with NaCl-gradient elution on the same MICRA-based material; retention time of the supercoiled plasmid strongly increased with temperature whereby no impact on the oc and the lin isoform could be observed.

Furthermore, the temperature influences the peak shapes thus a higher temperature (60°C) was preferred for the further experiments.

Influence of flow rate

Buffer A: 50 mM phosphate, pH 6.5, 0.1M NaCl

Buffer B: 50 mM phosphate, pH 7.5, 30% IPA

5 to 10% buffer B in 7 minutes, 10-60% buffer B in 8 minutes (t_{total}=15 min)

Flow rate: **x** mL/min

Column temperature: 60°C
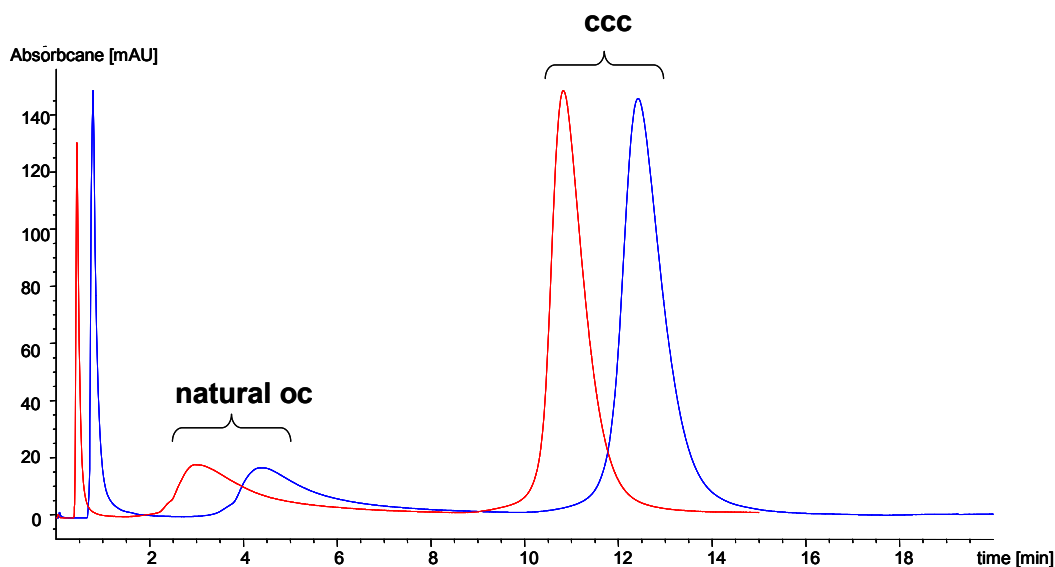
Figure 66: Influence of flow rate (supercoiled plasmid, 4.9 kb)

Column: Micra NPS PCQ without endcapping, HETP/dp=10.51
Column dimension: 33 x 4.6 mm ID
red: 0.7 mL/min, blue: 0.4 mL/min

The chromatogram above shows that the flow rate of the mobile phase has no strong impact on the separation. Thus, the analysis time can be cut down without loosing efficiency or selectivity by increasing the flow rate.

Significance of Endcapping

To proof the necessity of end-capping, the shielded material as well as the non end-capped material is compared in terms of their chromatographic performance. The difference between both materials is that the residual silanol groups are derivatized with hexamethyldisilazane to avoid deprotonation and consequently partly negatively charged surface of the stationary phase. Before, an elemental measurement revealed only a small difference between both materials (a negligible increase of carbon due to endcapping). So it can be expected that the

84

chromatograms of both materials are very similar. Concerning the packing of the columns (density and regularity), the non endcapped material showed higher reduced plate heights (10.5-16, normally 3-4) which can be due to sub-optimal packing.

Buffer A: 50 mM phosphate, pH 7.0

Buffer B: 50 mM phosphate, pH 7.6, 20% IPA

0 to 75% buffer B in 10 minutes

Flow rate: 0.7 mL/min

Column temperature: 60°C
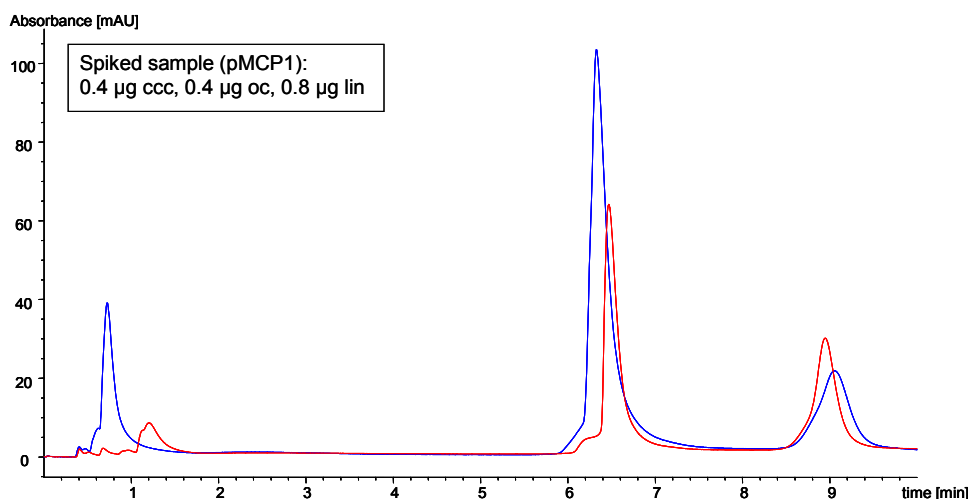
Figure 67: Comparison of end-capped and non end-capped material

red: endcapped, HETP/dp=10.72
blue: non-endcapped, HETP/dp=15.52
column dimensions: 33 x 4.6 mm ID

As it can be seen from Figure 67 the endcapped material delivered a better peak shape and the separation was slightly better. Therefore this material is preferable and the second step of the synthesis (endcapping of the residual silanol groups with hexamethyldisilazane) is not necessary but improves the chromatographic resolution.

Difference between glass wool and stainless steel frits

Previous experiments (carried out by M. Mahut, doctoral thesis (2010) *University of Vienna*) showed that the plasmids strongly adsorb to the glass wool which is used

as a filter for our packed columns. This phenomenon negatively affects the recovery of the plasmids or in worst case it can congest the column. However, to avoid or even reduce irreversible adsorption, the glass wool filters have been replaced by stainless steel frits. To investigate the significance of the glass wool, a spike sample was measured with the same method before and after replacing the glass wool by steel frits. While removing the filter the packing bed can be injured thus it has to be done with caution.

Buffer A: 50 mM phosphate, pH 7.0

Buffer B: 50 mM phosphate, pH 7.6, 20% IPA

0 to 75% buffer B in 10 minutes

Flow rate: 0.7 mL/min

Column temperature: 60°C
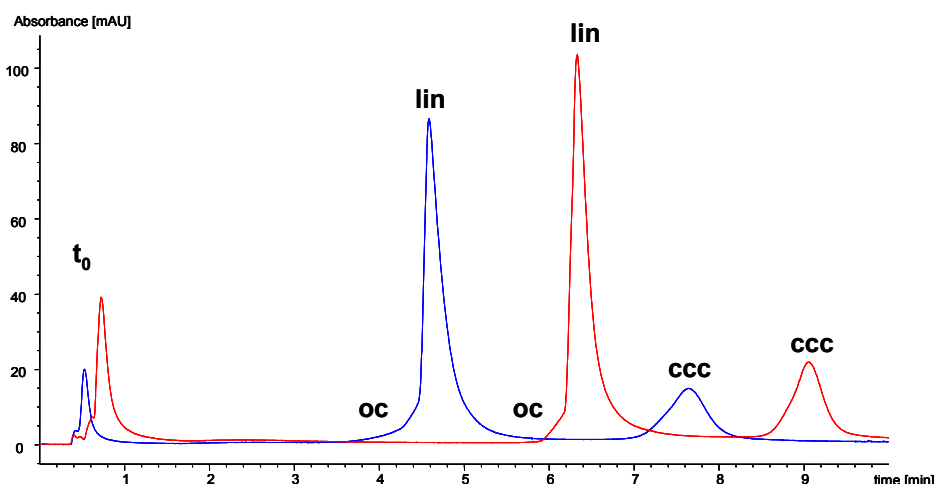
Figure 68: Comparison of glass wool and stainless steel frits

Sample (pMCP1): 0.4 µg ccc, 0.4 µg oc, 0.8 µg lin
red: glass wool frits,
blue: stainless steel frits
not endcapped, HETP/dp=15.52
Column dimensions: 33 x 4.6 mm ID

By comparing both chromatograms the higher signal of the glass wool can be a result of desorbed plasmid. However, the replacement of the filter just generated a shift in the elution time, but based on the results of the previous experiments stainless steel frits should be favoured.

Chromatograms of other plasmid (pMCP1, pAcMC1, pGNA3)

The separation of three plasmids with different sizes (4.9 kb, 10 kb, 15 kb) have been tested with pre-optimized conditions.

Method:

> Buffer A: 50 mM phosphate, pH 7.0
>
> Buffer B: 50 mM phosphate, pH 7.6, 20% IPA
>
> 0 to 75% buffer B in 10 minutes
>
> Flow rate: 0.7 mL/min
>
> column temperature: 60°C

- pMCP1

For stacked chromatogram of ccc and lin, see Figure 62 page 80.

- pAcMC1
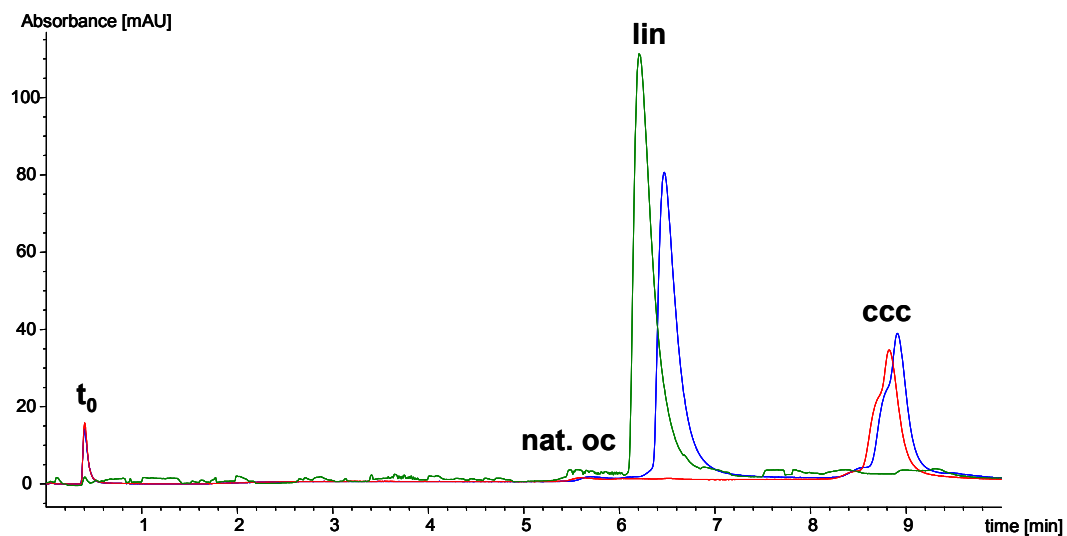
Figure 69: Chromatograms of different isoforms of p

AcMC1

red: 0.4 µg supercoiled pDNA
green: 0.8 µg linear pDNA
blue: 0.4 µg ccc + 0.8 µg linear
column: endcapped, HETP/d_p=10.72
column dimensions: 33 x 4.6 mm ID

- pGNA3
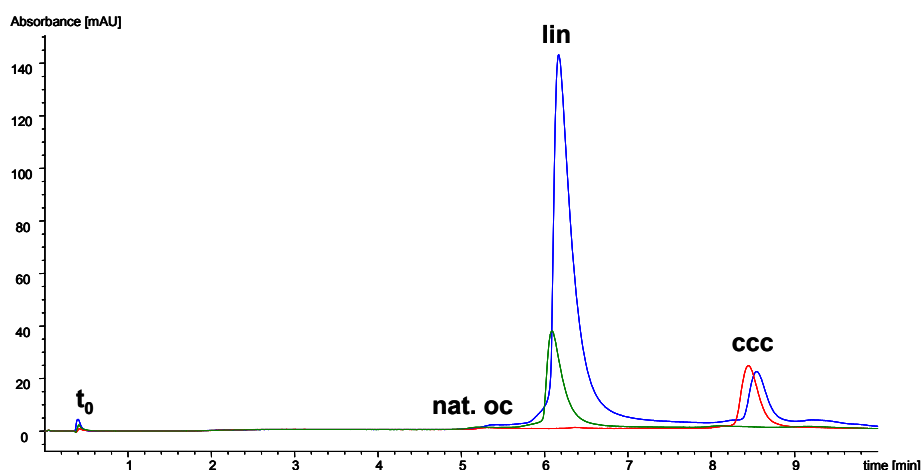
Figure 70: Chromatograms of different isoforms of pGNA3

red: 0.4 µg supercoiled pDNA
green: 0.8 µg linear pDNA
blue: 0.4 µg ccc + 0.8 µg linear
column: endcapped, HETP/d_p=10.72 (33 x 4.6 mm ID)

Figure 69 and 70 demonstrate the suitability of the method for 10 and 15 kb plasmids. However, the major problems are the selectivity between the linear and the open circular isoform and the preparation of oc standards. Thus this method can be used for the smaller plasmids (4.9 kb) but can still be further optimized. Moreover, a dilution error occurred preparing the 15 kb samples, thus peak areas do not fit to the injected amounts.

Optimization of gradient for pMCP1

Furthermore, appropriate method conditions considering also the regeneration and cleaning steps had to be developed. This optimized method should allow appropriate selectivity between linear and open circular isoform as well as reducing the cycle time to less than 15 minutes including cleaning and regeneration.

For this fine-tuning just the eluting gradient and the flow rate were modified, the mobile phases and the column temperature were adapted from the method before.

Buffer A: 50 mM phosphate, pH 7.0

Buffer B: 50 mM phosphate, pH 7.6, 20% IPA

Column temperature: 60°C

The column employed was column no. 5 (not endcapped).

Optimized method:
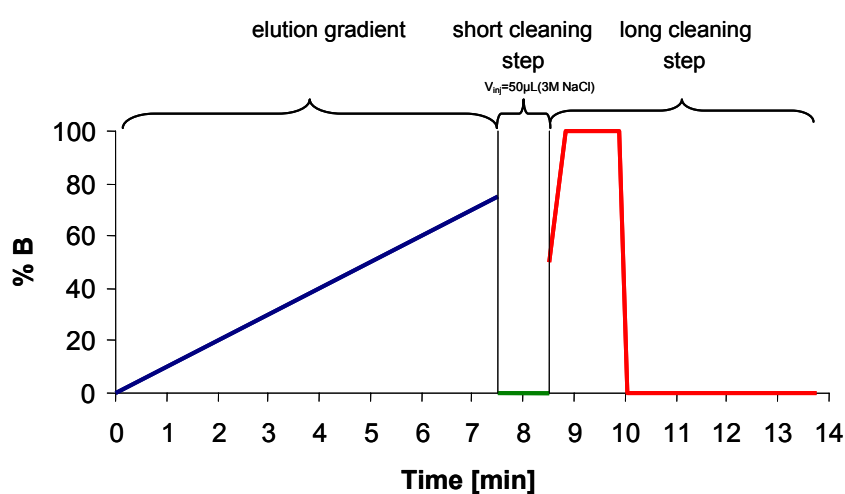
Figure 71: Graphic presentation of gradient

Table 42: Optimized method

elution gradient

%B	t [min]	flow rate [mL/min]
0	0	1
75	7.5	

short cleaning step

%B	t [min]	flow rate [mL/min]
0	0	1
0	1	

Long cleaning step & reequilibration

%B	t [min]	flow rate [mL/min]
50	0	1
100	0.35	
100	1.4	
0	1.54	
0	5.25	

Concerning this method, a total cycle time of 13.75 min can be achieved.
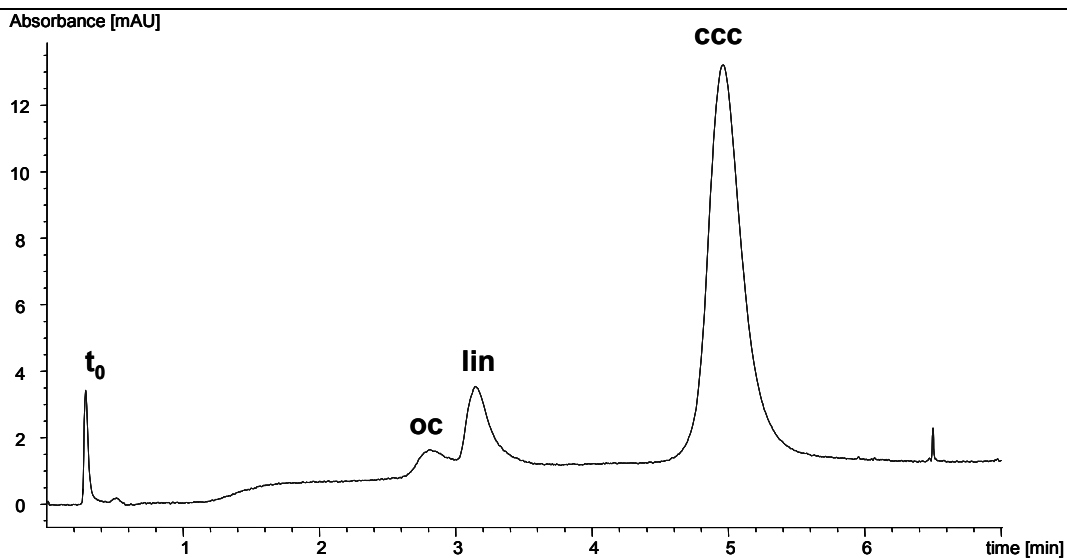
Figure 72: Chromatogram of spiked pMCP1 using optimized method

This sample contains 0.7 µg oc, 0.3 µg linear and 13.6 µg supercoiled isoform, oc and linear isoform were purified standards.

Table 43: Calculation of the selectivity and the resolution

	t_R [min]	α	R_s
t_0	0.285	-	-
lin	3.344	-	-
oc	3.003	1.13	0.70
ccc	5.122	1.58	2.41

The chromatogram above (Figure 72) illustrates an acceptable resolution of 0.7 between the linear and the open circular isoform and retention of 2.4 min between lin and oc form while the total cycle time is kept below 15 minutes. Taken together, this method fulfils requirements specified for quality control purposes. The separation was reasonably repeatable, yet the retention times were slightly shifted as a result of the decreasing stability of the support material.

Table 44: Comparison of injected and recovered peak ratio

	Injected amount on column	Recovered ratio of peak areas
ccc	93%	82%
oc	5%	5%
lin	2%	13%

In Table 44 spiked sample with well-known concentrations of isoforms, namely 13.6 µg ccc, 0.7 µg and 0.3 µg lin was injected into the Micra based PCQ column and the resulting peak area ratio between the isoforms was evaluated. It can be seen that the value of peak area ratio for the oc fits perfectly but the percentage of ccc is shifted to the linear form.

Furthermore, the recovery was calculated using the calibration curves for the supercoiled and linear isoform from the validation (see Figure 77-80). In Table 45 the calculated recoveries are compared with injected amounts. It can be seen that the recovered amount of supercoiled and linear isoform are considerably too less.

Table 45: Comparison of injected and recovered amount using calibration curves

	Injected amount on column [µg]	Recovered amount [µg]
Ccc	13.63	0.53
Oc	0.72	-
Lin	0.3	0.14

11.2   Validation protocol

Method validation with pDNA isoforms of pMCP1 was performed using the optimized method developed before (summarized in Table 42). Therefore the open circular standard has to be prepared again according to the protocol on page 28-2832.

Results:
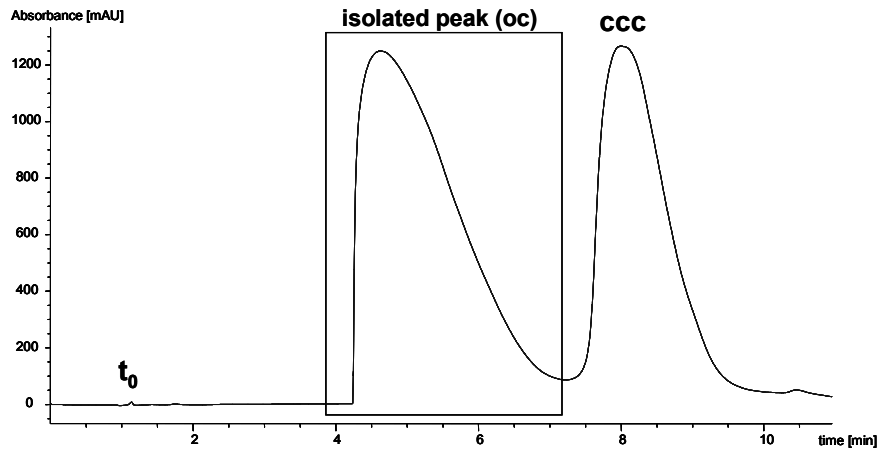
Figure 73: Isolation of open circular form (pMCP1, 55°C for 24h)

Column: propylcarbamoyl quinine PCQ based on Kromasil 100 Å, 5 µm
Column dimension: 150 x 4 mm ID
Buffer A: 50 mM phosphate, pH 7.2, Buffer B: A + 20% IPA pH 7.9,
0-100% buffer B in 15 min, column temperature: 60°C, flow rate: 0.7 mL/min
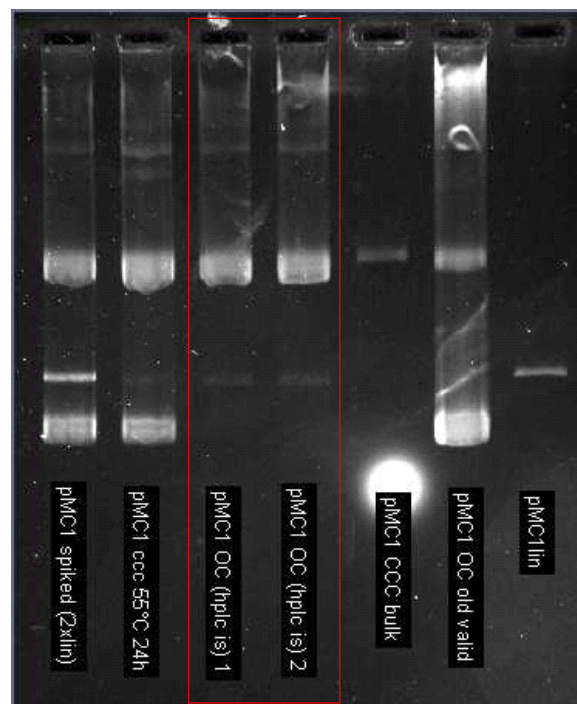
Figure 74: Agarose gel for the verification of oc standard

0.8% agarose, 1x TBE buffer, applied voltage: 200 V for 2 hours,
Staining: 2 µL EtdBr (10 mg/mL)

Figure 74 confirms that the isolated standards contain mainly the open circular form of the pDNA and a negligible amount of the linear form. However, this standard was used for the following measurements. Due to the fact that a completely new column was used for this validation, the steel frits had to be saturated with DNA to inhibit undesirable adsorptions of the sample. Therefore about 50 µg of oc form was injected.

11.3 Equipment and Instruments

The validation measurements were performed using a Rapid Resolution Agilent 1200 system equipped with a binary pump, a thermostatted autosampler (cooled to 4°C) and a diode array UV detector (DAD). All buffer solutions were filtered by a glass filtration unit (Millipore) through a 0.22 µm nylon filter before using.

11.4 Method Information

For the method information, see Table 42 page 89.

Stationary phase used for further measurements is endcapped and packed in-house (HETP/d_p=13.37, column dimension: 33 x 4.6 mm ID).

11.5 Results and evaluation

Amounts from 0.05 to 0.5 µg pDNA of each isoform were measured.

Linearity Range:

Initially, open circular form was injected (beginning with the lowest amount), followed by linear form and at last the supercoiled plasmid. The oc measurements showed barely any peak thus they can not be evaluated. Maybe the saturation with 50 µg oc form was not enough consequently the DNA absorbed at the filter and could not be detected.

a. Chromatograms

Supercoiled pDNA
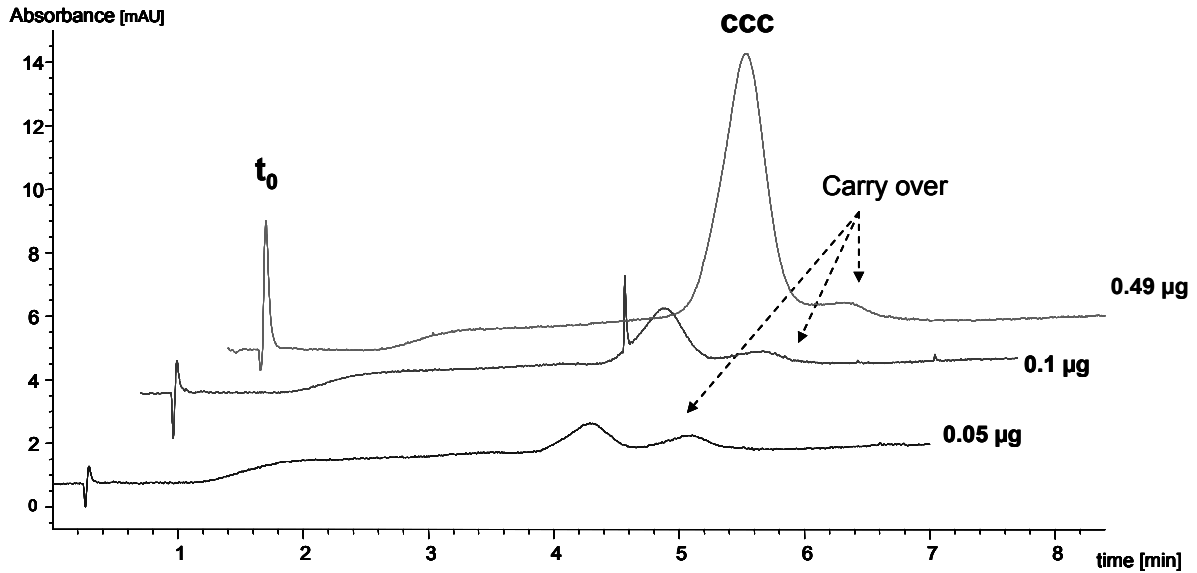
Figure 75: Stacked chromatograms of ccc form (0.05-0.49 µg)

Linear pDNA
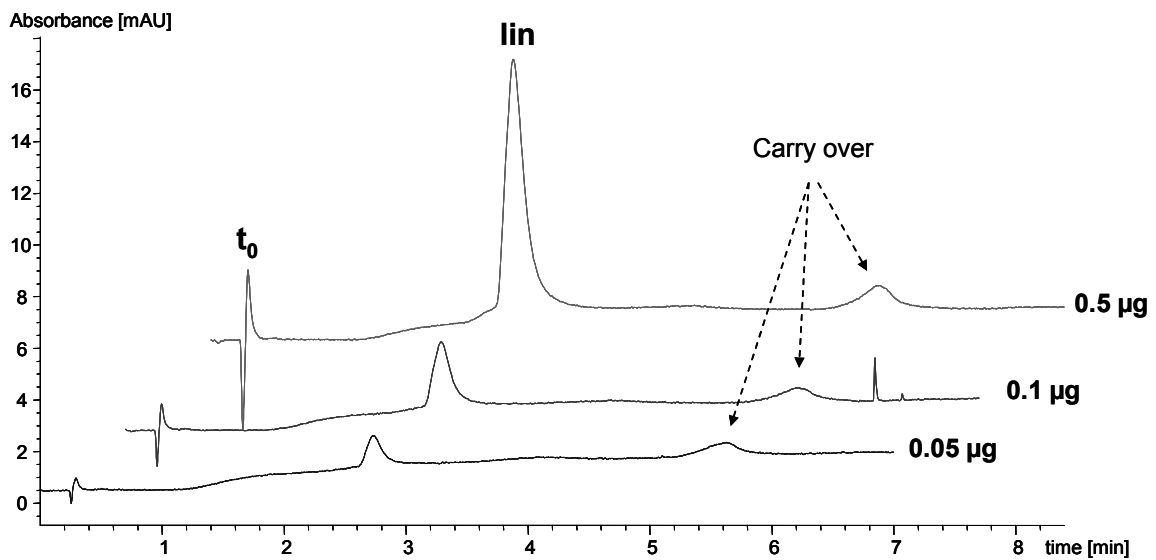
Figure 76: Stacked chromatograms of lin form (0.05-0.5 µg)

b. Calculated calibration curves

Injected amounts of plasmid are plotted against the resulting peak areas to determine the linearity range using the coefficient of determination.

Table 46: Results of the ccc plasmid

Sample	Inj. amount [µg]	1st measurement		2nd measurement	
		t_R [min]	A [mAU·s]	t_R [min]	A [mAU·s]
ccc	0.05	4.288	19.6	4.217	21.9
	0.11	4.166	36.2	-	-
	0.49	4.133	196.8	4.084	195.9

1st measurement

$$y = 409.81x - 4.5927$$
$$R^2 = 0.9983$$
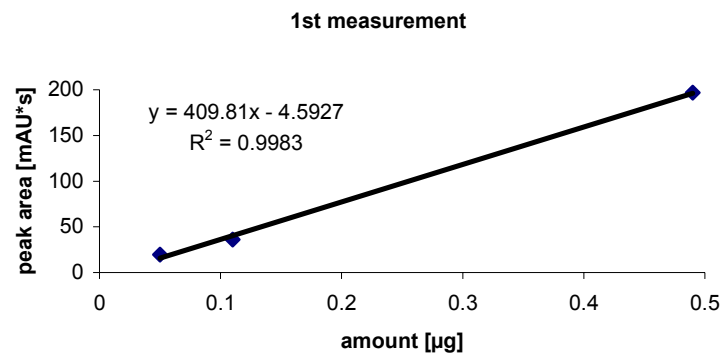
Figure 77: Results of the ccc plasmid (0.05-0.5 µg plasmid)

Table 47: Results of the lin plasmid

Sample	Inj. amount [µg]	1st measurement		2nd measurement	
		t_R [min]	A [mAU·s]	t_R [min]	A [mAU·s]
lin	0.04	2.73	10.30	2.67	10.10
	0.10	2.59	26.20	-	-
	0.49	2.48	122.20	2.41	118.40

1st measurement

$$y = 247.76x + 0.8696$$
$$R^2 = 0.9999$$
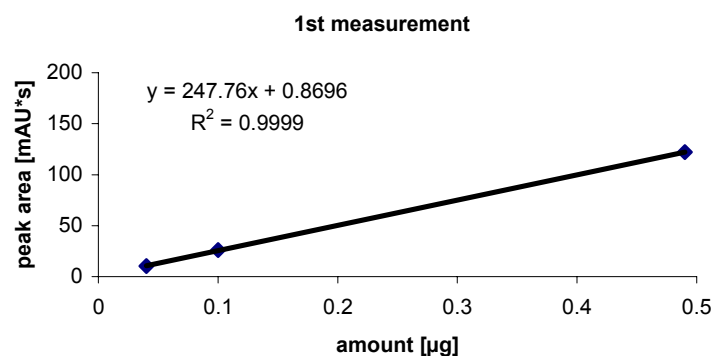
Figure 78: Results of the lin plasmid (0.04-0.49 µg plasmid)

As it can be seen in Figure 77 and 78 the peak areas increase linearly with increasing injected amounts, thus the measured concentration range from 0.05 to 0.5 µg can be assumed to be the linearity range for both isoforms (ccc, lin).

Determination of the precision (repeatability)

For the definition of precision see page 35.

0.49 µg supercoiled and 0.5 µg linear isoform were injected 2 times and the precision of peak areas was calculated. Based on the few measurements, the significance of these values is not very well.

Table 48: Precision calculation for ccc and lin isoform

		peak area [mAU·s]	Retention time [min]
Supercoiled pDNA	**Average value**	196.35	4.109
	Standard deviation	3.82	0.035
	Relative standard deviation	**1.94%**	**0.85%**
Linear pDNA	**Average value**	121.47	2.417
	Standard deviation	2.77	0.06
	Relative standard deviation	**2.28%**	**2.49%**
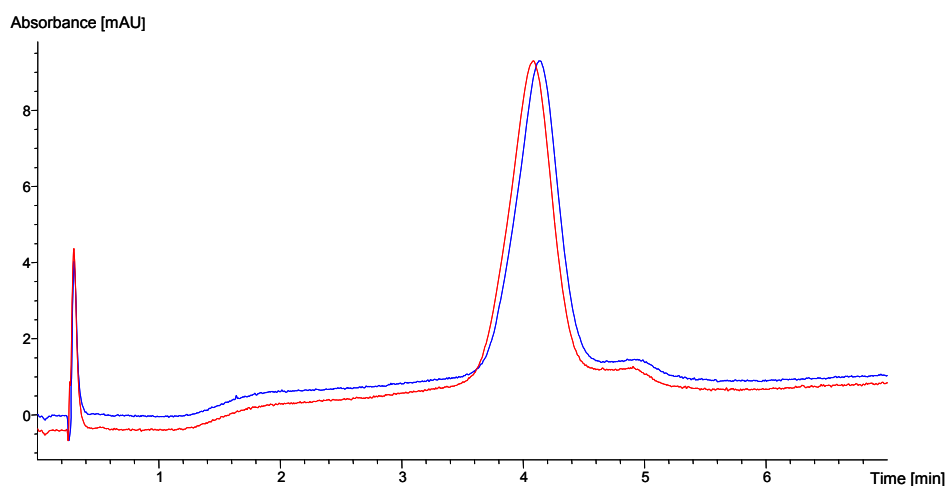
Figure 79: Chromatograms of precision measurements (0.49 µg) of ccc plasmid
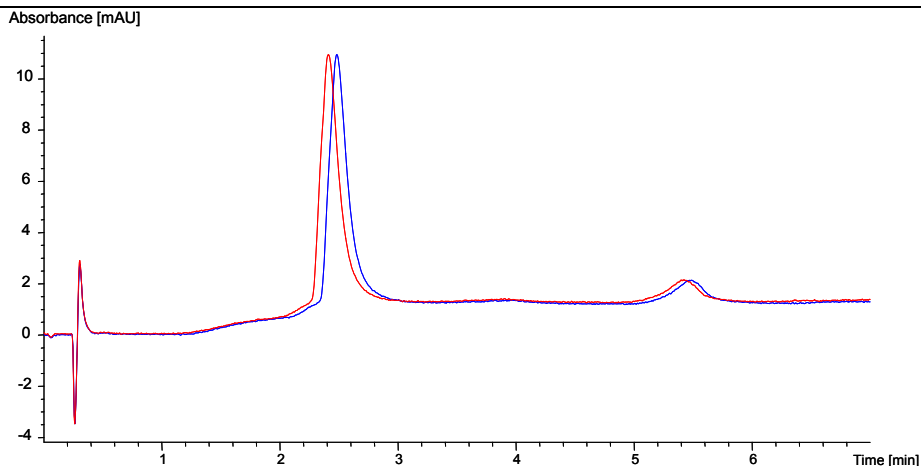
Figure 80: Chromatograms of precision measurements (0.5 µg) of lin plasmid

Figure 79 and Figure 80 illustrate the precision measurements.
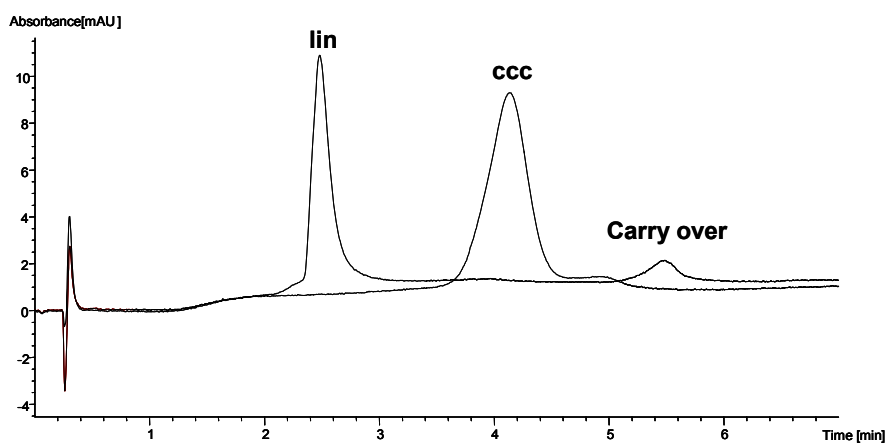
Figure 81: Overlayed Chromatgram of ccc and lin isoform (each 0.5 µg)

Determination of the Limit of Detection / Limit of Quantification

The LOD can only be estimated to be the lowest injected amount so approximately 0.05 µg for the linear and the supercoiled plasmid. To get an accurate LOD or LOQ, additional measurements would be necessary but could not be performed because of unusually high instability of the column.

11.6 Conclusions

An optimized gradient elution, which enabled an adequate resolution of oc and lin form as well as a separation between the oc/lin and ccc form. Furthermore a total cycle time below 15 minutes could be achieved. During the validation procedure, certain drawbacks concerning the support material were found: Its stability was

unexpectedly low resulting in a maximum of 30 injections per column life time employing optimized conditions. It may be concluded that the pH gradient in combination with a temperature of 60°C causes a degradation of the MICRA material. An alternative to the pH gradient would be a sodium chloride gradient elution but these additional measurements were not performed due to lack of time. Moreover, these conditions cause separation of topoisomers which is undesirable for process analysis.

Moreover, the stability of the propylcarbamoyl quinine modified MICRA material has to be improved by enhancing the bonding chemistry for further experiments.

12 Development of 2D HPLC method for analysis of topoisomer distribution in fermentation samples and application to In-Process-Control (IPC) samples

Previously our working group presented a HPLC method for chromatographic topoisomer analysis (M. Mahut, PhD thesis (2010) *University of Vienna*). This method works use of the chemoaffinity principle based on quinine carbamate. This stationary phase exhibits toposiomer selectivity, however, it does not allow injection of samples from fermentation without thorough prior precipitation. Host cell proteins, gDNA, RNA and various other components of the fermentation broth interfer with the pDNA topoisomer peak. T overcome this problem the goal was to develop a 2D HPLC method which allows to isolate the pDNA peak of SEC in the first dimension and transfer it to carbamate column in the second dimenstion for topoisomer analysis.

The aim of in-process controlling was to investigate the influence of the circadian rhythm (day/night cycle) and to define the harvest time point at which the topoisomer contribution offers the highest supercoiling.

12.1 2D-HPLC system:

Combination of size exclusion and anion exchange chromatography

Connecting two complementary chromatographic separation principles in a two-dimensional HPLC system enables faster and automated analysis of such complex samples, eliminating sample preparation steps and exchange of buffer. It is the method of choice if one chromatographic principle does not provide adequate selectivity to perform separation in one step. Additionally the purification and analysis can be done in one single run.

Characterization of size exclusion material

Sepax SRT-SEC phases are based on silica support material (5 µm, 1000 Å, column dimension: 150 x 7.8 mm ID) coated with hydrophilic and neutral nanometer thick films. The large pore volume (1 mL/g) enables high separation capacity.

Characterization of anion exchanger
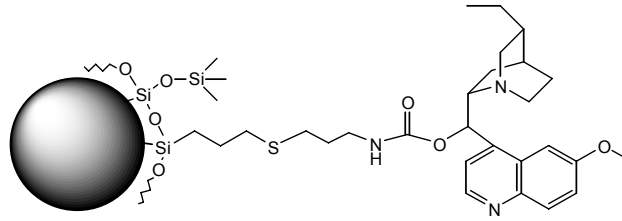
Figure 82: Molecule structure of O-9-allylcarbamoyl-10,11-dihydroquinine (endcapped, based on 5 μm Daiso, 120 Å)

As it can be seen in Figure 83 size exclusion chromatography (5 μm, 1000 Å) does not provide satisfactory results due to lack of topoisomer separation. However, the SRT-SEC column can be used for purification and isolation of the desired peak. Thus supplemental a complementary chromatography system which provides topoisomer selectivity has to be performed subsequently.
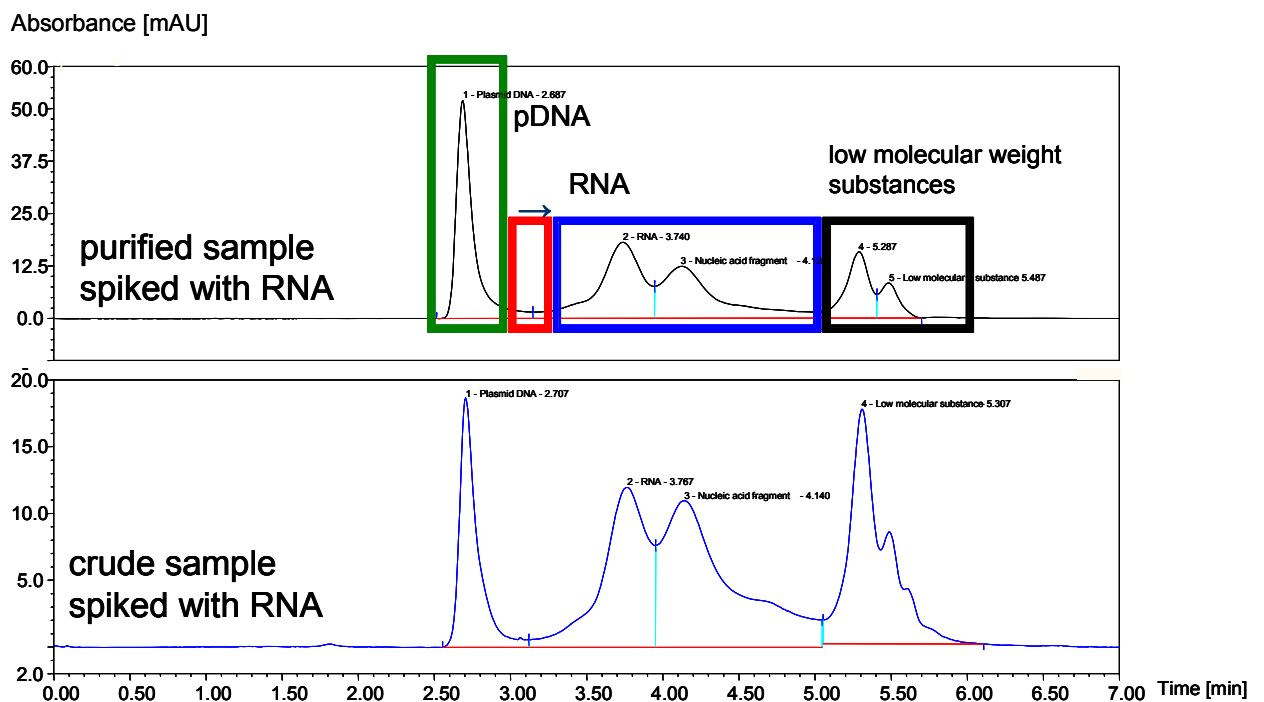
Figure 83: Resulting chromatograms using only size exclusion column

SRT-SEC 5 μm, 1000 Å, 150 x 7.8 mm ID (M. Mahut, PhD thesis (2010) *University of Vienna*)

The biomass sample of 4.9 kbp plasmid (pMCP1) was disintegrated performing alkaline lysis and spiked with RNA.
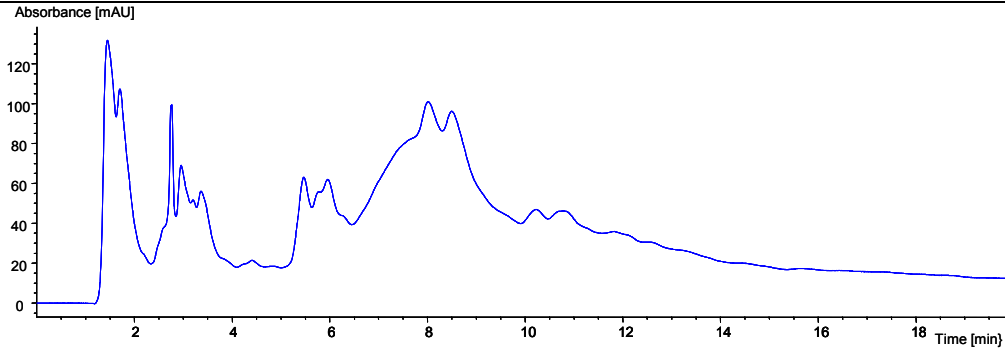
Figure 84: Chromatogram of pMCP1 lysate using only anion exchange column

(Results from M. Mahut) O-9-allylcarbamoyl-10,11-dihydroquinine (5 µm, 120 Å,: 150 x 4 mm ID)
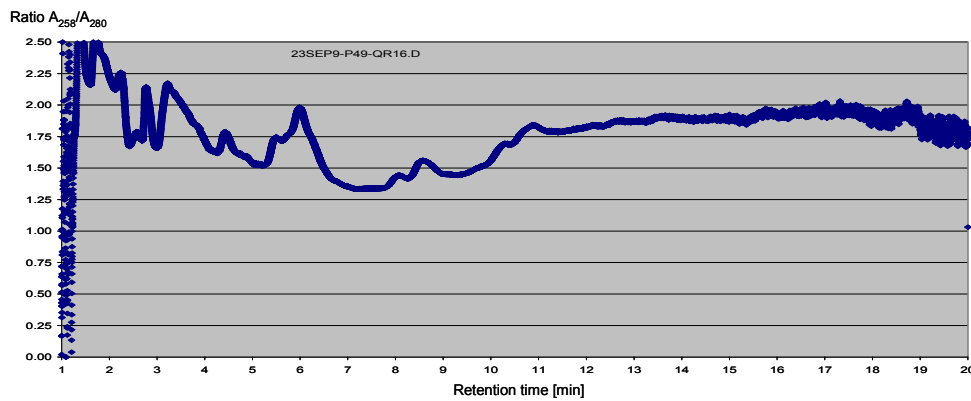
Figure 85: A_{258}/A_{280} plotted against retention time
(Results from M. Mahut)

As it can be seen in Figure 85, analysis of real samples with quinine carbamate based stationary phase does not enable sufficient separation between plasmidic DNA and impurities. In Figure 85, the plot A_{258}/A_{280} against retention time shows that the pDNA (A_{258}/A_{280} = 1.8-2.0) is highly contaminated as a result of insufficient selectivity. Thus, a purification step before analyzing with the quinine modified silica material is necessary.

However, size exclusion chromatography (Sepax SRT-SEC based on silica 5 µm, 1000 Å, 150 x 7.8 mm ID) in the first dimension enables purification and isolation of the desired DNA peak which is then directly loaded onto the second column (O-9-allylcarbamoyl-10,11-dihydroquinine on Daiso 5 µm, 120 Å, column dimension: 150 x 4 mm ID), which provides the separation of topoisomers.

Details of the 2D HPLC method

Measurements were performed with Ultimate 3000 (Dionex) system which provides two separate ternary gradient pumps, switching valve for fraction transfer in heartcut and comprehensive online 2D HPLC.

Figure 86 and 87 schematically visualize the 2D HPLC system. Initially, both valves are in the 10-1 port position thus both columns are not connected with each other i.e. they are operated individually by two distinct pump. The sample is injected into the SEC-SRT column using the loading pump followed by detection being wasted. In contrary, the micro pump transports the buffer into the sample loop followed by the quinine based column and is afterwards wasted without detection.

By switching both valves to the 1-2 port position, the buffer flows through the SEC SRT column too but the analytes can not be detected anymore because instead of getting to the detector they are transported into the sample loop and afterwards to the waste. Thus, the desired peak of the first size exclusion chromatogram containing the analyte can be cut out and collected in the sample loop. Before the analyte is wasted, the left valve has to be switched to the 10-1 position again, whereby the right valve stays in the 1-2 position. As a consequence, the analyte which is in the sample loop is transferred to the second column, namely the quinine carbamate phase. After being separated again, the analyte is detected and subsequently wasted. It would use implementation of another detector after the first dimension column.

This method enables combination of two steps, purification and topoisomer selectivity but only the analyte passing both columns can be detected. Detection directly after passing the size exclusion chromatography is not possible as a consequence of switching the right valve to the 1-2 port position.

Left valve: 10-1 port, right valve: 10-1 port

a) Loading pump → 1st column (SEC) → detector → waste
b) Micro pump → sample loop → 2nd column (QN) → waste

Left valve: 1-2 port, right valve: 1-2 port

a) Loading pump → 1st column (SEC) → sample loop → waste
b) Micro pump → 2nd column (QN) → detector → waste
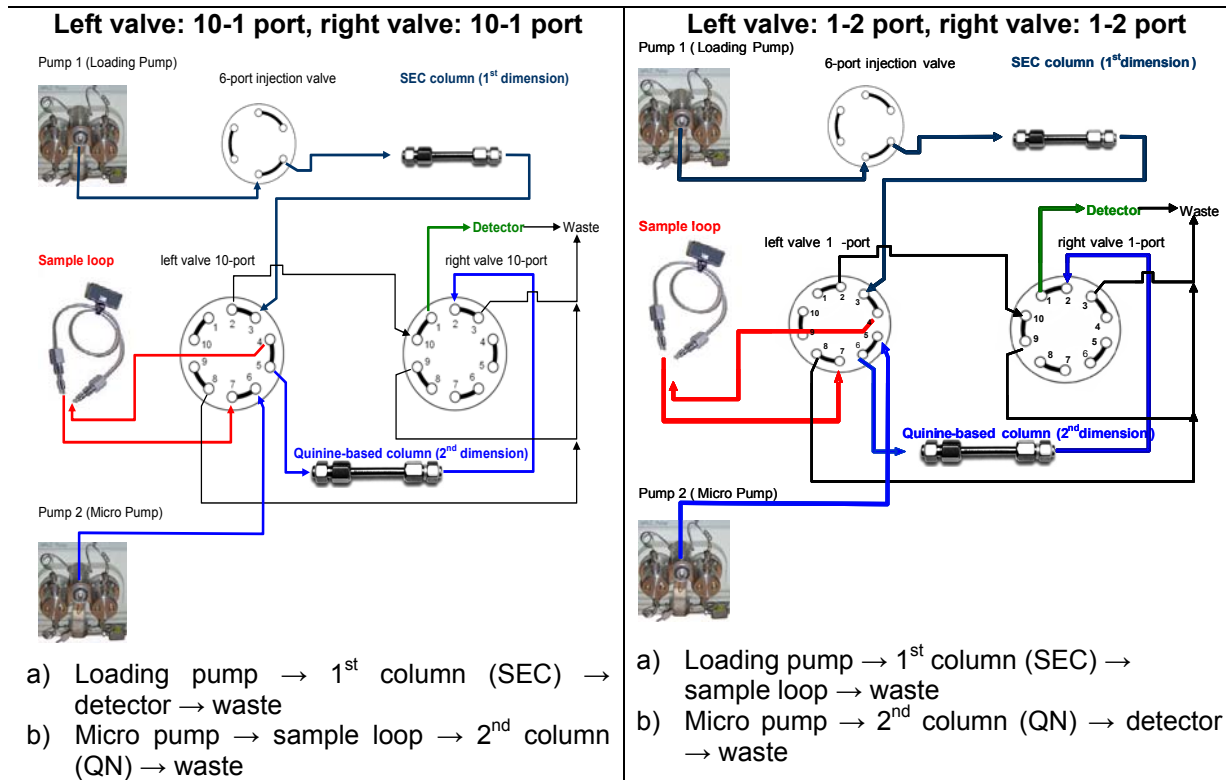
Figure 86: Scheme of the 2D HPLC setups (1)

Left valve: 10-1 port, right valve: 1-2 port

a) Loading pump → 1st column (SEC) → waste
b) Micro pump → sample loop → 2nd column (QN) → detector → waste
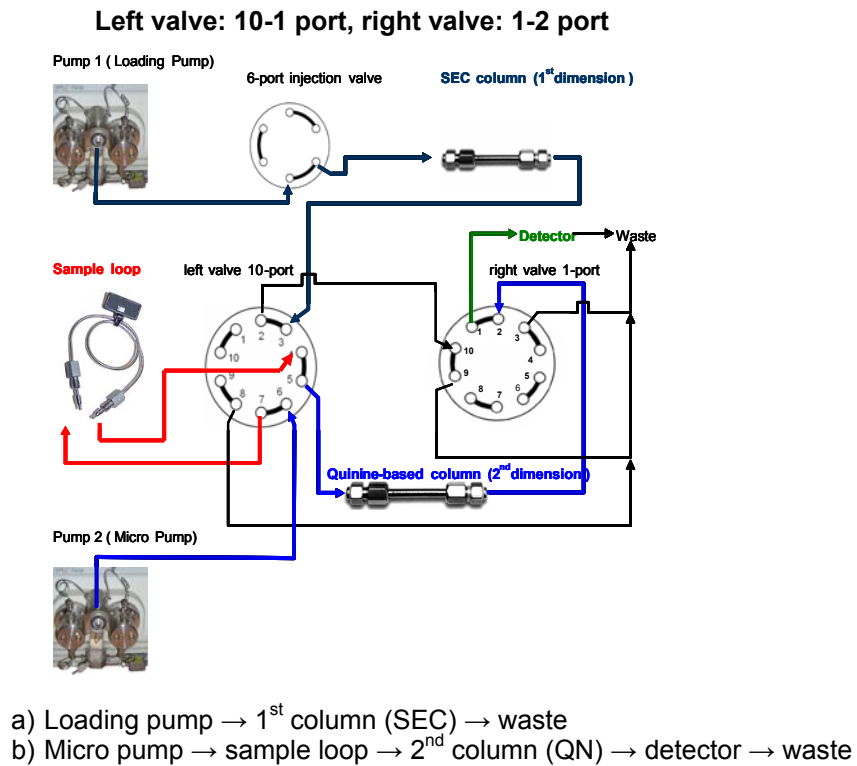
Figure 87: Scheme of the 2D HPLC setups (2)

12.2 Analysis of IPC samples

To investigate the influence of the circadian and harvest time point, the topoisomer distribution was analyzed. Therefore, biomass samples were taken every uneven hour (2 h intervals) during fermentation. Subsequently cell disintegration using alkaline lysis was carried out before analysis. Full topological analysis could be achieved by chromatographic separation of the crude lysate.

Two different plasmid samples (AS24 – 3347, pMCP1; bp, AS25 – 4892 bp) had to be investigated, whereby the biomass samples contained all cell compounds except of genomic DNA.

Notation of AS24 samples

Table 49: Numbering of samples concerning their feed time (3347 bp plasmid)

Sample no.	day time	feed time [h]
0	7 am	-
1	8 am	0
3	10 am	2
5	12 am	4
7	2 pm	6
9	4 pm	8
11	6 pm	10
13	8 pm	12
15	10 pm	14
17	12 pm	16
19	2 am	18
21	4 am	20
23	6 am	22
25	8 am	24
27	10 am	26
29	12 am	28

Notation of AS25 samples

Table 50: Numbering of samples concerning their feed time (4892 bp plasmid)

sample no.	day time	feed time [h]
0	10:30 am	-
1	01:30 pm	0
3	03:30 pm	2
5	05:30 pm	4
7	07:30 pm	6
9	09:30 pm	8
11	11:30 pm	10
13	01:30 am	12
15	03:30 am	14
17	05:30 am	16
19	07:30 am	18
21	09:30 am	20
23	11:30 am	22
25	01:30 pm	24
27	03:30 pm	26
29	05:30 pm	28

The biomass pellets were suspended in 2 mL buffer A (50 mM Tris-HCl, 10 mM Di-Na-EDTA adjusted to pH 7.9-8.1 with NaOH) for homogenization. Therefore 2 mL buffer B (0.2 M NaOH, 1% SDS) was added, mixed and incubated at r.t. for 3 minutes. Afterwards the suspension was neutralized with 2 mL buffer C (3 M potassium acetate adjusted to pH 5.4-5.6 with glacial acetic acid) and 3 minutes incubated at 4°C (in the fridge). For the removal of the solid particles the samples were centrifuged for 15 minutes at 4°C followed by a filtration using a 0.2 μm filter and then analyzed with a 2D-HPLC system (SEC-AIEX).

In general, the lysate of AS25 samples were less concentrated and needed to be enriched using a QIAGEN Kit followed by precipitation with isopropanol, washing with 70% ethanol and air-drying of the DNA pellets. The addition of alcohol or organic solvents changes the solvent polarity and inhibits therefore the interactions of the hydrophilic groups of the DNA surface with water. In further consequence, the molecules tend to precipitate because of their decreasing solubility. Afterwards the DNA was dissolved in about 100 μL 20 mM Tris-HCl (adjusted to pH 8.0).

By adding SDS to some samples of AS25 (no. 7-13, 25) started strongly to foam resulting in partial destruction of the samples. Thus no results for those samples could be obtained.

Optimized method for IPC analysis

Table 51: Column switching program

Time [min]	Right valve port	Left valve port
0	10-1	10-1
1.35	1-2	1-2
2	10-1	1-2
3.3	1-2	1-2

Table 52: Detailed method for topoisomer separation

	1st dimension]		2nd dimension	
Time [min]	Buffer	Flow rate [µL/min]	Buffer	Flow rate [µL/min]
0	100% Buffer A	2000	0% Buffer B	1000
1.35	100% Buffer A	2000	0% Buffer B	1000
2	100% Buffer A	2000	0% Buffer B	1000
2.1	100% Buffer A	500	0% Buffer B	1000
4	100% Buffer A	500	0% Buffer B	1000
19	100% Buffer A	500	100% Buffer B	1000
20	100% Buffer A	500	100% Buffer B	1000
20.1	100% Buffer A	500	0% Buffer B	1500
22	100% Buffer A	500	0% Buffer B	1500
22.1	100% Buffer A	500	0% Buffer B	1000

1st dimension: buffer A 0.1 M Tris-HCl, 0.1M NaCl, 1 mM EDTA, pH 7.5

2nd dimension: buffer A: 50 mM phosphate

buffer B: 50 mM phosphate + 0.6 M NaCl, 10% IPA, pH 7.2

To sum up, the analyte was purified using the SRT-SEC column in the first dimension, whereby the desired peak was collected in the sample loop. Subsequently, the transfered fraction of pDNA from the SEC column was separated in the quinine based modified silica column (AIEX) and detected. As a result, purification and separation of topoisomers could be performed within one step.
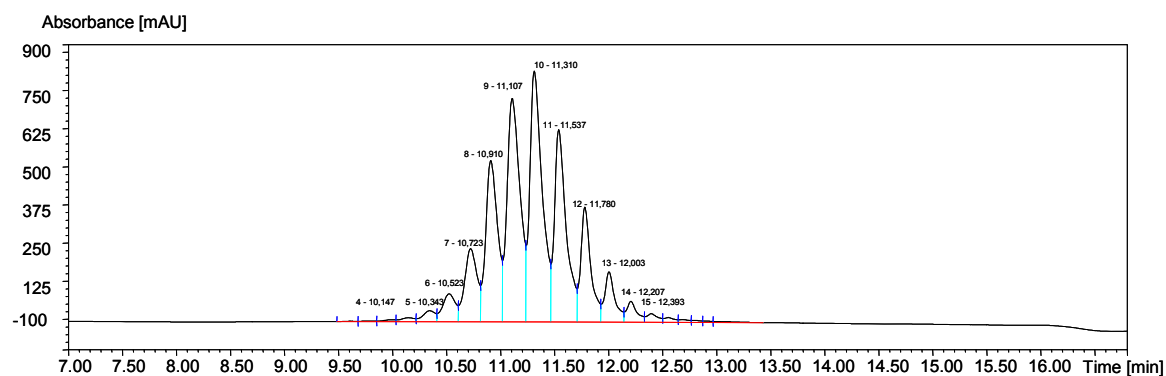
Figure 88: Chromatogram of supercoiled pMCP1 analyzed employing optimized 2D HPLC method described in Table 51-52

An example for this optimized method is given in Figure 88, which illustrates the topoisomers separation from the supercoiled pMCP1 plasmid.

12.3   Results

16 crude samples of each plasmid (AS 24, AS 25) were analyzed using the 2D HPLC system (1st dimension: SRT SEC, 2nd dimension: allylcarbamoyl dihydroquinine) and the optimized method (see Table 51-52).

In following chromatograms the arrows are indicating the peak of maximum of supercoiling of topoisomer distribution.

Analysis of AS24 plasmid (3347 bp)
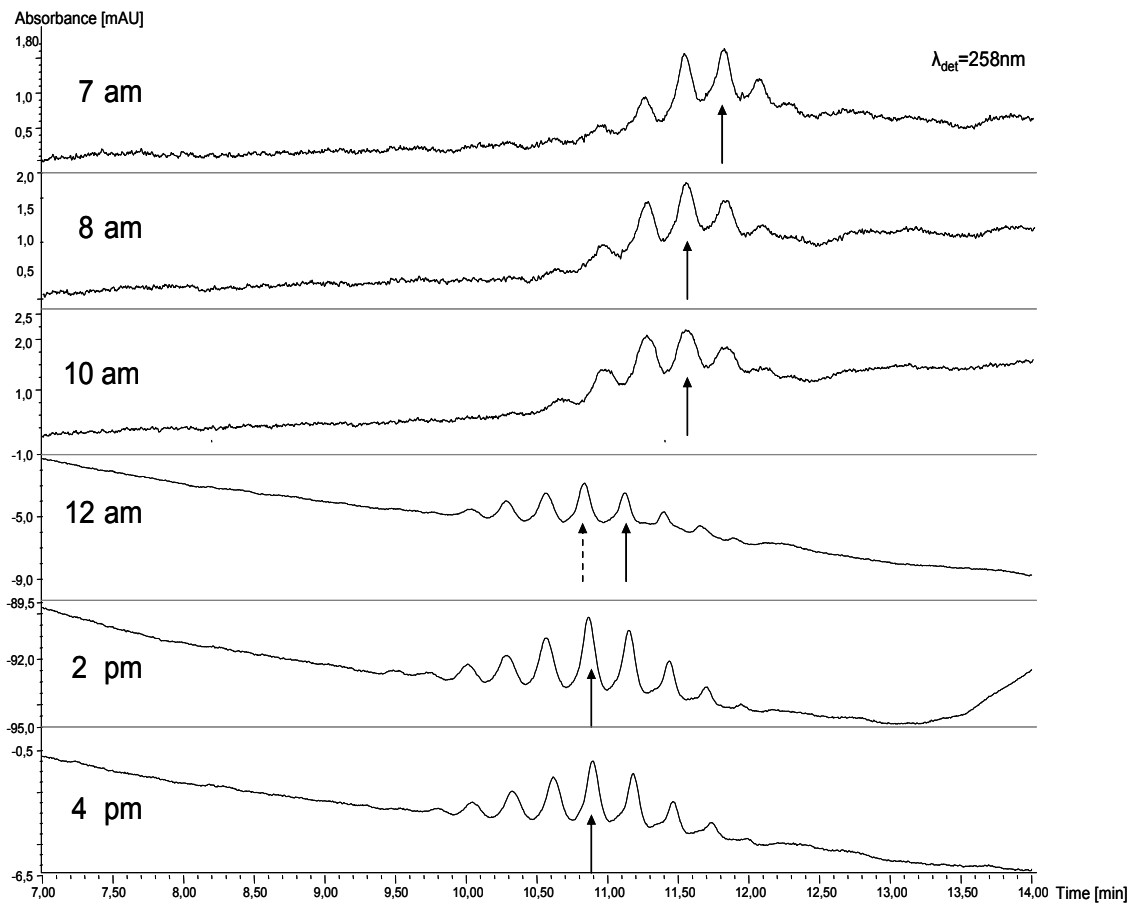
Figure 89: Topoisomer distribution of 3.3 kbp plasmid from 7 am to 4 pm
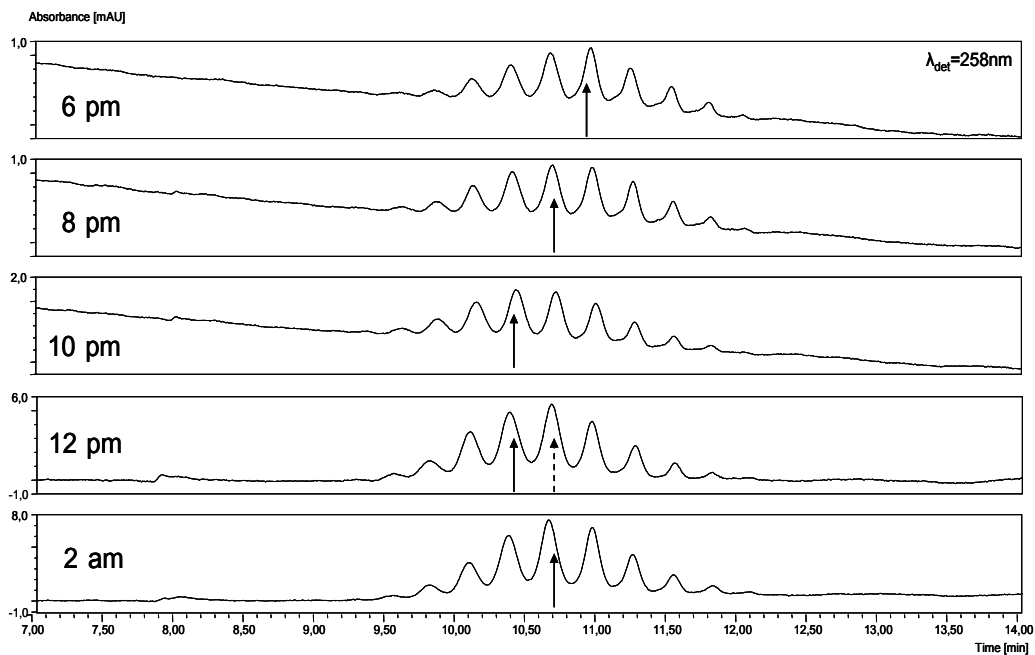
Figure 90: Topoisomer distribution of 3.3 kbp plasmid from 6 pm to 2 am
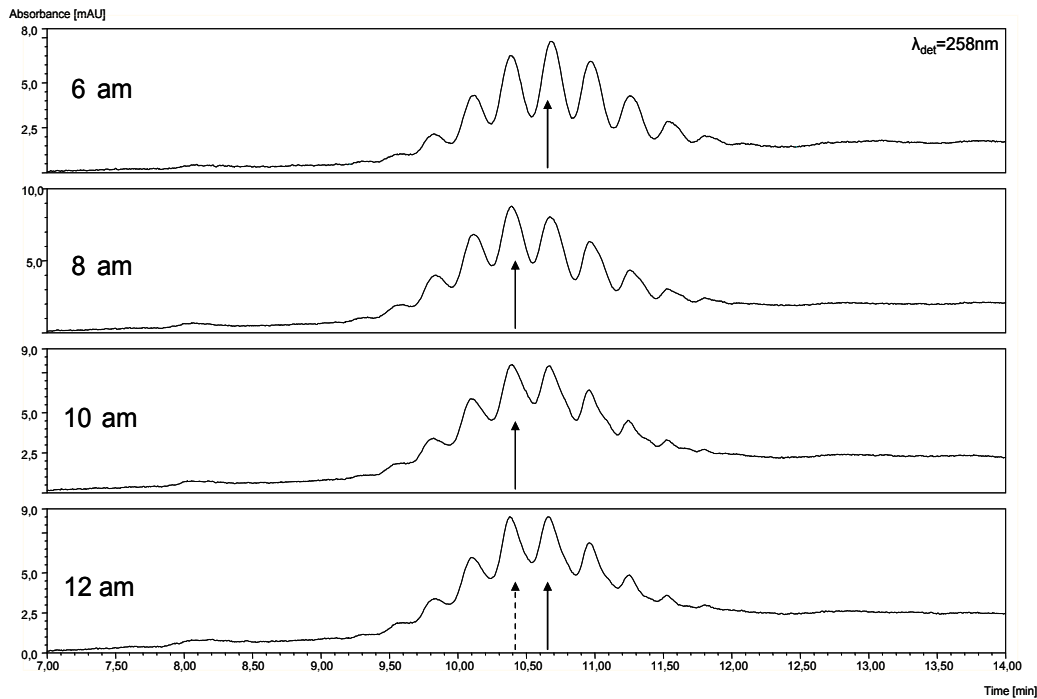
Figure 91: Topoisomer distribution of 3.3 kbp plasmid from 6 am to 12 am

In Figure 89-91 the topoisomer distribution with labelling of the maximum peak can be seen. At the beginning, the plasmid showed the highest supercoiling which is subsequently decreasing with increasing fermentation time. The longer the fermentation time was, the more concentrated the samples were resulting in a loss of resolution due to overloading phenomena.
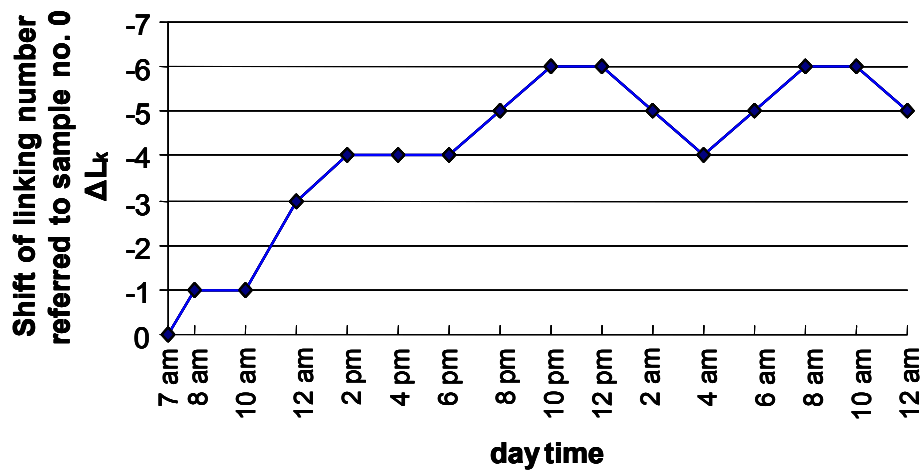
Figure 92: Change of linking number with fermentation time

This graph shows that after approximately 15 hours fermentation duration (10 pm) a maximum of linking number difference referred to the sample at the beginning (7 am) was reached. Afterwards the linking number fluctuates between -4 and -6.

Additionally, it should be mentioned that there is no dramatic shift between 6 pm and 12 am (after 11 hours of fermentation) and that the relative quantity of topoisomers (distribution pattern) does not change with the fermentation process anymore. Thus the equilibrium of topoisomers distributions is reached after approximately 11 to15 hours of fermentation.

<u>Analysis of AS25 plasmid (4892 bp)</u>
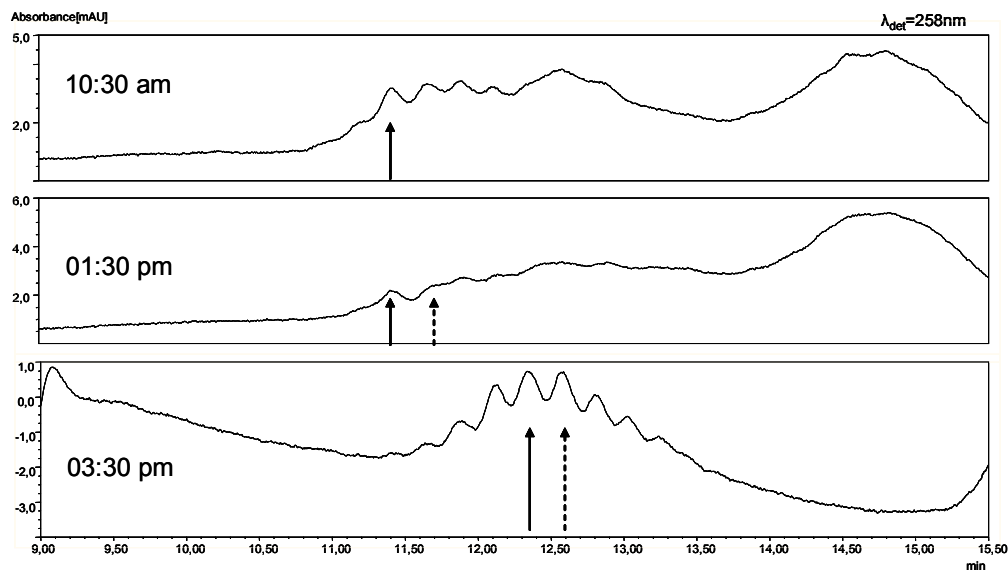
Figure 93: Topoisomer distribution of 4.9 kbp plasmid from 10:30 am to 03:30 pm
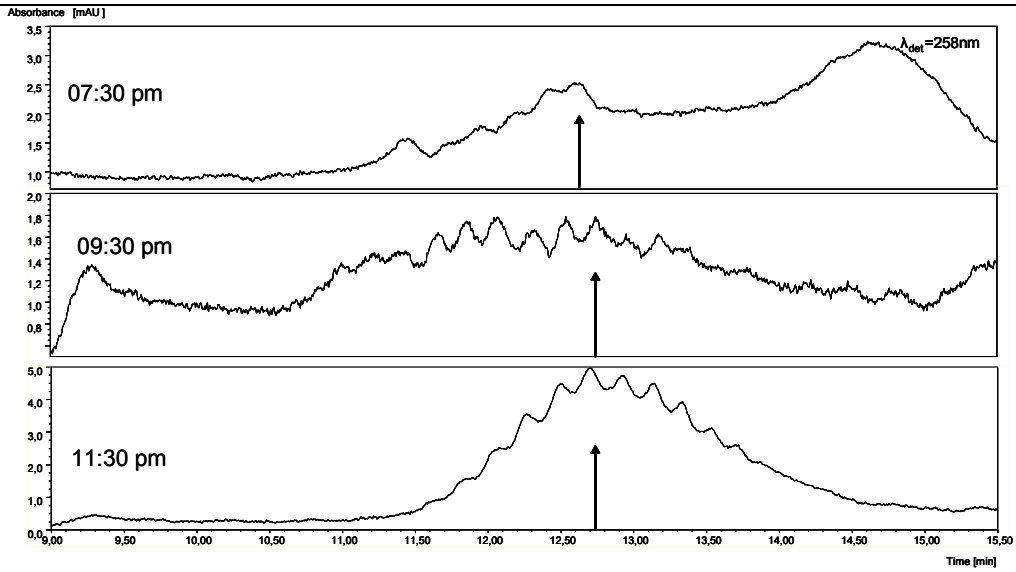
Figure 94: Topoisomer distribution of 4.9 kbp plasmid from 07:30 to 11:30 pm
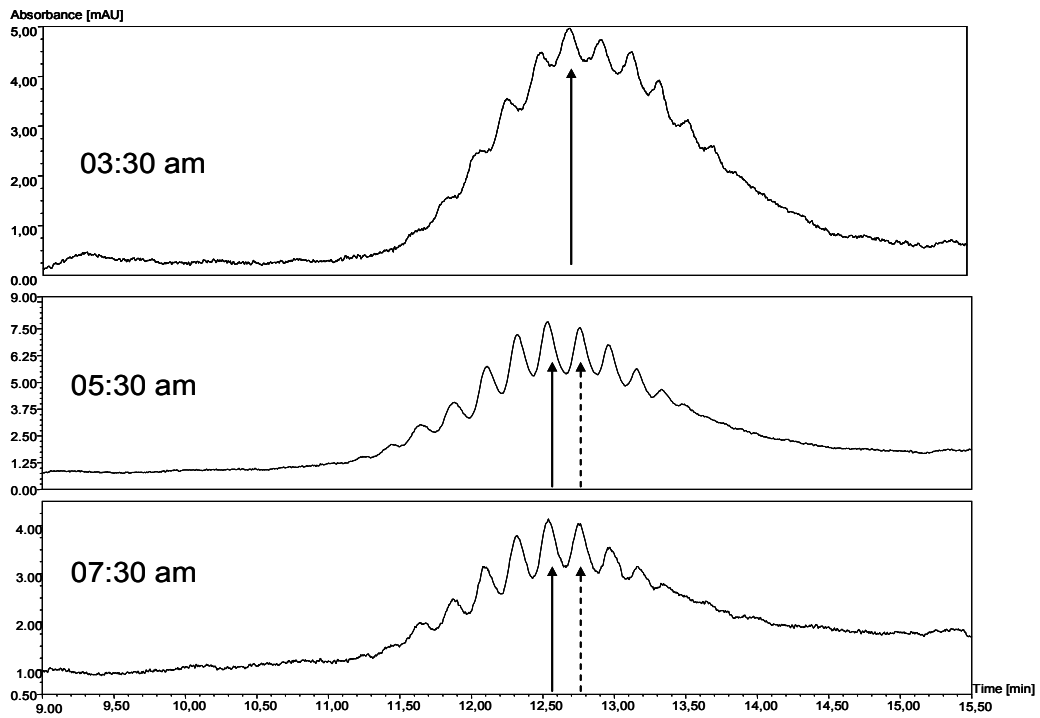
Figure 95: Topoisomer distribution of 4.9 kbp plasmid from 03:30 to 07:30 am
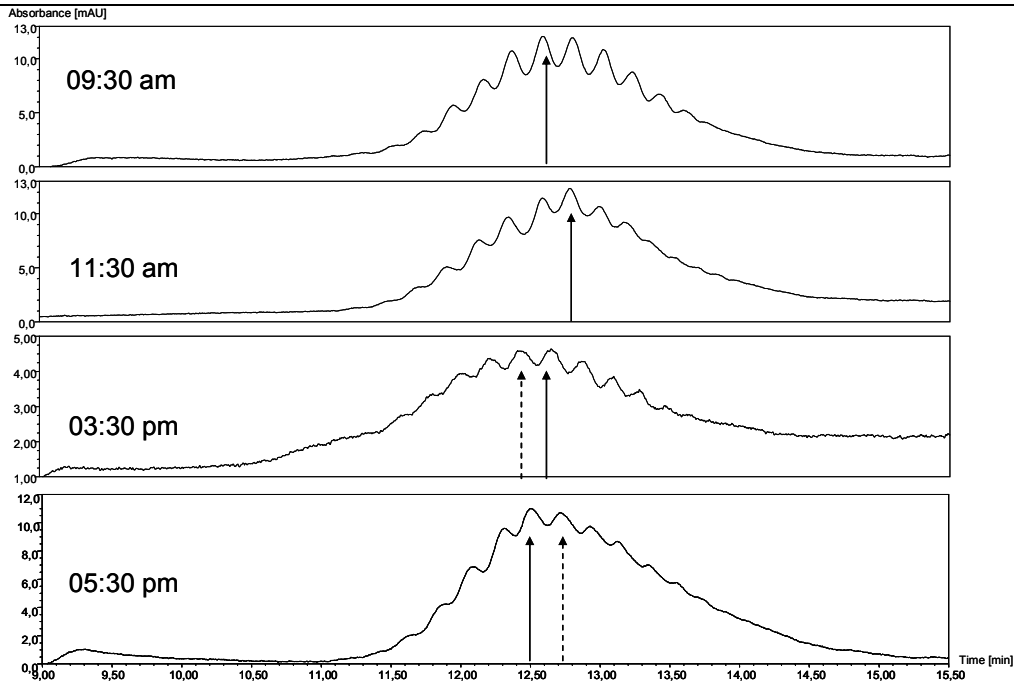
Figure 96: Topoisomer distribution of 4.9 kbp plasmid from 09:30 am to 05:30 pm

Figure 93-96 show the resulting chromatograms of crude samples of pMCP1 taken every uneven hour during fermentation process. The arrows indicate the maximum of supercoiling for each topoisomer distribution. The plasmidic samples were less concentrated compared to the AS24 plasmid, thus all samples except of no. 3 (03:30 pm) had to be concentrated using the QIAGEN-Kit (see page 103).

By comparing the arrows it can be seen that the supercoiling was increasing with increasing fermentation time and the equilibrium was reached somewhere between 03:30 am and 03:30 pm.

The samples between 05:30 pm and 11:30 pm do not exist due to a few problems which emerged during the alkaline lysis – after the addition of buffer B which contained 1% SDS, the solution foamed over and the sample could not be used for further measurements.
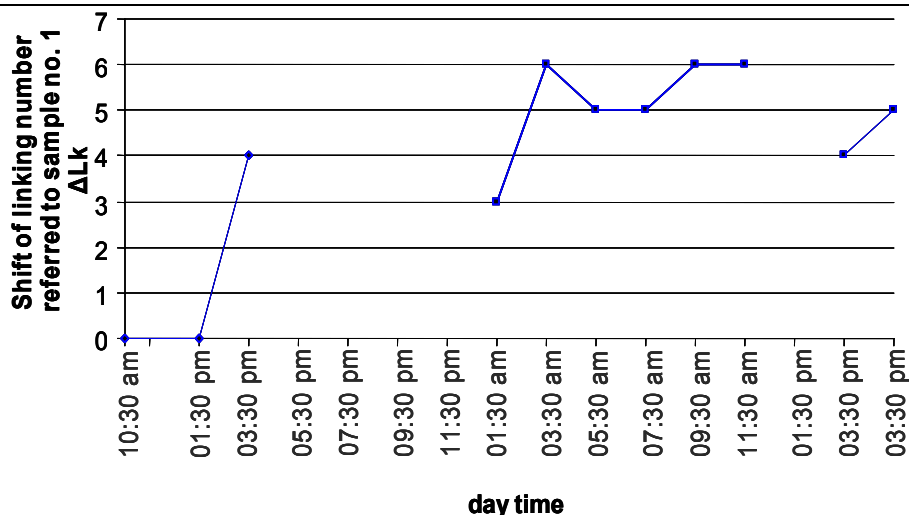
Figure 97: Change of linking number with fermentation

This graph illustrates that after approximately 15 hours of fermentation the maximum of linking number difference referred to the origin sample and equilibrium of topoisomer distribution is reached and then fluctuating around the shift of +5 supercoils.

Furthermore, there is no dramatic shift of the distribution between 03:30 am and 03:30 pm which indicates that there is no influence of the reaction time to the fermentation process anymore. Moreover, it should be mentioned that with these results, it is not possible to make an explicit distinction between the reaction time and the daytime.

It could be shown, that the online 2D HPLC can be successfully used for topoisomer analysis. The combination of size exclusion and anion exchange chromatography enables analysis within one step in an automated manner.

Furthermore, results mentioned above confirmed that the fermentation time indeed influences the topoisomer distribution in the first 13 to 15 hours before reaching an equilibrium of supercoiling.

The consequences of different topoisomers are not clarified yet because so far no preparation was possible. Eventually, the supercoiling can influence the transcription process and efficiency of vectors for therapeutic applications.

13 Summary

This diploma thesis is dealing with the analysis of plasmid DNA isoforms and topoisomers. Plasmids are extrachromosomal, double-stranded DNA molecules and they appear in different topologies: supercoiled (ccc), open-circular (oc) and linear (lin). They are used as vectors for gene therapy and vaccination, whereby the ccc form is believed to be the most active topological isoform. Plasmidic DNA can be analyzed using capillary gel electrophesis (CGE), agarose gel electrophoreses (AGE) or high performance liquid chromatography (HPLC), whereby an HPLC method is the one with the most promising future.

During my diploma thesis, validation of new methods employing new stationary phases based on two different chemoaffinity selectors based on quinine carbamate (PCQ) was performed for two different plasmids (4.9 kb and 15 kb). This study involved preparation of suitable standards for the oc form. It is critical and a difficult task to produce a representative oc standard with a similar topology to the natural occurring oc. Therefore heat treatment for the pMCP1 plasmid and the enzymatic reaction (enzyme: Nt.BstNBI) for the larger pGNA3 plasmid were optimized and subsequently isolated using the PCQ based stationary phase. The preparation was in both cases successful, as controlled with agarose gel electrophoresis. It is not completely sure how many nicks within one DNA strand were produced during these treatments but no obvious differences concerning the chromatographic or electrophoretic behaviour could be observed between the synthesized oc standards and natural oc form in ccc plasmid form. In literature, no useful production protocols of the open circular form could be found, thus it is still a content of research.

Another issue was the reliable detection and quantification of this oc form. Preliminary measurements performed from M. Mahut (PhD thesis (2010) *University of Vienna*) showed, that the poor recovery of this isoform exists due to its reversible but tight adsorption at the glass wool frits. To make the oc analysis more accurate glass wool frits were replaced by metal ones like stainless steel frits if possible.

Stainless steel columns (150 x 4 mm ID) were packed with porous PCQ modified silica particles (100 Å, 5 μm) and the experimental conditions optimized. Resultant method allowed separation of oc and ccc forms with high resolution, thus greatly improved compared to state-of-art DNA-NPR (Tosoh). Unfortunately, lin and oc coeluted. On the other hand, validation showed that recovery for oc form (pMCP1:

~112% recovery, pGNA3: ~102% recovery) is much better than with DNA-NPR (pMCP1: ~60 % recovery).

The linearity range of the DNA-NPR column yielded slightly wider or equal concentration ranges (pMCP1: 0.01-7µg ccc, 0.01-1 µg oc, 0.01-3 µg lin) compared to the novel material (pMCP1: 0.1-7 µg ccc, 0.04-7 µg oc and lin; pGNA3: 0.04-10 µg ccc and lin, 0.01-3 µg oc) but PCQ based column offers higher sample loadings and is therefore more suitable for semi-preparative applications. Furthermore the quinine carbamate based material offered better intra-assay precision (RSD of peak area: 0.6-1.5%; DNA-NPR: RSD of peak area: 0.8-6.4%) and in general lower limits of detection and quantitation. Based on these results, the novel material has a greater benefit.

However, the selectivity between the oc and the linear form was improved when using 1.5 µm NPS silica particles as support (R_s of 0.7 between oc and lin). In principle, the validation was completed successfully also for this stationary phase except for the oc standard sample that was degraded, reflecting the complexity of this topic. Precisions of 1.9% for the ccc and 2.3% for the lin isoform and a linearity range over the entire measured concentration range (0.05-0.5 µg pDNA) for both isoforms was found. Furthermore, the stability of this NPS chromatographic material was unsatisfactory enabling only approximately 20 injections. This approach is still promising, but the selector binding chemistry and therefore the stability of this column has to be improved.

The second part of this diploma work dealt with the in-process control (IPC) of the degree of supercoiling in the course of fermentation process. Thus, topoisomer distributions had been investigated on two different samples to study the influence of fermentation duration on relative topoisomer abundances. Therefore, an Ultimate 3000 system which provides two separate ternary pumps and switching valves for fraction transfer in heartcut and comprehensive online 2D HPLC was used for measurements. In the first dimension the sample was purified using a SRT-SEC column (5 µm, 1000 Å, 150 x 7.8 mm ID) and subsequently collected in the sample loop. Afterwards, the valves were switched enabling the separation of the collected analyte with allylcarbamoyl dihydroquinine based silica phase (5 µm, 120 Å, 150 x 4 mm ID) in the second dimension and detected. The 2D system is essential due to the fact that the size exclusion phase only enables purification of the plasmidic sample

and does not provide topoisomer selectivity. In contrast, the quinine carbamate based stationary phase does indeed provide an adequate toposelectivity but the material can not separate the plasmid from impurities. Thus this 2D HPLC method is essential for such a topic.

In process control samples were taken every 2 hours from the fermentation process and analyzed with the 2D HPLC method described before. The results of the smaller plasmid (3347 bp) showed that at the beginning the supercoiling is decreasing until reaching a linking number of -5 after approximately 15 hours. Afterwards the distribution pattern does not change with the fermentation process anymore. Analyzing the larger plasmid (4892 bp), a few problems associated with the alkaline lysis occurred. Moreover, the larger plasmid was less concentrated which required additional preconcentration steps causing a lack of data for several samples. Resultant chromatograms showed an increase of +6 supercoils during fermentation in the first 13 hours followed by fluctuation around the shift of +5 supercoils. Results of both samples revealed that in the first few hours the biggest shift of supercoiling takes place, but no influence of the circadian rhythm could be found.

To sum up, the results presented in this thesis point out important properties of a chromatographic material that is intended for use in pDNA isoform and topoisomer separation and analysis. Significantly improved chromatographic methods for this purpose have been developed in this work based on a chemoaffinity principle, and they have been successfully validated for pDNA isoform analysis of a 4.9 and 15 kb plasmid. Further on, a new online 2D-HPLC method based on SEC and quinine carbamate chemoaffinity chromatography has been presented for the in-process control of supercoiling and topoisomer distributions respectively in pDNA manufacturing during fermentation on two different plasmids. Ongoing investigations will hopefully enhance these types of chromatographic separations based on quinine carbamate and lead to materials with improved long term stability materials. Moreover, further research is needed for a full understanding of the fundamental mechanism of pDNA interaction with the quinine carbamate silica, especially concerning the various open circular isoforms.

14 Acknowledgments

First of all I would like to express my sincere gratitude to my professor Dr. Lämmerhofer for giving me the opportunity to write my diploma thesis in his working group. I would like to thank him explicitly for the continuous support of my study and research.

I would also like to acknowledge Professor Dr. Lindner for his support, help and participation in my thesis.

Furthermore, I owe my deepest gratitude to Marek. Without his patience, knowledge and the enormous time he invested in helping me, my thesis would not be the way it is. He always supported me mentally during my laboratory research and had faith in me. He proved right: After a huge disappointment, I measured one of the best resolutions up to this day. His guidance helped me in all times of research and compiling this thesis.

Moreover, I would like to thank all members of the working group (Lindner group) who accepted, motivated and encouraged me since my first day (especially with funny and entertaining movies). I thank you all for being patient and watching my favourite serials.

Special thanks to Andrea for the electronic music entertainment and also to Heli for accepting it.

I would like to mention my study colleagues, who accompanied me during the stressful but also very amusing study, as well as all my friends from Vienna and Linz.

Finally, I am grateful for my familiy's unrestricted support and for the chance to study in Vienna, even if I decided the subject of my studies very spontaneously. Their encouragement helped me throughout the years, even if I should be more cautious in the lab according to my dad. Last but not least, my sister Angela supported me mentally which I would like to thank her for.

Without the help of all the people mentioned above, I would not have been able to write this diploma thesis.

15 Table of Figures

16 References

Books and papers

Bates A. D., Maxwell A. (2005) DNA Topology, *Oxford University Press*, February 18

Bhikhabhai R., Plasmid DNA Purification using Divalent Alkaline Earth Metal Ions and two Anion Exchangers, *US Patent 6410274*

Birnboim H.C., Doly J. (1979) A Rapid Alkaline Extraction Procedure for Screening Recombinant Plasmid DNA, *Nucleic Acids Res* **7**: 1513-1523

Burda, Jaroslav V., Jiri Sponer, Jerzy Leszczynski and Pavel Hobza (1997) Interaction of DNA Base Pairs with Various Metal Cations (Mg^{2+}, Ca^{2+}, Sr^{2+}, Ba^{2+}, Cu^+, Ag^+, Au^+, Zn^{2+}, Cd^{2+}, and Hg^{2+}): Nonempirical ab Initio Calculations on Structures, Energies, and Nonadditivity of the Interaction, *The Journal of Physical Chemistry B* **101**, No. 46 (November 1): 9670-9677

Bussey L.B., Adamson R., Atchley A. (1998) Methods for Purifying Nucleic Acids by Tangential Flow Ultrafiltration, patent WO 9805673 (A1)

Center of Biologics Evaluation and Research (CBER, 1996) Points to Consider on Plasmid DNA Vaccines for Preventive Infectious Disease Indications (Draft Guidance), *US Food and Drug Administration*, 5600 Fishers Lane Rockville, Maryland 20852, USA

Colpan et al., Schorr J., Moritz P. (1999) Process for the Separation and Purification of Nucleic Acids from Biological Sources, Qiagen GmbH, Hilden, Germany, patent US005990301A

Cozzarelli, Nicholas R., Gregory J. Cost, Marcelo Nollmann, Thierry Viard and James E. Stray (2006) Giant Proteins that move DNA: Bullies of the Genomic Playground, *Nature Reviews Molecular Cell Biology* **7**, No. 8: 580-588

Dean et al., Krasnow M. A., Otter R., Matzuk M. M., Spengler S. J., Cozzarelli N. R. (1983) Escherichia Coli Type-1 Topoisomerases: Identification, Mechanism, and Role in Recombination, *Cold Spring Harbor Symposia on Quantitative Biology* **47**(2), page 769-777

Depew D. E. and J. C. Wang (1975) Conformational Fluctuations of DNA Helix, *Proceedings of the National Academy of Sciences of the United States of America* **72**, No. 11 (November): 4275-4279

Diogo M. M., Queiroz J. A., Monteiro G. A., Martins S. A. M., Ferreira G. N. M. and Prazeres D. M. F. (2000) Purification of a Cystic Fibrosis Plasmid Vector for Gene

Therapy using Hydrophobic Interaction Chromatography, *Biotechnol Bioeng* **68**: 576-583

Eon-Duval A., Burke G. (2004) Purification of pharmaceutical-grade Plasmid DNA by Anion-Exchange Chromatography in an RNase-free Process, *J. Chromatography B* **804**: 327-335

Ferreira G. N. M., Cabral J. M. S., Prazeres D. M. F. (1999) Development of Process Flow Sheets for the Purification of Supercoiled Plasmids for Gene Therapy Applications, *Biotechnol Prog* **15**: 725-731

Ferreira G., Monteiro G. D. (2000) Downstream Processing of Plasmid DNA for Gene Therapy and DNA Vaccine Applications, *Institute Superior Técnico*, Portugal

Green, A. P., Garance M., Helveston N. M., Taittinger B. E., Liu X., Thompson J. A. (1997) Preparative Purification of Supercoiled Plasmid DNA for Therapeutic Agents, *BioPharm (Eugene, Oregon)* No. **10**(5), page 52-42, 56, 59-60, 62

Horn N.A., Meek J.A., Budahazi G., Marquet M. (1995) Cancer Gene Therapy using Plasmid DNA: Purification of DNA for Human Clinical Trials, *Hum Gene Ther* **6**: 565-573

Huber C. G. (1998) Micropellicular Stationary Phases for High-Performance Liquid Chromatography of double-stranded DNA, *Journal of Chromatography A* **806**, No. 1 (May 8): 3-30

ICH Harmonised Tripartite Guideline (1994) Validation of Analytical procedures: Test an Methodology, Q2(R1), Current Step 4 version

Kelley B. D., Hatton T. A. (1991) The Fermentation/Downstream Processing Interface, *Bioseparations* **1** (5-6) page 333-349

Kutzler M. A., Weiner D. B. (2008) DNA Vaccines: Ready for Prime Time? *Nature Reviews Genetics* **9**, No. 10 (October): 776-788

Mahut M. (2010) PhD Thesis: Analysis of Plasmid Isoforms and Supercoiled Topoisomers by Liquid Chromatography, *University of Vienna*

Middaugh C. R., R. K. Evans, D. L. Montgomery and D. R. Casimiro (1998) Analysis of Plasmid DNA from a Pharmaceutical Perspective, *Journal of Pharmaceutical Sciences* **87**, No. 2: 130-146

Mihăsan M., Niță A., Artenie V. (2007) Optimal parameters for plasmid DNA preparation using the alkaline lysis method, *Analele Ştiinţifice ale Universităţii „Alexandru Ioan Cuza"*, Secţiunea Genetică şi Biologie Moleculară

Pulleyblank D. E., Shure M., Tang D., Vinograd J. and Vosberg H. P. (1975) Action of Nicking-Closing Enzyme on Supercoiled and Nonsupercoiled Closed Circular DNA: Formation of a Boltzmann Distribution of Topological Isomers, *Proceedings of the National Academy of Sciences of the United States of America* **72**, No. 11 (November): 4280-4284

Schleef M. (2001) Plasmids for Therapy and Vaccination, *Wiley-VCH*

Schmidt T., Friehs K., Schleef M., Voss C. and Flaschel E. (1999) Quantitative Analysis of Plasmid Forms by Agarose and Capillary Gel Electrophoresis, *Analytical Biochemistry* **274**, No. 2 (October 15): 235-240

Stadler J., Lemmens R., Nyhammar T. (2004) Plasmid DNA Purification, *J Gene Med* **6:** 54-66

Thatcher et al., Hitchcock A., Hanak J., Varley D. (1999) Method of Plasmid DNA Production and Purification, Int Patent WO 9636706

Travers A., Muskhelishvili G. (2005) DNA Supercoiling - A Global Transcriptional Regulator for Enterobacterial Growth? *Nature Reviews Microbiology* **3**, No. 2 (February): 157-169

Urthaler J. (2005) Improved Downstream Process for the Production of Plasmid DNA for Gene Therapy, *Acta Biochimica Polonica* **52** No. 3, 703-711, Boehringer Ingelheim Austria GmbH, Vienna, Austria

Wang J. C. (1971) Interaction between DNA and an Escherichia Coli Protein Omega, *Journal of Molecular Biology*, **55**(3), page 523-533

Werner R. G., Urthaler J. (2002) pDNA – From Process Science to Commercial Manufacture*, Boehringer Ingelheim*, CD-Biopharmaceuticals, Binger Str. 173, 55216 Ingelheim am Rhein (D)

Zhdanov R. I., Podobed O. V., Vlassov V. V. (2002) Cationic Lipid-DNA Complexes-Lipoplexes-for Gene Transfer and Therapy, *Bioelectrochemistry* **58**, no. 1 (November): 53-64

Websites

http://www.ema.europa.eu

http://www.neb.com

New England Biolabs ®, Product Details of enzyme Nt.BstNBI (#R0607)

http://www.separations.us.tosohbioscience.com

Tosoh Bioscience LLC, Product Details of DNA-NPR column

http://www.wiley.com/legacy/wileychi/genmed/clinical

Gene Therapy Clinical Trials Worldwide (2010) Vectors Used in Gene Therapy Clinical Trials

http://sandwalk.blogspot.com/2007/07/ethidium-bromide-binds-to-dna.html

Information of Ethidium Bromide binding to DNA

Curriculum Vitae

Elisabeth HALLER

Personal Details	
Nationality	Austria
Born in	October 18, 1986 in Linz
Address	Wagnerweg 2, 4060 Leonding, Austria
Study address	Weidmanngasse 41/8, A-1170 Wien, Austria
Contact	a0504862@univie.ac.at

Education	
March 2010 – January 2011	**Diploma Student** **University of Vienna,** *Faculty of Chemistry* Department of Analytical and Food Chemistry Research Group for Molecular Recognition Materials Währinger Straße 38, A-1090 Vienna
October 2005 – January 2011	**Student of Chemistry** **University of Vienna ,** *Faculty of Chemistry* Währinger Straße 38, A-1090 Vienna
September 1997– June 2005	**Secondary School** **BG/ WRG Körnerschule,** Linz Körnerstraße 9, A-4020 Linz Acquired qualification: matriculation
September 1993 – July 1997	**Primary School,** Leonding Alhartinger Weg 8, A-4060 Leonding
September 1992 – July 1993	**Preschool,** Leonding Alhartinger Weg 8, A-4060 Leonding